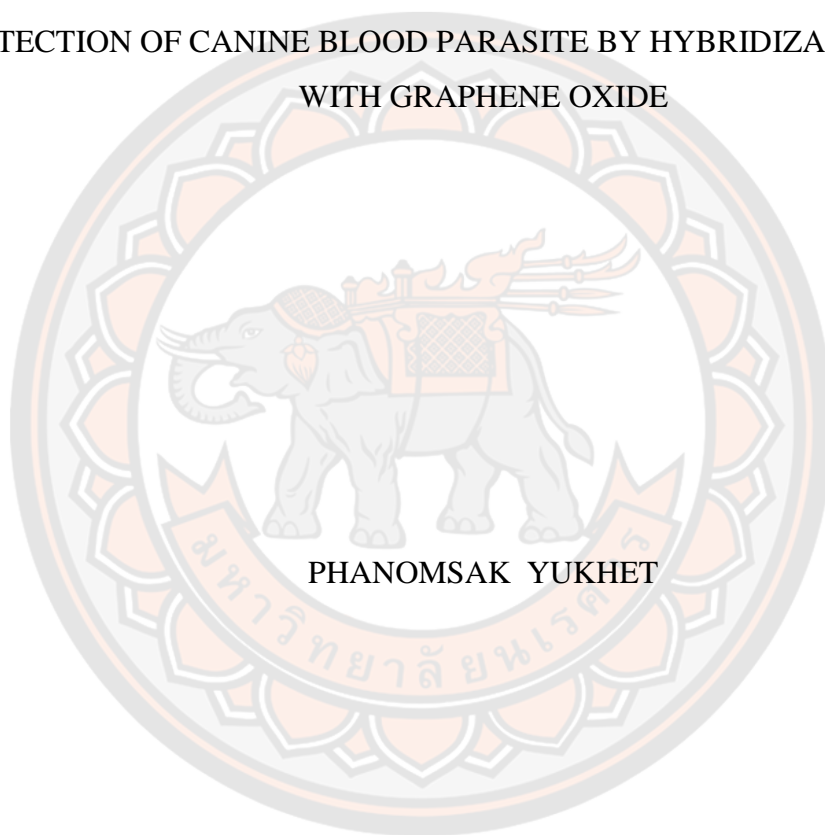




APPLICATION OF PYRROLIDINYL PEPTIDE NUCLEIC ACID FOR  
DETECTION OF CANINE BLOOD PARASITE BY HYBRIDIZATION PROBE  
WITH GRAPHENE OXIDE



PHANOMSAK YUKHET

A Thesis Submitted to the Graduate School of Naresuan University  
in Partial Fulfillment of the Requirements  
for the Master of Science in (Chemistry)

2020

Copyright by Naresuan University

APPLICATION OF PYRROLIDINYL PEPTIDE NUCLEIC ACID FOR  
DETECTION OF CANINE BLOOD PARASITE BY HYBRIDIZATION PROBE  
WITH GRAPHENE OXIDE



A Thesis Submitted to the Graduate School of Naresuan University  
in Partial Fulfillment of the Requirements  
for the Master of Science in (Chemistry)  
2020

Copyright by Naresuan University

Thesis entitled "Application of Pyrrolidinyl Peptide Nucleic Acid for Detection of Canine Blood Parasite by Hybridization Probe with Graphene Oxide"

By PHANOMSAK YUKHET

has been approved by the Graduate School as partial fulfillment of the requirements for the Master of Science in Chemistry of Naresuan University

**Oral Defense Committee**

..... Chair  
(Professor Tirayut Vilaivan, Ph.D.)

..... Advisor  
(Assistant Professor Chaturong Suparpprom, Ph.D.)

..... Co Advisor  
( Kittisak Buddhachat, Ph.D.)

..... Internal Examiner  
(Assistant Professor Boonjira Rutnakornpituk, Ph.D.)

**Approved**  
.....  
(Professor Paisarn Muneesawang, Ph.D.)  
Dean of the Graduate School

**Title** APPLICATION OF PYRROLIDINYL PEPTIDE  
NUCLEIC ACID FOR DETECTION OF CANINE  
BLOOD PARASITE BY HYBRIDIZATION PROBE  
WITH GRAPHENE OXIDE

**Author** PHANOMSAK YUKHET

**Advisor** Assistant Professor Chaturong Suparpprom, Ph.D.

**Co-Advisor** Kittisak Buddhachat, Ph.D.

**Academic Paper** Thesis M.S. in Chemistry, Naresuan University, 2020

**Keywords** Canine Monocytic Ehrlichiosis, PNA probe, Graphene  
oxide, Isothermal DNA amplification

### ABSTRACT

Canine Monocytic Ehrlichiosis (CME) caused by *Ehrlichia* spp., is a vector-borne disease with worldwide distribution. The dogs have primarily infected this bacteria through the bite of brown-dog ticks. Clinical symptoms are such as anorexia, enlarged lymph nodes, vomiting, diarrhea, leukopenia, and maybe led to death in terrible cases. A typical diagnosis for CME is a polymerase chain reaction (PCR) based on the amplification of a sequence-specific gene of interest. However, a requirement of thermocycler to control the PCR reaction-temperature becomes a majority limitation as high costs and loss of time. In recent years, an isothermal DNA amplification has been developed to reduce costs and time towards CME identification. These techniques are usually combined with a nucleic acid probe for the development of an uncomplicated and practical method as well as the enhancement of assay performance. Herein, a fluorescent-labeled conformational-constrained peptide nucleic acid (PNA) in the graphene oxide (GO) platform has been established towards *E. canis*'s DNA detection using the specific region of the 16S rRNA gene. This assay's principle is based on the use of excellently targeted binding of PNA probe with DNA target, producing PNA×DNA<sub>target</sub> duplex which was remained or recovered fluorescence signal under GO-suspended solution. Whereas, in the case of non-targeted DNA, unbound PNA would be adsorbed on the GO surface *via* p-p interaction, hydrophobic driving force, and hydrogen bonding between

unpaired nucleobases and functional groups of GO. Firstly, the comparison of two different types of pyrrolidiny PNA as acpcPNA and apc/acpcPNA was examined. The apc/acpcPNA was designed to create the positive charges within the acpcPNA backbone to relieve the non-specific binding of acpcPNA by replacing the 3'APC to ACPC spacers. However, the results showed that apc/acpcPNA could not be reduced the non-specific quenching between the probe and hydrophobic surface with indicating the fluorescence signal lower than acpcPNA. In addition, the binding property with single-stranded (ss) DNA target showed that acpcPNA has a great performance to discriminate the targeted DNA from other mismatched sequences rather than apc/acpcPNA and provided the sensitivity to target with a limit of detection (LOD) in the range of 7-9 nM. Hence, an acpcPNA probe was further used in double-stranded (ds) DNA detection by developing the recombinase polymerase amplification (RPA) in combination with Deoxyribonuclease I (DNase I) enhancement and PNA/GO system (RPA-DPG assay). The results found that acpcPNA could hybridize with a sequence-specific region within targeted dsDNA at low temperature and displayed the fluorescence signal in GO-suspended solution upon digesting of non-targeted dsDNA by DNase I enzyme. The study of specific detection for targeted *E. canis* in comparison with pUC57-based plasmid DNAs including *Ehrlichia canis*, *Anaplasma platys*, *Babesia canis vogeli*, and *Hepatozoon canis*, showed that the developed RPA-DPG assay has an excellent performance to distinguish the *E. canis* from others species and giving LOD = 2.22 fg/mL (2.47 fM). Notably, the fluorescent visualization under LED transilluminator was clearly observed with naked-eye when the concentration of the DNA template at least 10 pg/mL (11.15 pM). Based on these results, the developed RPA-DPG assay could be adopted to identify *E. canis* in real samples by using a general heating block with successful detection and visualization under LED transilluminator. However, the protein interference that presented in extracted DNA from the whole blood sample becomes the limitation of the RPA process (gel electrophoresis is undetectable), providing a low fluorescence signal in the detection of real clinical DNA samples.

## ACKNOWLEDGEMENTS

Firstly, I would like to express my sincere gratitude and appreciation to my advisor Assistant Professor Dr.Chaturong Suparpprom as well as co-advisor Dr.Kittisak Buddhachat for their supervision, invaluable advice, guidance, kindness, and integrative knowledge on my logical and critical thinking skills. I also would like to thank the committee members for their helpful comments and guides me in understanding and solving problems on my research and writing this thesis. Furthermore, I would like to express my thankfulness to Professor Dr.Tirayut Vilaivan, Mrs. Chotima Vilaivan, Miss Penthip Muangkaew, and TV research group from the Department of Chemistry, Faculty of Science, Chulalongkorn University as well as CS and KB research groups from the Department of Biology, Faculty of Science, Naresuan University for their important support, constant inspiration valuable comments and suggestions throughout this study. I would like to thank the Development and Promotion of Science and Technology Talent project (DPST) for the financial support of my study and research. I am also grateful to SC4-501 members and all officers of the Faculty of Science, Naresuan University for their stimulating discussion, friendship, advice, and co-operation. Finally, I am indebted to my family for moral supports and encouragement throughout my life.

PHANOMSAK YUKHET

## TABLE OF CONTENTS

	<b>Page</b>
ABSTRACT.....	C
ACKNOWLEDGEMENTS.....	E
TABLE OF CONTENTS.....	F
LIST OF TABLES.....	I
LIST OF FIGURES.....	K
LIST OF ABBREVIATIONS.....	O
CHAPTER I INTRODUCTION.....	1
Peptide nucleic acid and graphene oxide.....	1
The identification of <i>Ehrlichia canis</i> .....	3
The combination of RPA and GO-based acpcPNA probe.....	5
Research objectives.....	6
Scope of research.....	6
CHAPTER II LITERATURE REVIEWS.....	7
The adsorption-desorption ability of nucleic acid on GO.....	8
GO-based fluorescent-labeled probe in nucleic acid detection.....	14
The combination of GO-based PNA probe with amplification technique.....	20
The detection of <i>E. canis</i> DNA is based on isothermal amplification.....	25
CHAPTER III RESEARCH METHODOLOGY.....	27
General procedure.....	27
1. Instruments.....	27
2. Materials.....	28
Experimental procedure.....	29
1. RPA primers and PNA probe designs.....	29
2. Pyrrolidiny PNA monomers and spacers.....	29
2.1 Synthesis of N-Fmoc-T-OPfp <sup>49</sup> .....	31

2.2 Synthesis of N-Fmoc-ACPC-OPfp <sup>5</sup> .....	31
2.3 Synthesis of N-Fmoc-APC(Tfa)-OPfp <sup>50</sup> .....	32
3. Synthesis of pyrrolidinyl PNA <i>via</i> solid-phase peptide synthesis <sup>49</sup> .....	32
3.1 Solid support preparation and experimental setup .....	34
3.2 General protocol of manual SPPS in PNA synthesis .....	35
3.3 The side chain deprotection.....	35
3.4 The cleavage of pyrrolidinyl PNA .....	35
4. The purification and characterization of pyrrolidinyl PNA .....	36
4.1 PNA purification by using reverse-phase HPLC .....	36
4.2 The determination of PNA concentration and T <sub>m</sub> analysis.....	36
5. The ssDNA detection by PNA probe in the GO platform.....	37
5.1 Fluorescence measurement.....	37
5.2 The optimization of GO.....	37
5.3 Sequence selectivity .....	37
5.4 Sensitivity .....	37
6. The combination of a PNA/GO platform and PCR.....	38
6.1 Fluorescence measurement.....	38
6.2 PCR and nested-PCR (nPCR) amplification .....	38
6.3 Effect of PCR components to GO-based PNA probe.....	39
6.4 The optimization of GO.....	39
6.5 The fluorogenic detection for dsDNA of PCR reaction .....	39
7. The isothermal detection of dsDNA by RPA-DPG assay .....	39
7.1 The optimization of RPA .....	40
7.2 The determination of optimal GO.....	40
7.3 The detection of dsDNA by RPA-DPG assay .....	40
7.4 Specific <i>E. canis</i> detection.....	41
7.5 Sensitive detection for <i>E. canis</i> .....	41
7.6 PAGE analysis .....	41
7.7 Clinical samples .....	41

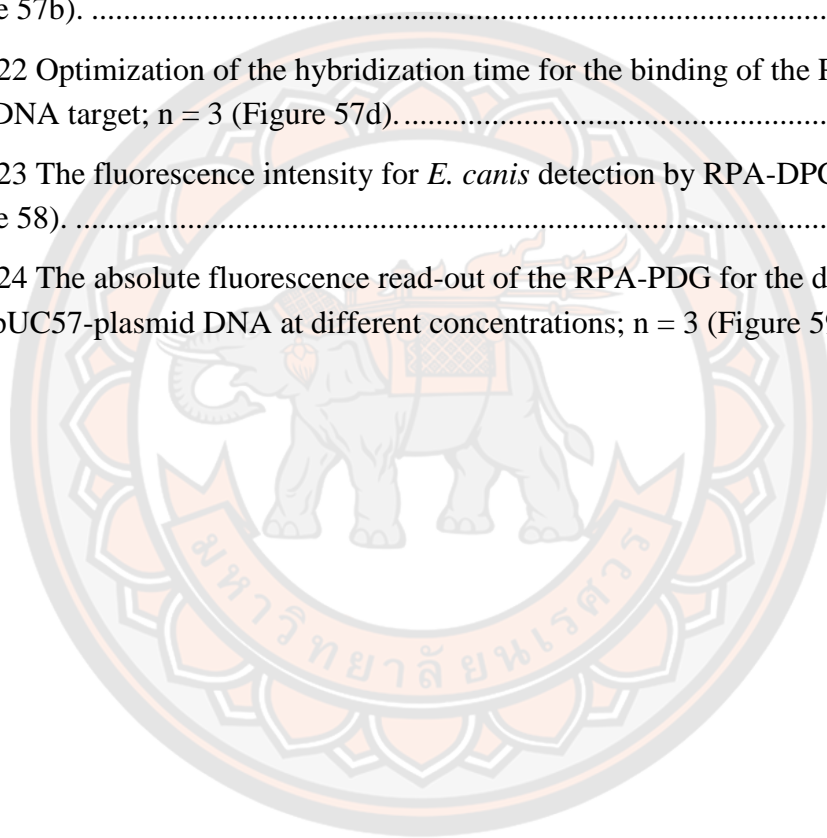


CHAPTER IV RESULTS AND DISCUSSION .....	42
Design of primers and pyrrolidinyl PNA probe .....	42
The detection of ssDNA by PNA probe in the GO platform.....	45
1. Fluorescence stability of PNA probe in Tris-HCl buffer .....	45
2. Fluorescence quenching ability of GO to Flu-labeled pyrrolidinyl PNA .....	47
3. The sequence specificity of PNA probe in the GO platform .....	50
4. The sensitivity DNA detection by PNA probe in the GO platform .....	53
The preliminary study for dsDNA detection .....	55
1. Effect of PCR components .....	55
2. The detection of dsDNA (PCR product) by PNA probe in the GO platform.....	58
2.1 Specificity of primers .....	58
2.2 Detection of dsDNA obtained from PCR.....	60
Isothermal detection for dsDNA by RPA-DPG assay .....	63
1. The optimization of the RPA reaction process.....	64
2. dsDNA detection by RPA-DPG assay .....	65
2.1 The optimization for the DNase I-treatment .....	66
2.2 Specificity.....	69
2.3 Sensitivity.....	70
2.4 Clinical samples .....	72
CHAPTER V CONCLUSION.....	75
REFERENCES .....	76
APPENDIX.....	81
BIOGRAPHY .....	102

## LIST OF TABLES

	<b>Page</b>
Table 1 16S rRNA genes used for primer and probe designs.....	29
Table 2 The stock solutions and related reagents in SPPS. ....	33
Table 3 Reverse-phase HPLC program. ....	36
Table 4 All sequences of primer and pyrrolidinyl PNA probe used in this study. ....	42
Table 5 PNA and Oligonucleotide sequences in the sequence-specific study.....	50
Table 6 The experiment setup for studying of PCR reagent-induced PNA desorption. .....	56
Table 7 DNA primers in PCR and nPCR amplification. ....	59
Table 8 Several methods for DNA detection by fluorogenic nucleic acid-GO system .....	71
Table 9 Fluorescence read-out of PNA in Tris-HCl buffer (Figure 39a-b). ....	85
Table 10 Fluorescence emission data of PNA in Tris-HCl buffer with different concentration of GO (Figure 41a-b). ....	86
Table 11 Average percentage of fluorescence quenching (%Q) of PNA in Tris-HCl buffer with different concentrations of GO for 1 hour (Figure 41c).....	87
Table 12 Average percentage of fluorescence quenching (%Q) of PNA-GO complex (200 nM: 10 µg/mL) in Tris-HCl buffer decreased over time (Figure 41c).....	87
Table 13 Fluorescence emission data for specific ssDNA detection by pre-mixing DNA with PNA before adding GO (Figure 43a-b).....	88
Table 14 Fluorescence emission data for specific ssDNA detection by post-mixing DNA with PNA-GO complex (Figure 43c-d).....	89
Table 15 Fluorescence emission data for sensitive ssDNA detection of PNA1-GO complex (Figure 44a).....	90
Table 16 Fluorescence emission data for sensitive ssDNA detection of PNA2-GO complex (Figure 44b).....	91
Table 17 The linearity range of relative fluorescence intensities at 530 nm ( $F_{530nm}$ ) and concentration of DNA1 of PNA/GO system towards targeted ssDNA detection (Figure 41c-d). ....	92

Table 18 Average fluorescence intensities of PNA-GO complex in PCR reaction-solution; n = 3 (Figure 47). .....	92
Table 19 Fluorescence intensity of PNA1 in PCR reaction-solution with different concentrations of GO which was re-determined and their percentage of fluorescence quenching (Figure 49). .....	93
Table 20 The percentage of fluorescence quenching (%Q) of 10 pmol PNA1 when adding different amounts of GO in range of 0-9.6 $\mu$ g; n = 3 (Figure 57a). .....	93
Table 21 Measured fluorescence for the detection of targeted RPA products; n = 3 (Figure 57b). .....	93
Table 22 Optimization of the hybridization time for the binding of the PNA probe to the dsDNA target; n = 3 (Figure 57d). .....	94
Table 23 The fluorescence intensity for <i>E. canis</i> detection by RPA-DPG assay; n = 3 (Figure 58). .....	94
Table 24 The absolute fluorescence read-out of the RPA-PDG for the detection of <i>E. canis</i> pUC57-plasmid DNA at different concentrations; n = 3 (Figure 59). .....	94



## LIST OF FIGURES

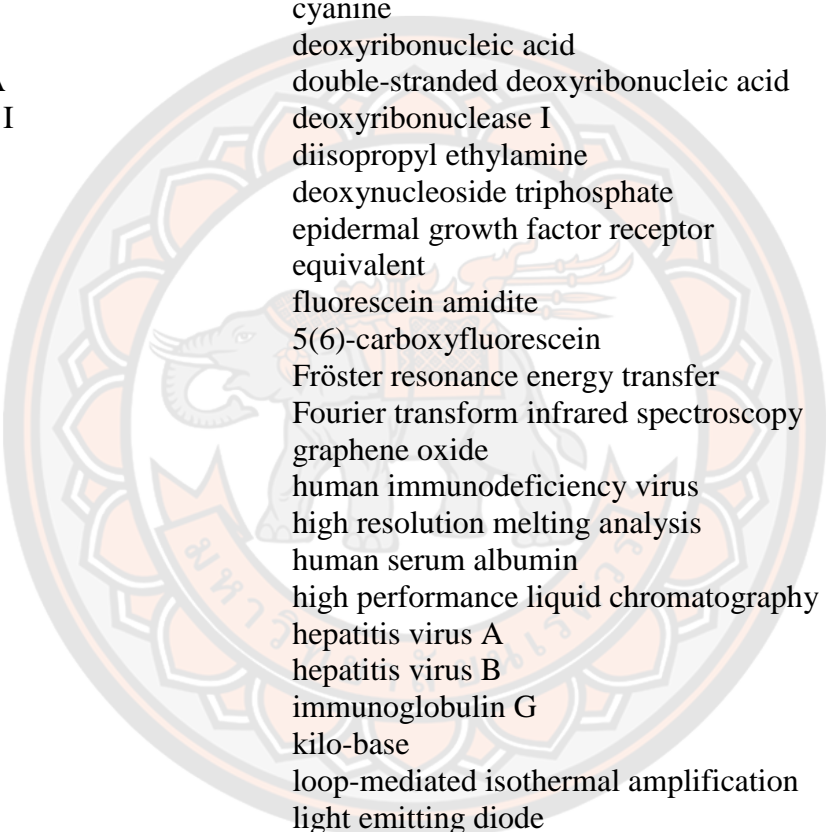
	<b>Page</b>
Figure 1 Structures of (a) DNA, (b) aegPNA, and (c) acpcPNA.....	1
Figure 2 Schematic illustration of GO-based nucleic acid probe for DNA detection. ....	2
Figure 3 The worldwide distribution of CME ( <a href="https://cvbd.bayer.com">https://cvbd.bayer.com</a> ). ....	3
Figure 4 Schematic illustration of recombinase polymerase amplification (RPA). ....	4
Figure 5 Schematic illustration of the detection of <i>E. canis</i> 16S rRNA gene by the combination of RPA, GO-based fluorescent-labeled pyrrolidiny PNA and DNase I treatment as RPA-DPG assay. ....	5
Figure 6 Schematic illustration of graphene derivatives.....	7
Figure 7 The MD simulation of FAM-tagged ssDNA and dsDNA with GO.....	8
Figure 8 Schematic illustration for studying the several effects of DNA/GO desorption.....	9
Figure 9 The possibilities of binding mode between a GO-adsorbed DNA probe and its complementary DNA. ....	10
Figure 10 The study of hybridization kinetics. ....	11
Figure 11 Schematic illustration of the addition of complementary or non-complementary pdsDNA into F-ssDNA-GO complex and fluorescence intensity variations for (A) 10 $\mu\text{g/mL}$ and (B) 3 $\mu\text{g/mL}$ of GO. ....	12
Figure 12 Schematic illustration for BSA blocking to prevent (a) the nonspecific adsorption of PNA on a hydrophobic surface, and (b) PNA-DNA duplex on GO surface. ....	13
Figure 13 Fluorescence spectra of Fluorescein-labeled PNA in GO solution in the (a) absence and (b) presence of 0.01% BSA. ....	13
Figure 14 Schematic illustration for target-induced fluorescence changes of the FAM-ssDNA-GO complex.....	14
Figure 15 Fluorescence emission spectra of GO-based fluorogenic assay.....	15
Figure 16 Fluorescence emission spectra of FAM-DNA tagged aptamer in GO platform with (a) the presenting of various concentrations of human thrombin and (b) different proteins.....	15
Figure 17 The multicolor DNA detection in homogeneous solution.....	16

Figure 18 Structure of DNA (I-CF), aegPNA (II-CF), and PCNA (III-, IV-CF) analogs. ....	16
Figure 19 Fluorescence quenching of (a-d) I-CF-IV-CF and its restoration upon adding DNA (V). ....	17
Figure 20 The study of PNA-assembled GO for DNA detection. ....	18
Figure 21 Multiple target detection of three viral genes in a single solution. ....	19
Figure 22 Schematic illustration for miRNA21 detection by the combination of RCA process and PNA probe in the GO platform. ....	20
Figure 23 The specific detection of miRNA21 by the combination of the RCA process and PNA probe in the GO platform. ....	21
Figure 24 (a) Schematic illustration for PCR product detection by GO-based FAM-labeled DNA probe and its fluorescence recovery (%) after PCR clean-up.....	22
Figure 25 Scheme for specific detection of EGFR mutation using the RCA-based fluorogenic PNA probe based on the GO platform. ....	23
Figure 26 The fluorescence signaling of specificity validation using F-DP in the presence of mutant, wildtype, or random DNA as RCAPs.....	24
Figure 27 The fluorescence signaling of sensitivity which was evaluated with various concentration of EGFR mutant DNA. ....	24
Figure 28 The colorimetric DNA detection based on p30 DNA by gold nanoparticles and its corresponding change in the UV-Vis spectrum. ....	25
Figure 29 The detection of <i>E. canis</i> based on the <i>p30</i> gene by LAMP. ....	26
Figure 30 The chemical structure of pyrrolidinyl PNA monomers and spacers.....	30
Figure 31 Schematic illustration for <i>N</i> -Fmoc-T-OPfp synthesis. ....	31
Figure 32 Schematic illustration of <i>N</i> -Fmoc-ACPC-OPfp synthesis. ....	31
Figure 33 Schematic illustration of <i>N</i> -Fmoc-APC(Tfa)-OPfp synthesis.....	32
Figure 34 The general SPPS cycle in PNA synthesis.....	34
Figure 35 The selected region of the 16S rRNA gene of <i>E. canis</i> for designing the sequences of primers and PNA probe.....	43
Figure 36 The snapshot for <i>in silico</i> sequence-specific analysis of the PNA probe....	44
Figure 37 The structure of acpcPNA and apc/acpcPNA probe. ....	45
Figure 38 Schematic illustration of possibly non-specific adsorption occurred between PNA and hydrophobic 96-well plate.....	46

Figure 39 The decreasing of fluorescence signals of (a) PNA1 and (b) PNA2 in Tris-HCl buffer over 1 h period.....	47
Figure 40 Schematic illustration for studying fluorescence quenching of GO to Flu-labeled pyrrolidinyI PNA.....	47
Figure 41 The study of GO-quenching PNA1 and PNA2. ....	49
Figure 42 Schematic illustration of specific ssDNA detection.....	50
Figure 43 The fluorescence emission spectra of specific ssDNA detection by Route A; DNA pre-mixing of (a) PNA1 and (b) PNA2, and Route B; DNA post-mixing of (a) PNA1 and (b) PNA2 in GO platform. ....	52
Figure 44 Schematic illustration for sensitivity ssDNA detection by PNA/GO system. ....	53
Figure 45 The fluorescence emission spectra of (a) PNA1 and (b) PNA2 upon the increasing concentration of DNA1. The linear calibration curve plots between relative fluorescence intensity at 530 nm of (c) PNA1 and (d) PNA2 with different concentrations of DNA1. ....	54
Figure 46 Schematic illustration of the effect of PCR reagents to PNA/GO complex. ....	55
Figure 47 (a) Relative fluorescence intensity of PNA with and without GO in the presence of different PCR reagents and (b) their $F_1 / F_0$ values.....	57
Figure 48 Schematic illustration of PCR reagents induce the release of PNA from the GO surface. (a) The PNA desorbed from GO by forming a hydrogen bonding with formamide or DMSO. (b) The PNA was stabilized into the solution phase by glycerol. ....	57
Figure 49 The re-determination of optimal GO for quenching PNA1 in presence of PCR reaction-components. (a) The relative fluorescence intensities of PNA1 and (b) their %Q upon increasing GO.....	58
Figure 50 Conceptual image of (a) PCR and (b) nested-PCR. ....	59
Figure 51 Gel electrophoretic analysis of PCR products that used F2 and R2 as DNA primers. ....	60
Figure 52 Schematic illustration of GO quenching-based fluorogenic detection of dsDNA obtained from PCR. ....	61
Figure 53 The visual image of GO quenching-based fluorogenic detection of PCR product by the combination of GO-based PNA probe and DNase I treatment.....	62

Figure 54 (a) Gel electrophoresis of nPCR products and (b) fluorescence images based on DNase I-treated PNA/GO system. ....	63
Figure 55 The gel electrophoresis for the optimization of RPA conditions. ....	65
Figure 56 Schematic illustration for <i>E. canis</i> dsDNA detection by RPA-DPG assay in this research. ....	66
Figure 57 The optimization for dsDNA detection based on RPA-DPG assay. ....	68
Figure 58 The specificity of RPA-DPG assay for <i>E. canis</i> detection. ....	69
Figure 59 Sensitivity of RPA-DPG assay for <i>E. canis</i> detection. ....	70
Figure 60 Agarose gel electrophoresis of PCR products using extracted DNA from whole blood as a DNA template. ....	72
Figure 61 Agarose gel electrophoresis of RPA products using extracted DNA from whole blood as a DNA template. ....	73
Figure 62 (a) Fluorescence intensity of RPA-DPG assay for the detection of <i>E. canis</i> DNA samples from dogs' blood and (b) fluorescence images obtained by LED transilluminator. ....	74
Figure 63 RP-HPLC chromatogram of PNA1. The product was observed at 31.9 min with the presence of two peaks corresponding to the 5(6)-isomers of fluorescein. ....	82
Figure 64 RP-HPLC chromatogram of PNA2. The product was observed at 30.0 min with the presence of two peaks corresponding to the 5(6)-isomers of fluorescein. ....	82
Figure 65 MALDI-TOF spectrum of PNA1. (calculated $[M+H]^+$ 3810.064, found 3811.282). ....	83
Figure 66 MALDI-TOF spectrum of PNA2. (calculated $[M+H]^+$ 3813.028, found 3812.985). ....	83
Figure 67 (a) $T_m$ analysis of PNA1·DNA1 (targeted DNA) in 0.1 M phosphate buffer pH 7.0 and (b) first-derivative curve showed $T_m = 59^\circ\text{C}$ . ....	84
Figure 68 (a) $T_m$ analysis of PNA2·DNA1 (targeted DNA) in 0.1 M phosphate buffer pH 7.0 and (b) first-derivative curve showed $T_m = 55^\circ\text{C}$ . ....	84

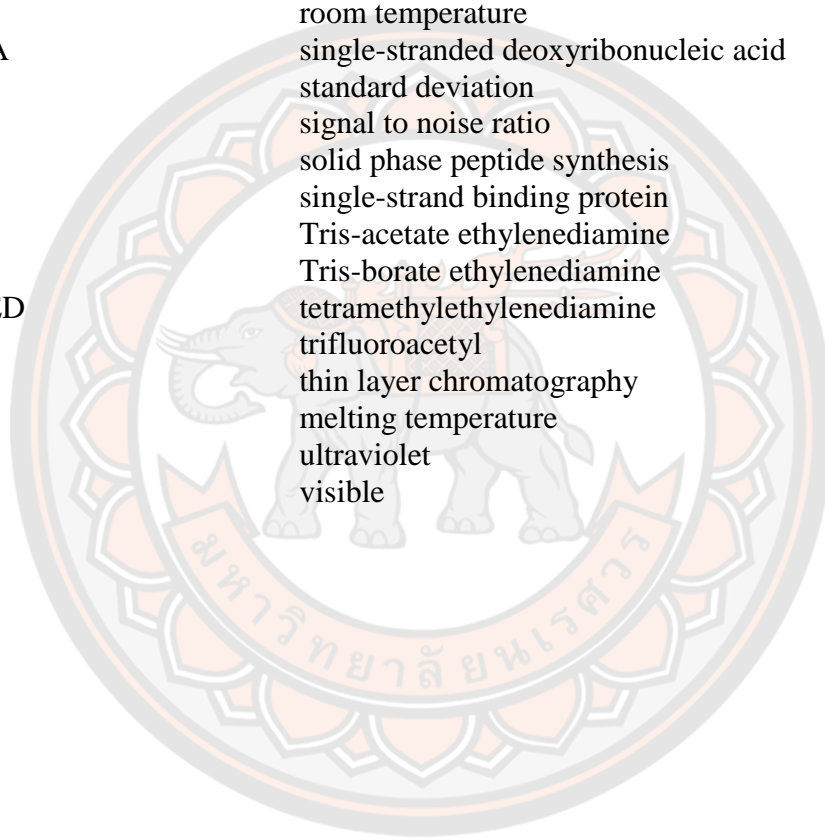
## LIST OF ABBREVIATIONS



ACPC	aminocyclopentane carboxylic acid
aegPNA	aminoethylglycine peptide nucleic acid
APC	aminopyrrolidine carboxylic acid
APS	ammonium persulfate
ATR	attenuated total reflection
BSA	bovine serum albumin
CME	canine monocytic ehrlichiosis
Cy	cyanine
DNA	deoxyribonucleic acid
dsDNA	double-stranded deoxyribonucleic acid
DNase I	deoxyribonuclease I
DIEA	diisopropyl ethylamine
dNTP	deoxynucleoside triphosphate
EGFR	epidermal growth factor receptor
equiv	equivalent
FAM	fluorescein amidite
Flu	5(6)-carboxyfluorescein
FRET	Fröster resonance energy transfer
FT-IR	Fourier transform infrared spectroscopy
GO	graphene oxide
HIV	human immunodeficiency virus
HRM	high resolution melting analysis
HSA	human serum albumin
HPLC	high performance liquid chromatography
HVA	hepatitis virus A
HVB	hepatitis virus B
IgG	immunoglobulin G
kb	kilo-base
LAMP	loop-mediated isothermal amplification
LED	light emitting diode
LOD	limit of detection
LNA	lock nucleic acid
MALDI-TOF	matrix-assisted laser desorption/ionization
MB	molecular beacon
miRNA	micro ribonucleic acid
MHz	megahertz
NMR	nuclear magnetic resonance
nPCR	nested polymerase chain reaction
PAGE	polyacrylamide gel electrophoresis
PCNA	polycarbamate nucleic acid
PCR	polymerase chain reaction
pdsDNA	partially complemented ssDNA of dsDNA
PEG	polyethylene glycol
Pfp	pentafluorophenyl



PNA	peptide nucleic acid
Q	quenching
RCA	rolling cycle amplification
RCAP	rolling cycle amplification product
RCT	rolling cycle template
RDP	ribosomal database project
RNA	ribonucleic acid
ROX	carboxy-X-rhodamine
RPA-DPG	recombinase polymerase amplification in combination with DNase I treatment and PNA probe in GO platform
rRNA	ribosomal ribonucleic acid
RT	room temperature
ssDNA	single-stranded deoxyribonucleic acid
SD	standard deviation
S/N	signal to noise ratio
SPPS	solid phase peptide synthesis
SSB	single-strand binding protein
TAE	Tris-acetate ethylenediamine
TBE	Tris-borate ethylenediamine
TEMED	tetramethylethylenediamine
Tfa	trifluoroacetyl
TLC	thin layer chromatography
$T_m$	melting temperature
UV	ultraviolet
Vis	visible



# CHAPTER I

## INTRODUCTION

### Peptide nucleic acid and graphene oxide

For three decades, the first peptide nucleic acid (PNA) has been reported by P.E. Nielsen's research group since the 90s.<sup>1</sup> PNA is a nucleic acid mimic in which sugar-phosphate backbone is replaced completely by nucleobase-substituted *N*-2-aminoethyl glycine (aeg) scaffold (as shown in **Figure 1b**). This aegPNA shows a high affinity to targeted DNA *via* Watson-Crick base-pairing recognition. It readily salt-independent hybridizes to complementary sequence with high thermal stability rather than natural nucleic acid due to lacking electrostatic repulsion.<sup>2</sup> The other outstanding properties are, such as high stability under acid-base conditions as well as enzymatic degradation.<sup>3</sup> So, aegPNA was considerably studied and developed by modifying the chemical structure to improve the properties and apply them in various-biological fields. In practical uses as nucleic probes, the flexibility of hydrophobic PNA backbone becomes the majority of a problem because it usually found the self-hybridization or folding characteristic, leading to aggregation in aqueous-based solution and obstruction for application use.

In 2001-2005, a novel conformational-constrained pyrrolidinyl PNA has been developed by Vilaivan's research group. The chemical structure comprises the alternated sequence of (*4R*)-nucleobase-substituted proline monomer which is linked by (*1S,2S*)-2-aminocyclopentane carboxylic acid spacer (so called acpcPNA).<sup>4,5</sup> This rigid conformation exhibits the stable binding to targeted DNA and forming a PNA·DNA helix in a sequence-specific manner (only antiparallel direction mode) with a melting temperature ( $T_m$ ) higher than flexible aegPNA. Additionally, acpcPNA indicates a low tendency towards self-hybridization and aggregation, exclusively base-mismatched discrimination.<sup>5-7</sup> Hence, acpcPNA has been adopting extensively as miscellaneous tools in DNA sensor applications, for example, SNP genotyping,<sup>8</sup> fluorogenic probes,<sup>9,10</sup> paper-based colorimetric DNA sensors,<sup>11,12</sup> and cell imaging.<sup>13</sup>

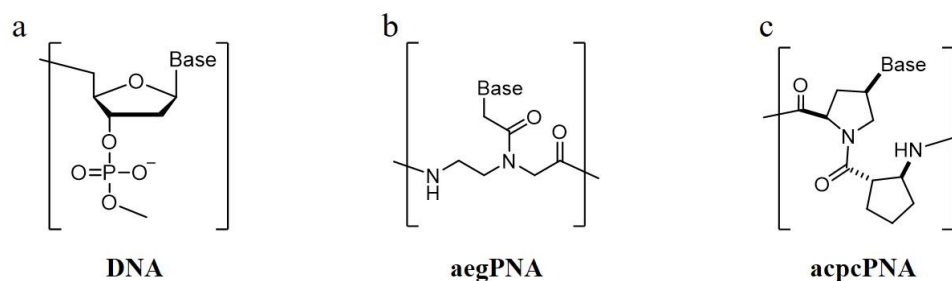


**Figure 1 Structures of (a) DNA, (b) aegPNA, and (c) acpcPNA.**

In the development of a nucleic acid probe as a DNA sensor, various types of the probe have been reported as molecular beacon (MB), Fröster Resonance Energy Transfer (FRET) probe, nucleic acid-template reaction, and light-up probe with an external quencher. MB is a hairpin-loop with dual-labeling of the reporter and quencher at both ends of the complementary-stem sequence. FRET is a tool for the detection of nucleic acid sequences by a pair of fluorescent probes placed nearby in appropriate distance. When probes bind with targeted DNA (template DNA), an excited electron (by light) of donor fluorophore transfers its energy to an acceptor fluorophore during FRET or occurs reaction between two molecules, resulting in a new reporter-compound. In recent years, graphene and its derivatives especially graphene oxide (GO) has been reported as an external quencher to quenching fluorescence of light-up probe. The advantages of graphene oxide are easy to prepare and cheaper than other commercial quenchers. GO is one of the graphene derivatives with bearing epoxy, hydroxyl, and carboxyl groups. An oxygenated carbon sheet is generated by oxidizing graphene following with exfoliation.<sup>14</sup> It shows a long-range absorption, excellent aqueous processability, and amphiphilicity that making GO as a useful material in biosensor research particularly in the nucleic acid detection field.<sup>15,16</sup> As displayed in **Figure 2**, the strong interaction between unpaired nucleobases of single-stranded (ss) nucleic acid probe and GO surface contributes to the adsorption process, leading to quenching emission signals of tagged-dye *via* FRET principle.<sup>17</sup> For the double-stranded (ds) molecule, nucleobases are paired and effectively hidden in a helical structure, preventing the directed adsorption that fluorescence would be remained or recovered. On the other hand, in the case of a non-targeted sequence, the unbound probe would simultaneously be adsorbed on the GO surface by  $\pi$ - $\pi$  stacking, hydrophobic interaction, and hydrogen bonding, resulting in a quenching fluorescence of the tagged dye.<sup>18</sup> Therefore, this simple platform has been used in a fluorogenic assay for DNA detection, for instance, multicolor ssDNA detection,<sup>19,20</sup> RNA imaging,<sup>21</sup> and amplified DNA detection.<sup>22-24</sup>

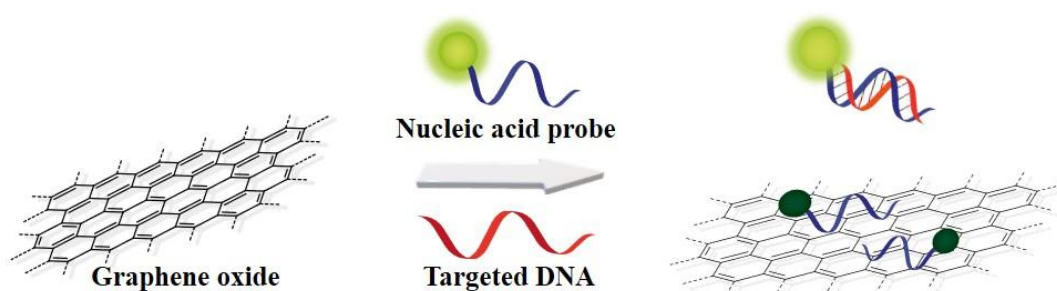


**Figure 2** Schematic illustration of GO-based nucleic acid probe for DNA detection.

### The identification of *Ehrlichia canis*

Canine Monocytic Ehrlichiosis (CME) is a major infectious disease in dogs with worldwide distribution (**Figure 3**). It is caused by *Ehrlichia canis* (*E. canis*) which is carried on brown dog tick (*Rhipicephalus sanguineus*) as a vector-borne.<sup>25</sup> *E. canis* is a small, highly pleomorphic shape and gram-negative bacteria, belonging to the family *Anaplasmataceae*.<sup>26</sup> It could be transmitted into canine monocytes *via* a bite of the all-state tick carrier (larvae, nymphs, or adults). Typically, clinical signs are commonly associated with hypothermia, loss of appetite, weight loss, or death in severe cases. However, stray dogs often remain subclinical regular carriers for long periods which transport to other regions and developed the disease in years later.<sup>27</sup> For traditional CME diagnosis, cell culture is the most difficult method because it requires a high-level biosafety laboratory and time of cell incubation (2-3 weeks). Meanwhile, serologic detection usually found false-positive testing due to initial-stage results may be negative in dogs, and cross-reactivity possibly presented.<sup>28</sup> Thus, the CME diagnosis with rapidity, sensitivity, specificity, and accuracy is an essential tool for CME identification and prevention of its spreading, particularly in resource limiting fields. For example, the standard-conventional polymerase chain reaction (PCR), has been widely and extensively used for *E. canis* identification based on the amplification of specific DNA such as *16S rRNA*, *trp36*, and *p30*.<sup>29-33</sup>

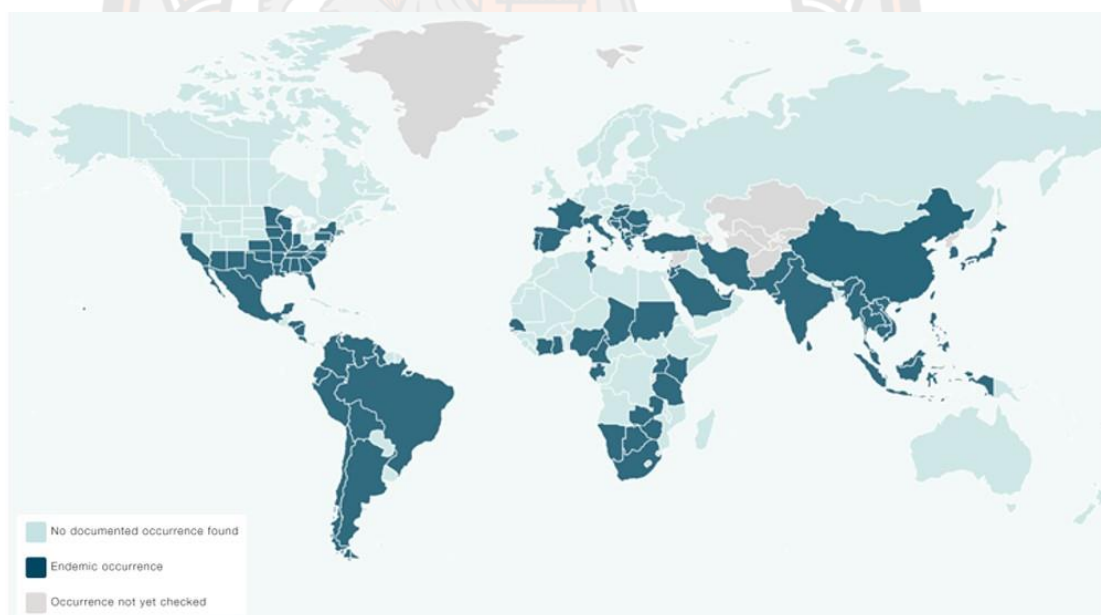


**Figure 3** The worldwide distribution of CME (<https://cvbd.bayer.com>).

In recent years, an advance in molecular detection as isothermal amplification has been developed and become a popular technique instead of PCR amplification because it is easy to set-up, rapidly, and accurately. This assay is not requiring an advanced instrument for reaction-temperature control, for example, loop-mediated isothermal amplification (LAMP), rolling cycle amplification (RCA), and recombinase polymerase amplification (RPA). RPA is an isothermal-enzymatic process to generate a specific fragment of dsDNA by working enzymes consist of recombinase, single-strand binding (SSB) proteins, and DNA polymerase.<sup>34,35</sup> Firstly, the recombinase proteins have interacted with primers, forming recombinase-primer complexes, and invaded within specific regions of the targeted gene. The strand invasion was formed in the D-loop structure, stabilizing by SSB proteins. Second, the synthetic process is performed by DNA polymerase in parental strand separation, providing targeted amplicons as RPA products as shown in **Figure 4**. This amplified DNA could be self-perpetuated to yielding billion copies of the DNA molecule.<sup>36</sup> Moreover, the reaction is carried out at a constant temperature in the range of 35-40°C which is easily operated.

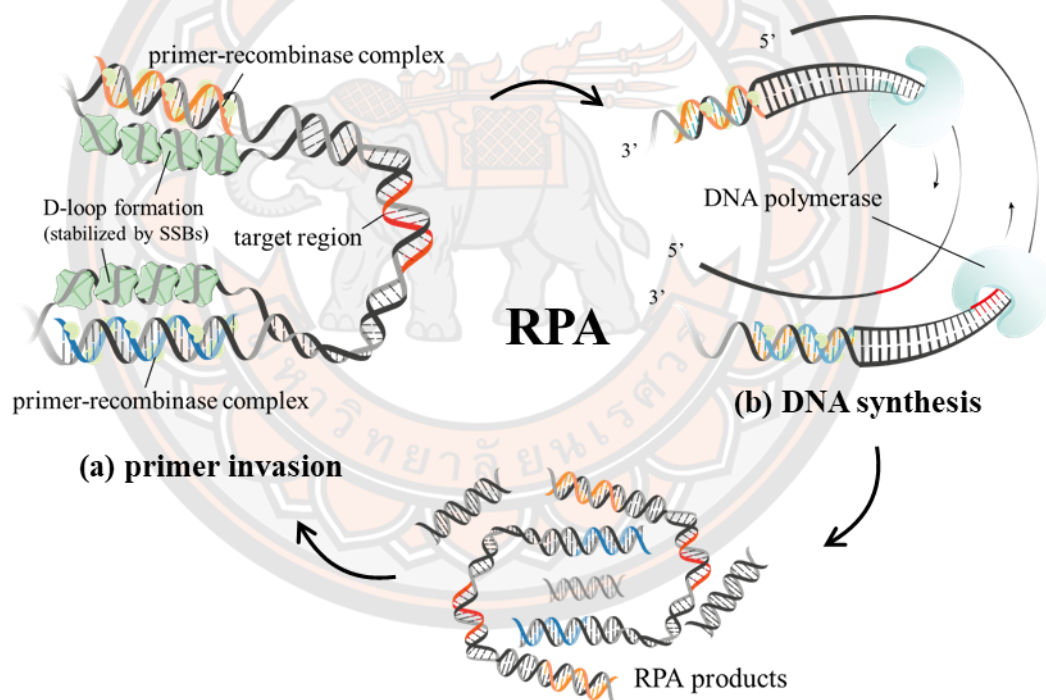


**Figure 4 Schematic illustration of recombinase polymerase amplification (RPA).**

### The combination of RPA and GO-based acpcPNA probe

Recently, the GO-based PNA probe was successfully demonstrated in the detection of ssDNA<sup>20,37</sup> as same as RCA products,<sup>24</sup> and RNA imaging<sup>21</sup> but in the detection of dsDNA has been challenging.<sup>23</sup> Likewise, the combination of RPA and GO-based DNA detection assay by PNA has been not reported yet. RPA can operate at low temperatures using SSB proteins stabilized D-loop formation of PNA·dsDNA invasion strand.<sup>38</sup> Besides, PNA·DNA strand could resist under strong-digested enzyme particularly a deoxyribonuclease (DNase I), whereas non-targeted DNA was simultaneously degraded,<sup>39</sup> contributing to the possibility of methodology for detection of dsDNA by RPA in combination with DNase I treatment and PNA probe in GO platform (RPA-DPG assay). Thus, this research focused on the detection of the *E. canis* 16S rRNA gene by using the combination of RPA and fluorescently labeled pyrrolidinyl PNA in the GO platform. This developed assay is also investigated in association with enzymatic treatment (DNase I) as shown in the overview picture in **Figure 5**.

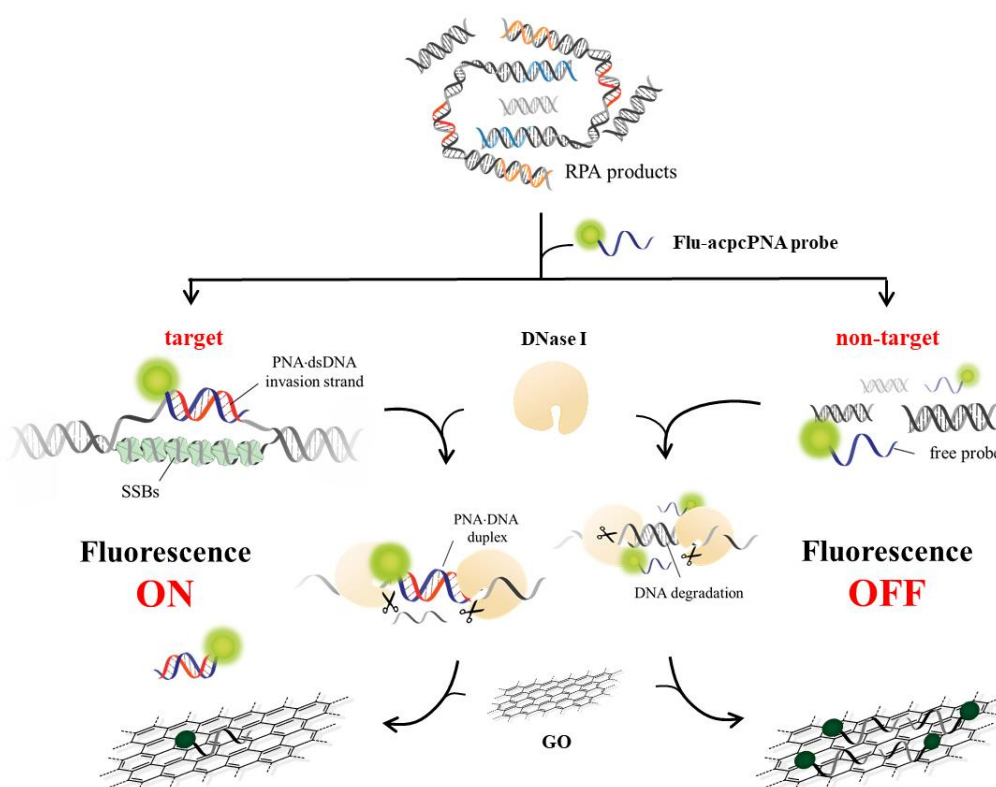


**Figure 5** Schematic illustration of the detection of *E. canis* 16S rRNA gene by the combination of RPA, GO-based fluorescent-labeled pyrrolidinyl PNA and DNase I treatment as RPA-DPG assay.

### Research objectives

1. To design, synthesize, and characterize the conformational-constrained pyrrolidinyl PNA to recognizing the specific-sequence of *E. canis* 16S rRNA gene.
2. To study the capability of the GO-based PNA probe as a DNA sensor for *E. canis* detection based on the amplification of the 16S rRNA gene by RPA.

### Scope of research

The specific-sequence of the PNA probe was designed by *in silico* analysis using a probe match on the RDP-11 database. The pyrrolidinyl PNA was synthesized *via* solid-phase peptide synthesis methodology without structure modification. The 5(6)-carboxyfluorescein was used as a reporting molecule without a modified linker at the *N*-terminus of the pyrrolidinyl PNA probe. GO-based fluorescently labeled PNA probe was employed with synthetic ssDNA and RPA products for assay evaluation. PCR and RPA methods were performed by using plasmid DNA (pUC57) of *E. canis*, *A. platys*, *B. vogeli*, *H. canis* as a DNA template. DNase I treatment was applied in this system for the enhancement of the fluorescent signal. Finally, the fluorescence intensity of assay in small volume was measured on a microplate reader and FAM channel of real-time PCR.

## CHAPTER II

### LITERATURE REVIEWS

Molecular detection especially nucleic acid has been widely used for diagnostic applications to identify or screening the early state of infectious diseases mostly caused by a bacterial pathogen. In the past decades, several methods for nucleic acid detection have emerged, such as amplification, sensor chips, or molecular DNA, RNA, LNA, or PNA probes. These probes are comprising of two parts. Firstly, an oligonucleotide that recognizes a sequence-specific region of the targeted gene, and another is a reporting unit, such as radioactive molecules, organic dyes, antigen, antibody, etc. Herein, literature reviews about the focus on fluorescently labeled nucleic acid or nucleic acid mimic as molecular probes in combination with graphene oxide were reviewed including the concept of method, theory, and applications.

GO is one of those materials prepared by powerful oxidation of graphite and chemical exfoliation (**Figure 6**). GO is easy to process since dispersing in water or other polar solvents. It is also highly hydrophilic and forms stable aqueous colloids to facilitate the assembly of macroscopic structures by simple and cheap solution processes.

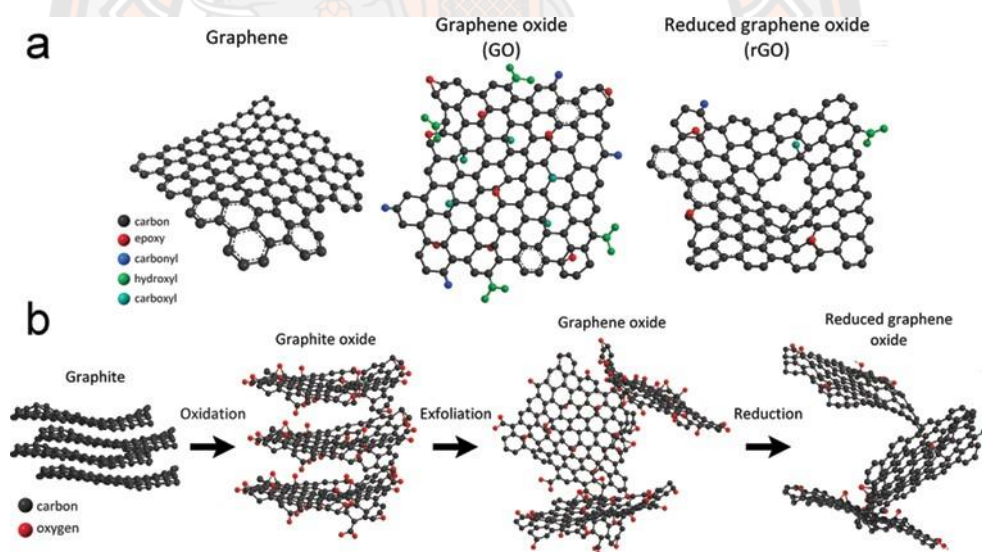


**Figure 6** Schematic illustration of graphene derivatives.

(a) The chemical structures of graphene, graphene oxide, and reduced graphene oxide. (b) Route of graphite to reduce graphene oxide.<sup>40</sup>



### The adsorption-desorption ability of nucleic acid on GO

In 2010, Fan and co-workers<sup>19</sup> reported the utilization of the FAM-labeled DNA/GO system for multicolor DNA detection. Molecular dynamic simulation (MD) was carried to interrogating the observed large discrepancy for interactions between ss- and ds-DNA with GO. **Figure 7**, the snapshot indicated that the nucleobase of ssDNA was formed planar nearby GO surface and stably adsorbed on GO surface *via*  $\pi$ - $\pi$  stacking driving force. Besides, this process has been confirmed by the degree of adsorption measurement. The result showed that very sharp peaks were achieved at  $\sim 3.5 \text{ \AA}$ , indicating the value between GO's carbon atom and functional group of nucleobases closely to van de Waals distance. In contrast, the dsDNA was not stably adsorbed on GO and retained its helical structure. The nucleobase pair was formed inner of duplex and effectively shielded. The snapshot displayed that hydroxyl groups on GO might interact with phosphate groups of dsDNA and observed minimal hydrogen bonding between them.

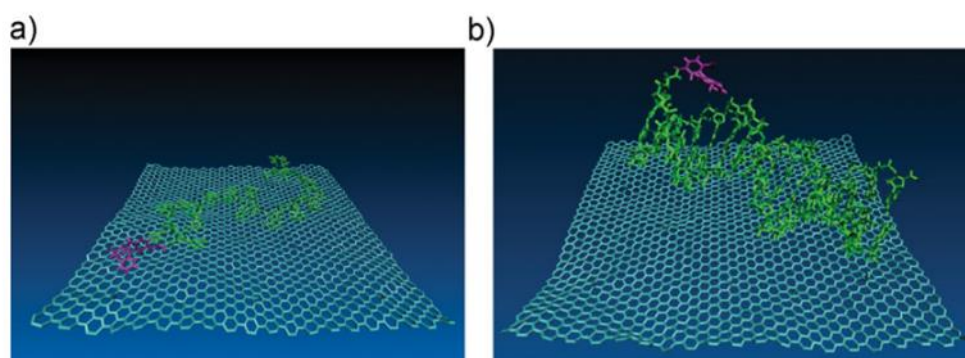


**Figure 7** The MD simulation of FAM-tagged ssDNA and dsDNA with GO. The snapshots, (a) FAM-tagged (red) ssDNA is tightly adsorbed at the GO surface and (b) dsDNA does not adsorb on GO.

In 2011, the effect of DNA adsorption and desorption on GO was reported by Liu and co-workers<sup>41</sup>. The several factors consisting DNA length (12-, 18-, 24-, and 36-mers), pH, salt concentration, and the solvent was studied on the binding between fluorescein-tagged DNA and GO (DNA-GO complex) by adding the complementary DNA (reaction 1), exchanging GO-adsorbed DNA with the same DNA sequence (reaction 2), or increasing temperature to desorb DNA (reaction 3) as shown in **Figure 8**.

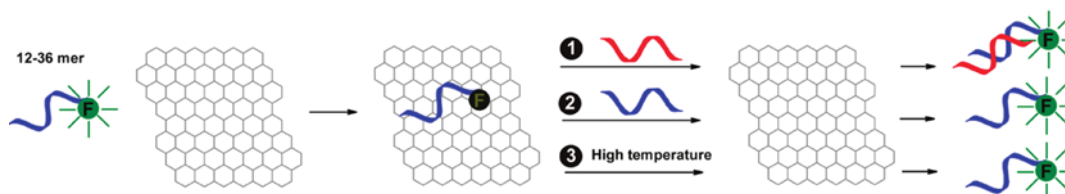


**Figure 8 Schematic illustration for studying the several effects of DNA/GO desorption.**

**The GO-desorbed FAM-ssDNA induced by (1) adding complementary DNA, (2) exchanging DNA-GO complex, and (3) increasing temperature.**

The study of capable FAM-ssDNA absorption on GO revealed that in the presence of salt, the percentage of fluorescent quenching was an increase according to salt concentration and close to 100% at the high ionic strength. On the other hand, the absence of salt stabilization led to reducing the quenching efficiency of all DNA lengths in this study because the polyanion of phosphate-backbone and GO's carboxyl group could be protonated at neutral pH, introducing to the repulsion of anion molecules. Meanwhile, the nucleobases which contain aromatic rings could bind to GO *via* hydrophobic and  $\pi$ - $\pi$  stacking interaction. The electrostatic interaction between DNA (36-mers) and carboxyl groups on the GO surface was also confirmed by employing various pH in the range of 4-8. The results showed that at the low pH (less than 6), the binding efficiency between ssDNA and GO was effectively more than neutral, and high pH respectively.

The investigation of FAM-ssDNA desorption showed that fluorescence has restored rapidly when complementary DNA was added into the saturated ssDNA/GO solution (reaction 1) because when complementary DNA could bind to FAM-ssDNA, the nucleobases of FAM-ssDNA have hidden inside the helical structure and no longer available for surface binding. However, the capability of FAM-ssDNA desorption could be interrupted by free ssDNA exchange (reaction 2), and the observed fluorescence signal was dependent on DNA concentration. Additionally, the thermal desorption study (reaction 3), the fluorescence remained a low value, suggesting that the temperature is ineffective to desorption ability in this study.

In 2013, the mechanism of DNA sensing on graphene oxide was reported by Liu's group.<sup>18</sup> The three possibilities for desorbing DNA probe including Langmuir–Hinshelwood (pathway A), Eley–Rideal (pathway B), and displacement mechanisms (pathway C) were investigated by adding complementary DNA into saturated ssDNA/GO as implied in **Figure 9**. If the reaction follows the Langmuir–Hinshelwood mechanism, the complementary DNA will adsorb on the GO surface firstly and join with a complemented probe to forming a duplex structure. The helix structure can release from the GO surface, resulting in recovering fluorescent signals simultaneously. Second, if the DNA probe directly reacts to complementary DNA in the solution phase (not adsorbed on the GO surface), the reaction is explained by the Eley–Rideal mechanism (Pathway B). Third, displacement mechanism, the complementary DNA readily interacts with the GO surface *via* nonspecific interaction (DNA displaced to probe on GO). Then, some released DNA probe will be hybridized with free complementary DNA in the solution phase (Pathway C).

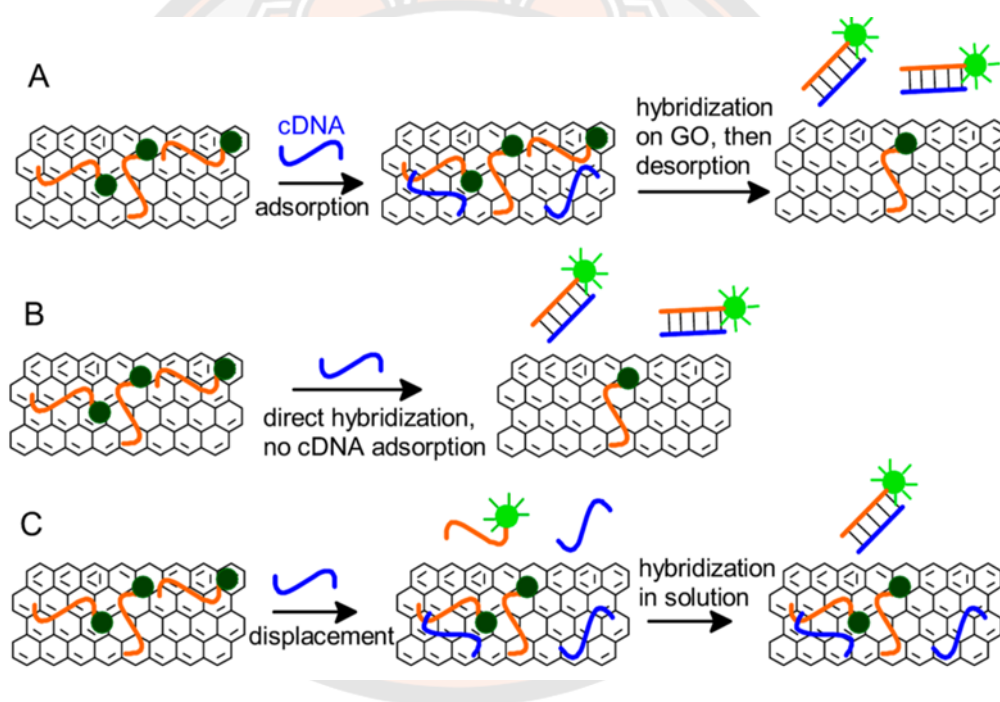


**Figure 9** The possibilities of binding mode between a GO-adsorbed DNA probe and its complementary DNA.

(A) Langmuir–Hinshelwood, (B) Eley–Rideal, and (C) displacement mechanisms.

The FAM-labeled homothymine ( $T_{15}$ ) and homoadenine ( $A_{15}$ ) were employed to study these binding mechanisms. FAM- $T_{15}$  or FAM- $A_{15}$  probe were adsorbed to the GO surface before adding complemented DNA or non-targeted DNA. The results found that only a lower affinity between FAM- $T_{15}/A_{15}$  could be desorbed from the GO surface but the FAM- $A_{15}/T_{15}$  could not release. Because purine bases of the FAM- $A_{15}$  probe are affined strongly with GO. The addition of non-targeted  $A_{15}$  to GO-adsorbed FAM- $A_{15}$ , the fluorescence was efficiently enhanced rather than the addition of targeted  $T_{15}$  pathway, implying that reactions might be the rate-limiting step as the role out of Eley–Rideal and Langmuir–Hinshelwood mechanisms. Therefore, the displacement mechanism is a general conclusion for this DNA/GO system.

Moreover, the investigation of the hybridization rate of nonstructural and MB probes with targeted DNA in the presence and absence of GO indicated in **Figure 10**. In the case of absent GO, the nonstructural DNA probe was readily hybridized with its target, whereas the MB probe was bound in slower (red curves in **Figure 10C** and **10D** respectively). However, in the presence of GO, the kinetic of the hairpin was similar to the previous study (**Figure 10D**, black curve). But the nonstructural DNA as a GO-adsorbed probe displayed a slow kinetic in the binding to its target (**Figure 10C**, black curve). The hybridization rate of MB-DNA with and without GO indicates that the displacement reaction should have a similar rate and GO is not a catalyst for DNA hybridization even when an artificial energy barrier is introduced, proving that the mechanism follows the displacement.

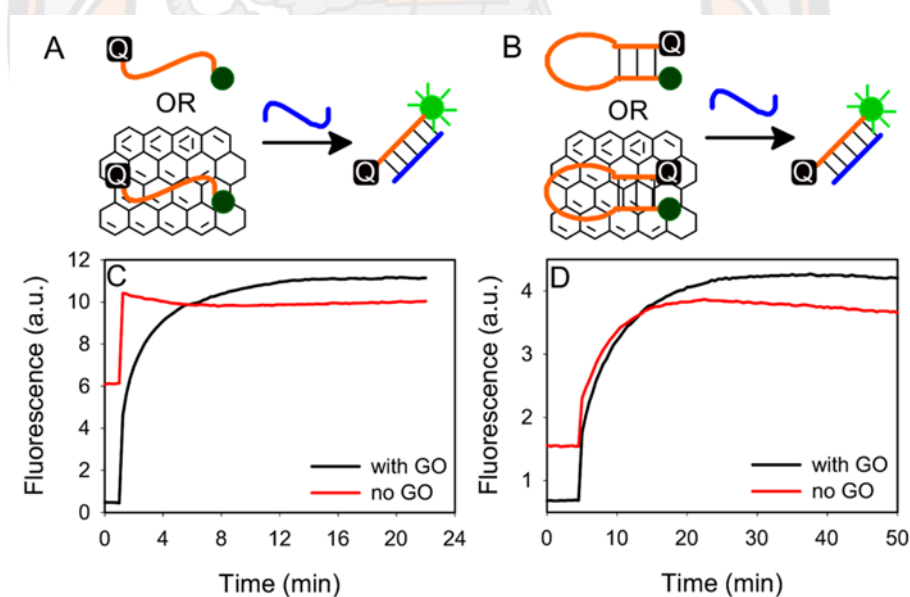


**Figure 10** The study of hybridization kinetics.

Schematic illustration of (A) Nonstructural and (B) MB probe with and without GO to its complemented DNA. (C) Hybridization kinetics for reaction A and (D) reaction B.

In 2014, Kim and co-workers<sup>42</sup> reported the displacement mechanism of GO-based fluorogenic assay by using an F-ssDNA probe that recognizes to partially complemented ssDNA tail of dsDNA (pdsDNA). As displayed in **Figure 11**, when the pdsDNA strand has been added into the F-ssDNA/GO solution at high and low concentrations of GO (10 and 3  $\mu\text{g}/\mu\text{L}$  respectively), the desorption pattern by displacement mechanism was changed in case of high GO concentration. Likewise, the fluorescence signal was not observed yet upon adding the non-complemented pdsDNA because an unbound DNA could be adsorbed with an ample amount of GO. However, at low GO concentration, the fluorescences were presented from F-ssDNA release when adding targeted and non-targeted pdsDNA (**Figure 11B**). These results suggest that this platform is depending on the amount of GO and the dsDNA harboring targeted ssDNA tail is an effective tool to reduce nonspecific adsorption in GO-based fluorogenic assay.

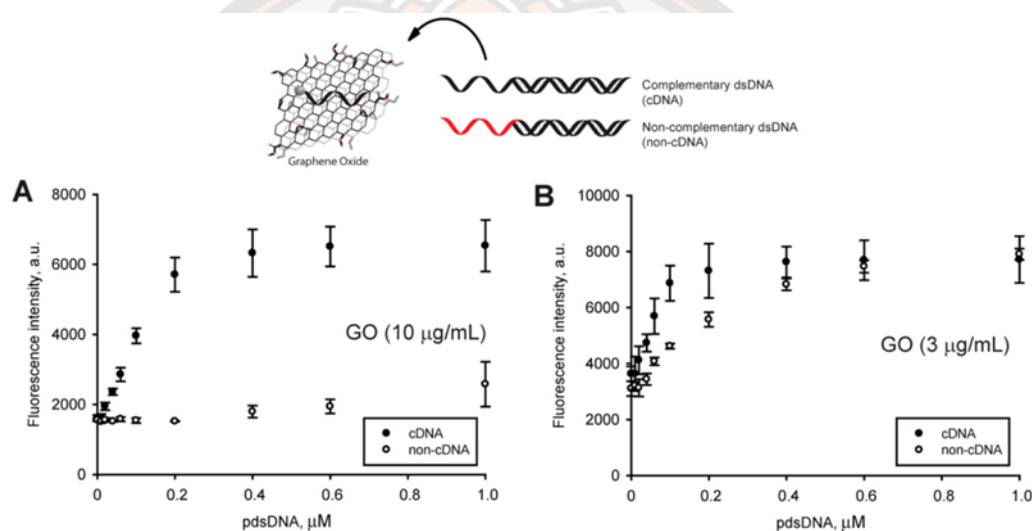


**Figure 11** Schematic illustration of the addition of complementary or non-complementary pdsDNA into F-ssDNA-GO complex and fluorescence intensity variations for (A) 10  $\mu\text{g}/\text{mL}$  and (B) 3  $\mu\text{g}/\text{mL}$  of GO.

In 2015, Min and co-workers<sup>43</sup> reported the critical tool to enhance the stability of the PNA-GO complex by using bovine serum albumin (BSA) as an additive agent. **Figure 12**, PNA consisting of hydrophobic backbone usually occurs non-specific interaction with a hydrophobic surface container. The loss of desorption ability of the PNA-DNA helix strand from the GO surface leads to loss fluorescence restoration of PNA-DNA duplex. In absence of BSA, fluorescence was decreased largely around 91% (**Figure 13**). When employing BSA for GO-based PNA probe assay, the result found that just 0.01% v/v of BSA could stabilize the free PNA significantly with the fluorescent decrease around 18% of the initial fluorescence intensity.

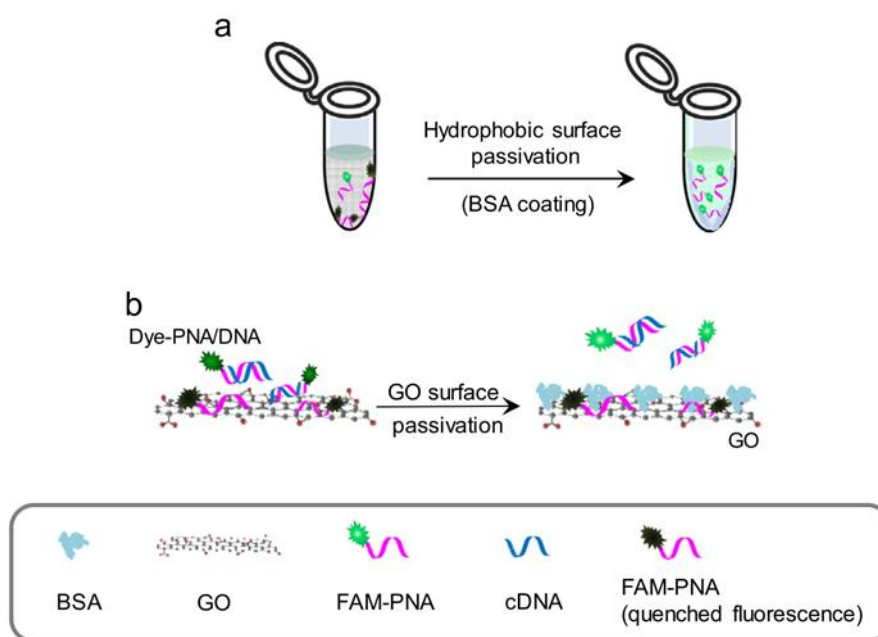


**Figure 12** Schematic illustration for BSA blocking to prevent (a) the nonspecific adsorption of PNA on a hydrophobic surface, and (b) PNA-DNA duplex on GO surface.

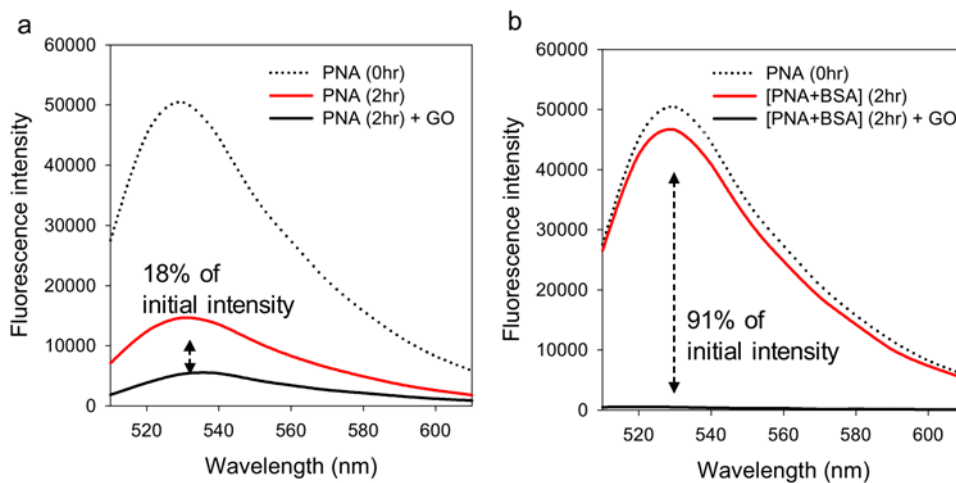


**Figure 13** Fluorescence spectra of Fluorescein-labeled PNA in GO solution in the (a) absence and (b) presence of 0.01% BSA.

### GO-based fluorescent-labeled probe in nucleic acid detection

The graphene platform in biomolecular sensors has emerged firstly in 2009. Yang and co-workers<sup>44</sup> reported the using of FAM-based aptamer-labeled DNA oligonucleotides (P1) to detect the targeted HIV1 in human thrombin (**Figure 14**).

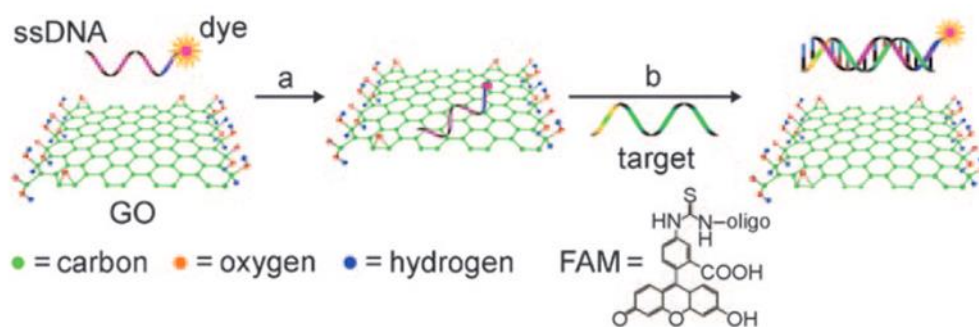


**Figure 14 Schematic illustration for target-induced fluorescence changes of the FAM-ssDNA-GO complex.**

**Figure 15**, the fluorescence spectrum of P1 (a-line) was readily quenched upon adding GO (c-line) which observed the percentage of quenching up to 97%. When complementary-targeted DNA has been added to the P1-GO complex, the fluorescence restoration was presented in the solution (d-line). The inserted graph showed that the fluorescence ( $F/F_0 - 1$ ) were enhanced significantly with logarithms of targeted concentration. The sensitivity and specificity of FAM-DNA linked with human thrombin aptamer were studied by using targeted human thrombin, human serum albumin (HSA), bovine serum albumin (BSA), human IgG, and bovine thrombin. The results, the strong fluorescence intensity was observed in the only presence of targeted-human thrombin with a high  $S/N$  ratio. The limit of detection was achieved at 2.0 nM and exhibiting fluorescence intensity higher than other proteins as shown in **Figure 16**.

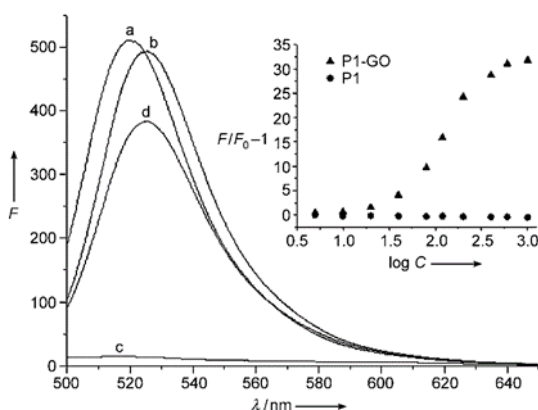


**Figure 15** Fluorescence emission spectra of GO-based fluorogenic assay. The spectra included (a) P1, (b) P1·DNA<sub>HIV1</sub> in Tris-HCl buffer, P1-GO complex and (d) P1·DNA<sub>HIV1</sub> in GO platform. Inserted graph, the fluorescence increases with increasing targeted DNA<sub>HIV1</sub>.

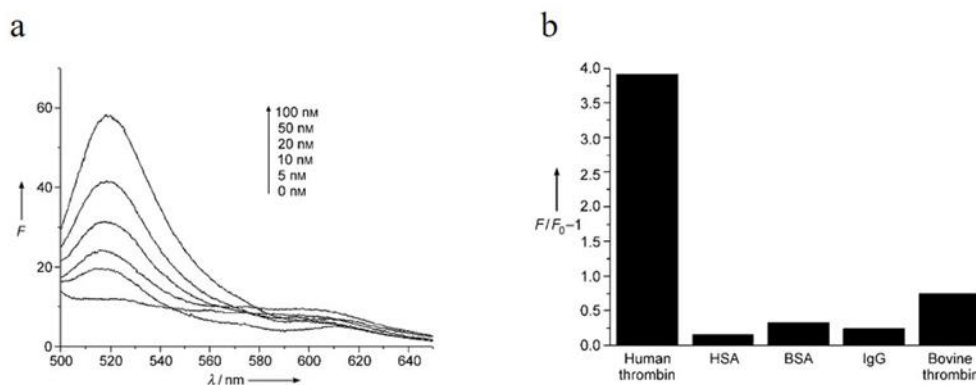


**Figure 16** Fluorescence emission spectra of FAM-DNA tagged aptamer in GO platform with (a) the presenting of various concentrations of human thrombin and (b) different proteins.

In 2010, the multicolor DNA sensor using GO-based DNA probe in a single solution was reported by Fan and co-workers.<sup>19</sup> The probes were labeled with different fluorescence dyes including FAM- (P5), Cy5- (P6), ROX-DNA (P7) towards the detecting its targeted DNA (D5, D6, and D7 respectively), as displayed in **Figure 17**. The representative spectra of probe mixture in the presence of different targets indicated that this assay was high sequence-selectivity observing the emission from corresponding wavelength of T5; blue, T6; red, T7; orange, respectively.



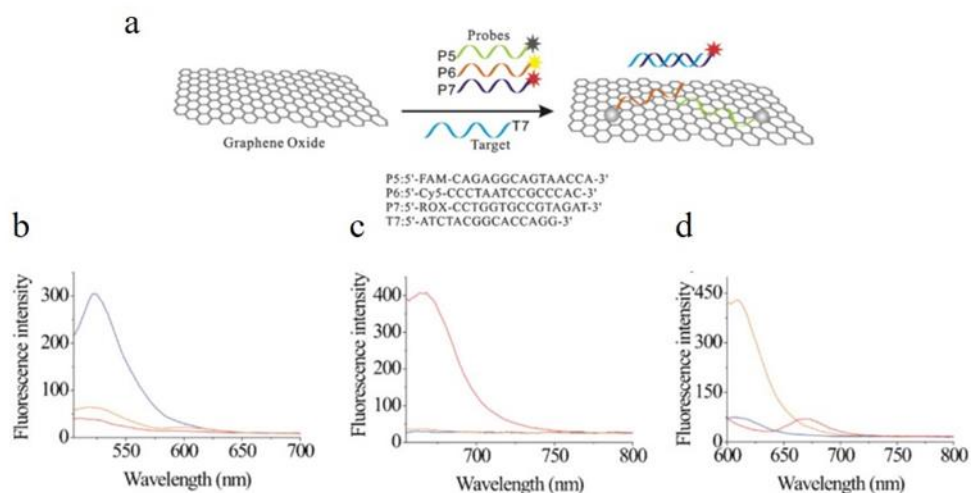


**Figure 17** The multicolor DNA detection in homogeneous solution. (a) Schematic representation of assay, and fluorescence spectra of the mixed probe including P5, P6, P7 in the presence of (b) T5, (c) T6, and (d) T7, respectively.

In 2012, Kumar and co-workers<sup>45</sup> reported a new type of PNA as polycarbamate nucleic acid (PCNA). The conformation of PCNA was designed in two enantiomeric structures as D-, and L-PCNA calls III-CF, IV-CF, and carboxyfluorescein was labeled at the end of the PNA chain. The DNA probe (I-CF), aegPNA (II-CF) with its complementary DNA (V) were included in comparing nucleic acid interaction with GO-based platform (structures as shown in **Figure 18**). The homothymine octamers (T<sub>8</sub>) were synthesized by solid-phase peptide synthesis (SPPS) with attending carboxyfluorescein dye at the N-terminus. The study of thermal stability of PCNA·DNA<sub>target</sub>, showed a strong affinity with high  $T_m$  value (50.1°C for L-isomer, and 56.1°C for D-isomer) rather than original aegPNA (45.0°C).

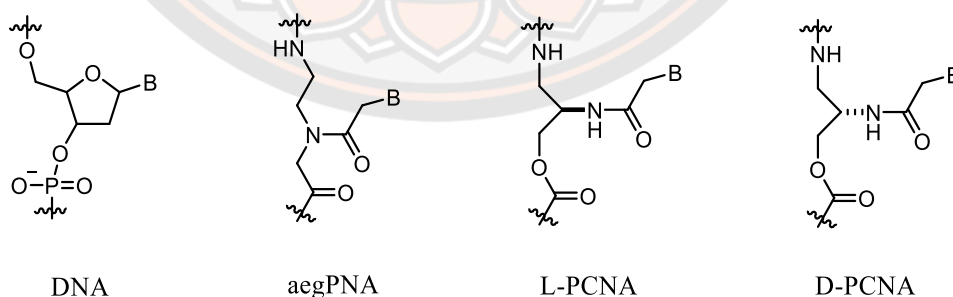


**Figure 18** Structure of DNA (I-CF), aegPNA (II-CF), and PCNA (III-, IV-CF) analogs.

**Figure 19**, the study of fluorescence quenching or restoration of developed PCNAs in the GO platform was demonstrated. The results indicated that the fluorescence of PNAs was quenched instantly (up to 90-95%), whereas the fluorescence quenching of dye-labeled DNA as I-CF was observed less than 20% because the negative charge of phosphate backbone interacted less competently with the GO surface (when compared to uncharged PNA oligomers). When complementary DNA (V) has been added to GO-preadsorbed II-CF, III-CF, and IV-CF as probe-GO complexes, the fluorescence restorations were observed slightly. However, the addition of targeted DNA (5-fold) to PNA solution leads to increase fluorescence up to 40% only IV-CF because DNA (V) could introduce a helical PNA·DNA duplex. Notably, it also binds to the GO surface and therefore fluorescence cannot be restored.

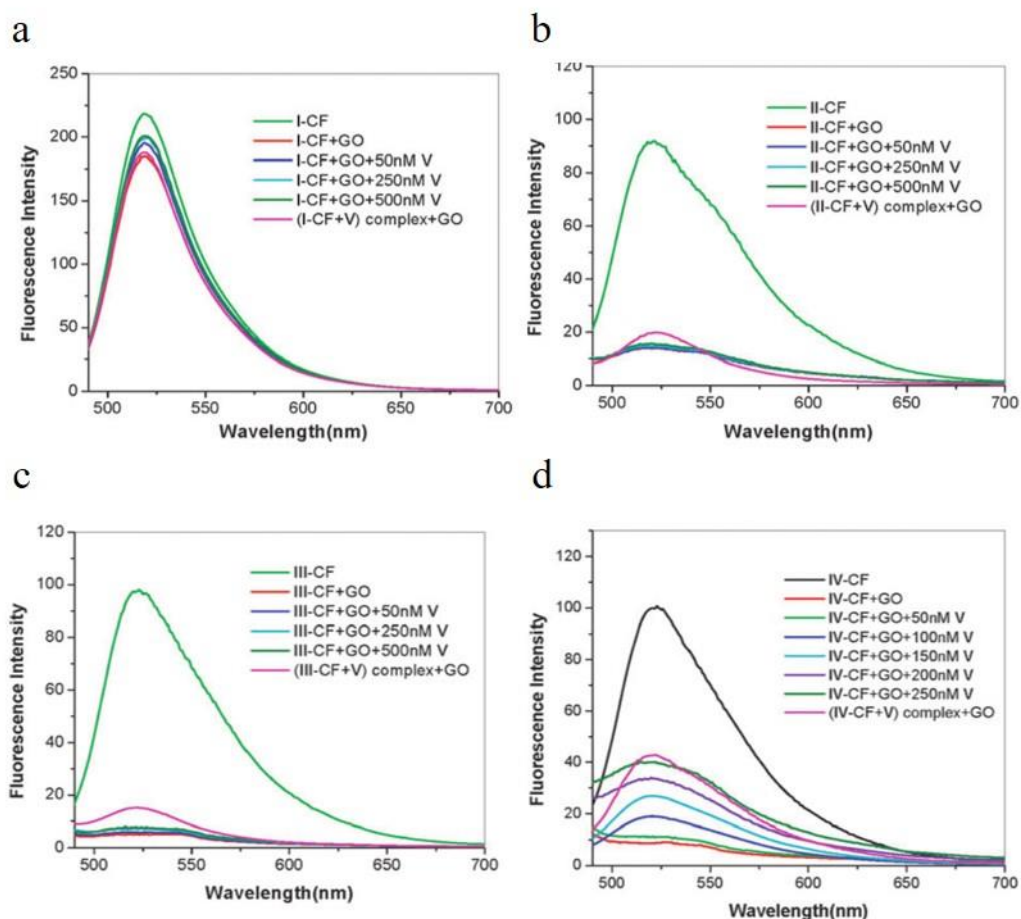


**Figure 19** Fluorescence quenching of (a-d) I-CF-IV-CF and its restoration upon adding DNA (V).

In 2013, Zhang and co-workers<sup>37</sup> reported the PNA-assembled GO for sensitive and selective DNA detection in comparison with the long-chain oligomeric DNA (**Figure 20a**). The study of thermal-induced desorption, when the temperature has been increased (lower than  $T_m$ ), the ability of PNA-DNA desorption from GO surface was enhanced according to increasing temperature (**Figure 20b**). Notably that if the temperature is too high, it makes higher noise (fluorescence of background) because of the dissociation of PNA-GO interaction. The sensitivity and selectivity were also demonstrated. This DNA detection assay was carried out 50 nM of PNA probe with 1.0  $\mu\text{g/mL}$  of GO and various targeted concentrations ranging from 0 nM to 200 nM (**Figure 20c**). The good linear relationship between the relative fluorescence intensity and the different concentration of target was achieved until 50 nM, giving  $y = 1.59x + 63.82$ ,  $R^2 = 0.9831$ , and displaying good detection limit as 800 pM ( $3 \times \text{SD}_{\text{blank}} / \text{slope}$ ). **Figure 20d**, the study of mismatched discrimination found that relative fluorescence intensity ( $F/F_0$ ) of the perfected match was remarkable as a value = 2.70 rather than a single mismatch (1.21) and non-complementary (1.03).

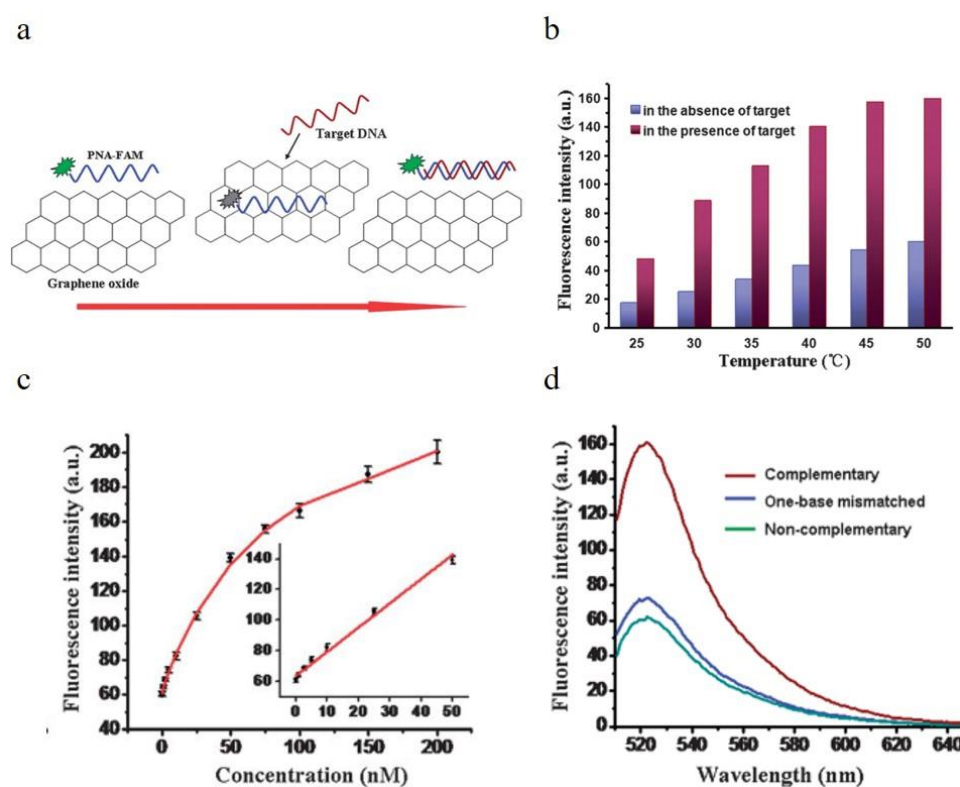


**Figure 20** The study of PNA-assembled GO for DNA detection.

(a) Scheme of the assay. (b) Fluorescence desorption of PNA-assembled GO in the presence and absence of targeted DNA with different temperatures. (c) The relationship between fluorescence intensity and increasing DNA concentration. (d) Fluorescence spectra of an assay in presence of targeted, and mismatched sequences.

In 2014, Min and co-workers<sup>20</sup> reported the GO-based PNA probe as an assay for directly sequence-specific detection of synthetic dsDNA without the denaturation step. Three probes were designed by attending FAM, ROX, and Cy5 and recognizing to its targeted sequences as related to viral diseases including hepatitis A virus Vall7 polyprotein gene (HVA), HIV, and hepatitis B virus surface antigen gene (HVB). The aliquot probe showed emission maxima at 518 nm (green), 608 nm (orange), and 670 nm (red) with excitation at 492 nm, 587 nm, and 650 nm respectively. In a single solution, each targeted dsDNA or the combination was added to probe mixtures, following with the addition of GO. The fluorescence emission spectra were recorded on a microplate reader. The results found that green, orange, and red emission were obtained in the sample contained each corresponding HVA-, HIV-, and HVB-targeted dsDNA (Figure 21).

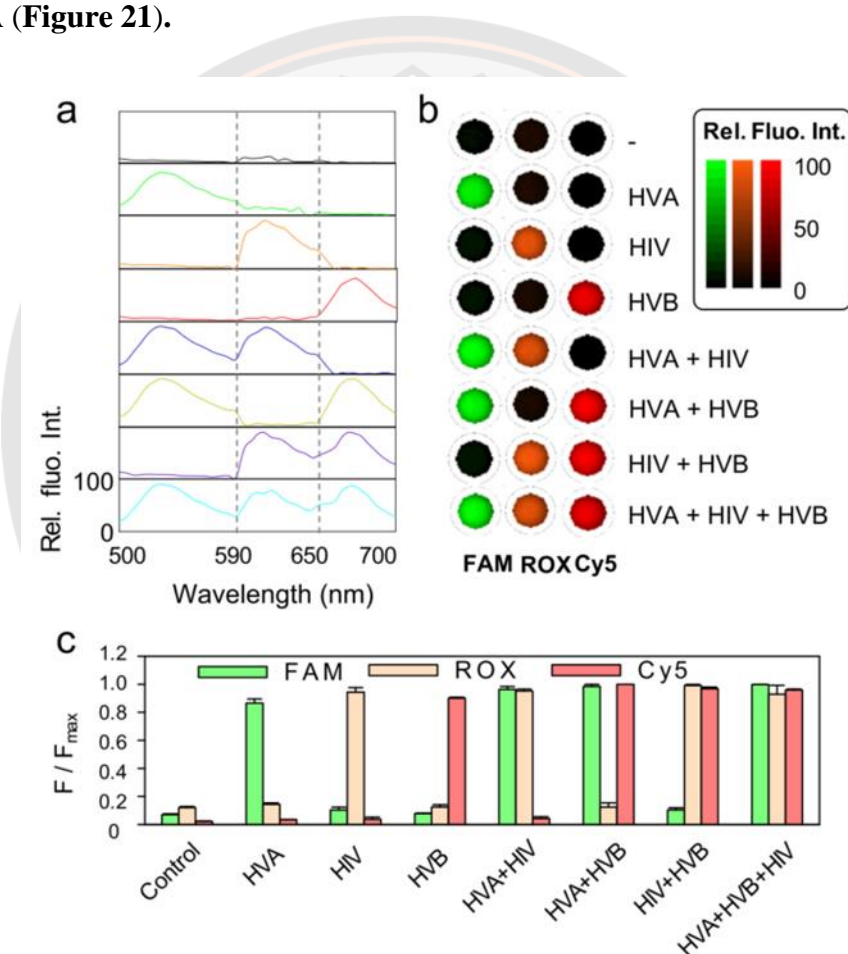


**Figure 21 Multiple target detection of three viral genes in a single solution.** (a) Fluorescence spectra of three dye-labeled PNAs in presence of target dsDNA. (b) Fluorescence images of reaction mixtures for multiple detections. (c) A bar graph, showing the relative fluorescence intensity of three dye-labeled PNAs in the presence of each target dsDNA.

### The combination of GO-based PNA probe with amplification technique

In 2016, Kim and co-workers<sup>24</sup> reported the facility of fluorogenic microRNA (miRNA) detection by using the GO-based PNA probe in combination with the RCA technique. The single-strand RCA product (RCAP) was generated in tandem repeats by RCA which is an isothermal-enzymatic process (**Figure 22**). The padlock DNA as a rolling circle template (RCT) was designed to complementary for both ends of the targeted miRNA. In the case of the present target miRNA, the RCT would be hybridized to target and achieved by the addition of the T4 DNA ligase enzyme, leading to the ligation step. The RCA has been initiated by phi29 DNA polymerase using the circular DNA as the template, and miRNA became the primer for DNA synthesis. The long-chain RCAP harboring the specific-complemented region could be annealed to the F-PNA probe to forming F-PNA/RCAP duplex. When GO has been added, the fluorescence signal also presented that so-called “Fluorescence ON”. On the other hand, in the absence of targeted miRNA, the RCA process could not generate DNA amplicons, leading to quenching fluorescence signal of F-PNA (Fluorescence OFF).

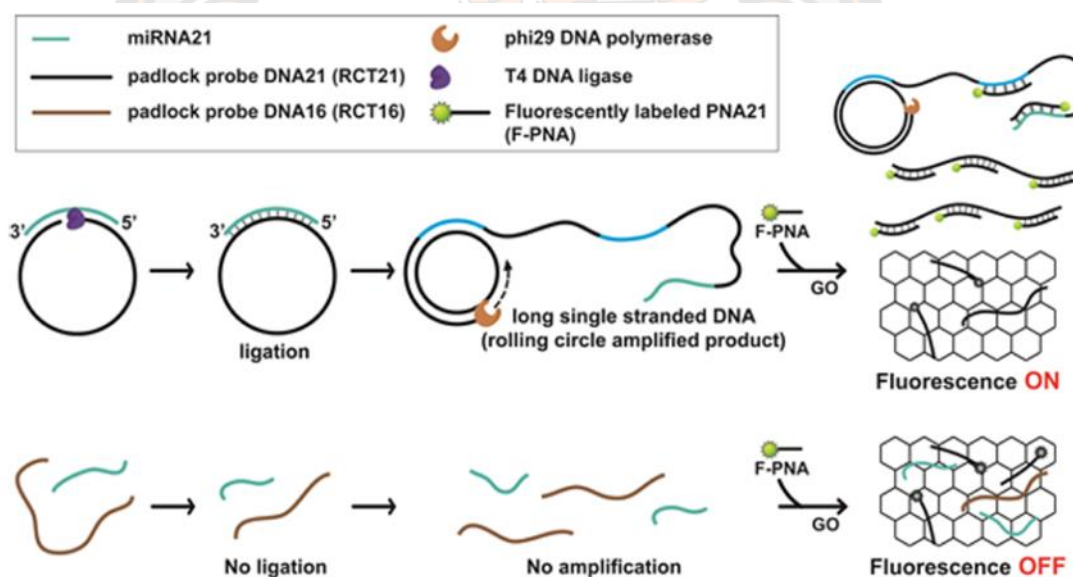


**Figure 22** Schematic illustration for miRNA21 detection by the combination of RCA process and PNA probe in the GO platform.

The assay was demonstrated by using miRNA 21 as a target, single-mismatched miRNA sequences (mismatch G and A), and non-target miRNA (miRNA 16) as shown in **Figure 23a**. The results found that the high molecular weight product and strong fluorescence were observed only in presence of targeted miRNA 21, but not observed in single-mismatched sequences and miRNA 16 (**Figure 23b-c**). Based on this finding, indicating that this combination assay would be a simple and convenient method for the quantitative detection of miRNA.

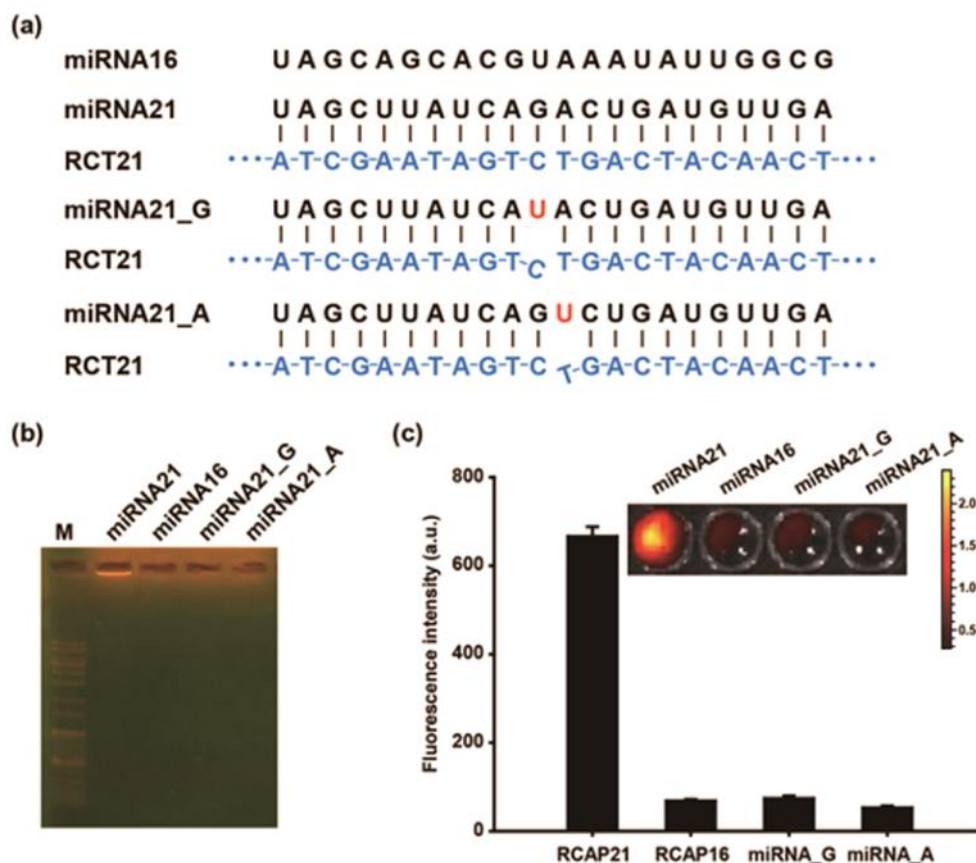


**Figure 23** The specific detection of miRNA21 by the combination of the RCA process and PNA probe in the GO platform.

(a) The miRNA sequences consist of non-target, target, and single-mismatched miRNA in binding with RCT21. (b) The gel electrophoresis of RCAP and (c) its fluorescence in combination with the PNA/GO system.

In 2017, Giuliadori and co-workers<sup>23</sup> reported the sequence-specific detection of dsDNA by using the combination with PCR and GO-based DNA probe (FAM-P) assay. The FAM-P was designed to specifically recognize with the targeted *cspC* gene. In the detection at the end of the PCR process, the probe-mixed amplicons have been denatured firstly, before allowing it to room temperature and adding GO respectively (**Figure 24a**). However, the purification step of PCR products must be required to avoid the non-specific binding that interfered with DNA adsorption on GO. In the absence of PCR primers, the results found that the targeted *cspC* DNA was successfully detected by FAM-P, and presenting fluorescence recovery around 2 folds of mismatched DNA (*cspE*) and 4 folds of non-targeted DNA (*hupA*), respectively (**Figure 25b**).

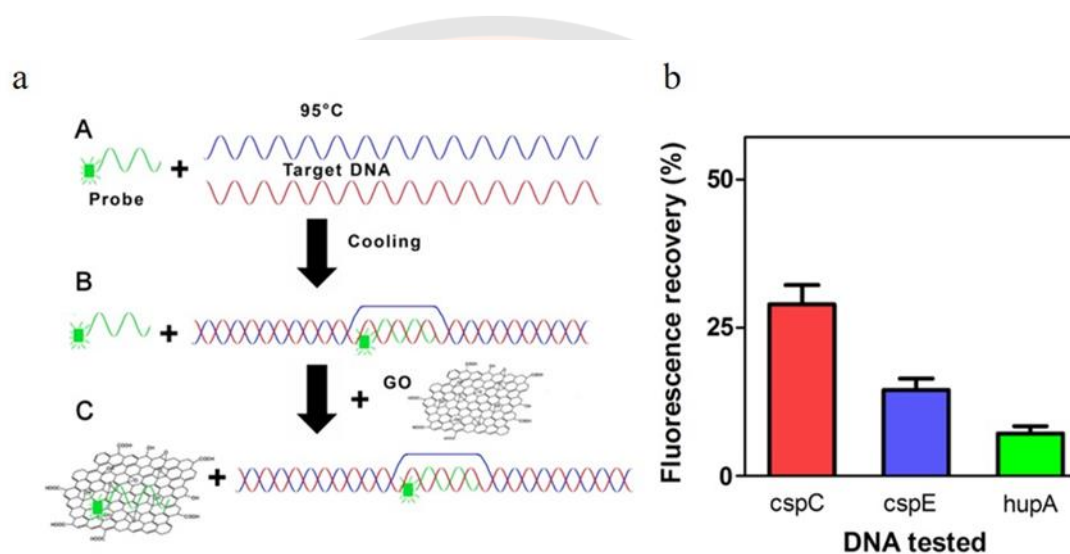


**Figure 24 (a) Schematic illustration for PCR product detection by GO-based FAM-labeled DNA probe and its fluorescence recovery (%) after PCR clean-up.**

In 2019, Zhao and co-workers<sup>46</sup> reported the highly sensitive and specific screening of epidermal growth factor receptor (EGFR) mutation using a PNA microarray-based fluorogenic assay in the GO platform and combination with RCA assay. This assay processes include: firstly, the EGFR gene sequence was efficiently captured by the 96-well surface-embedded PNA probe, secondly, this capped gene was specifically amplified by RCA using the RCA method to provide single-stranded RCA product (RCAP), and finally, RCAP was detected by GO-based fluorescently labeled PNA probe as shown in **Figure 25**.

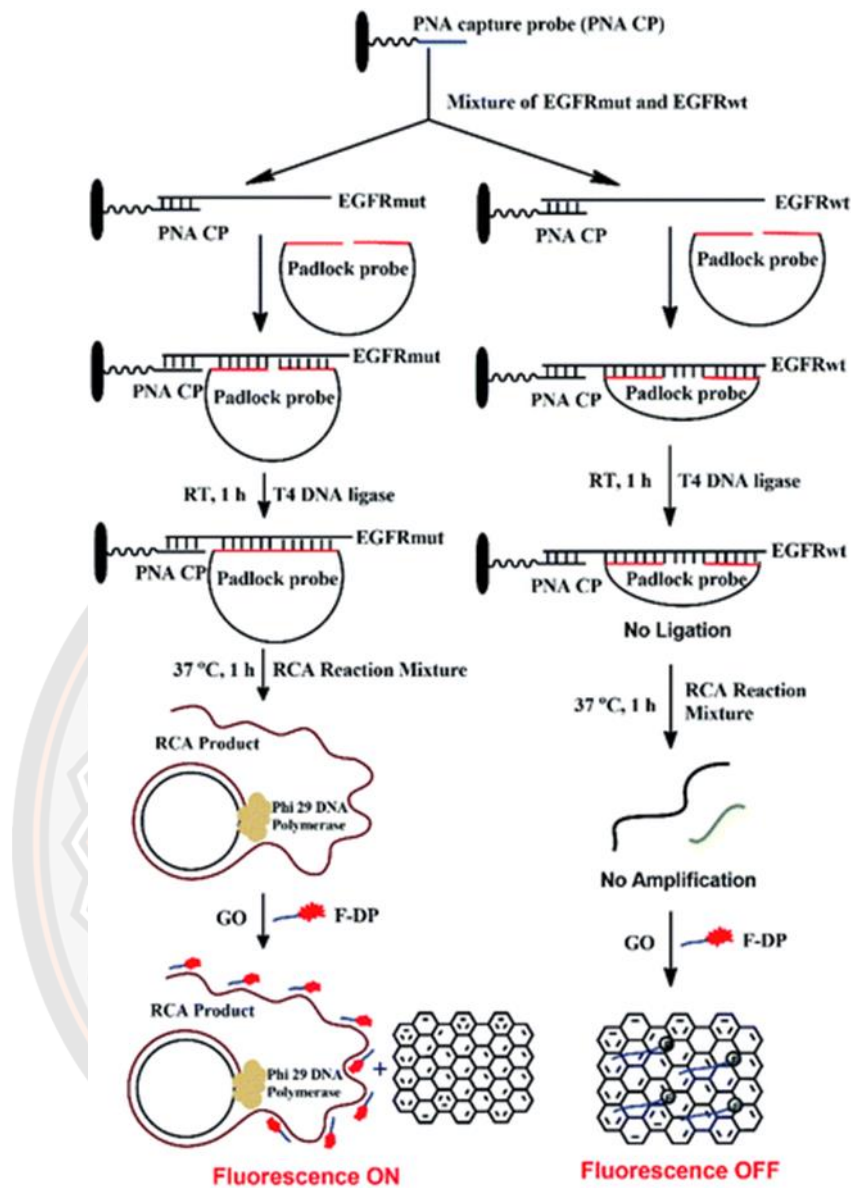
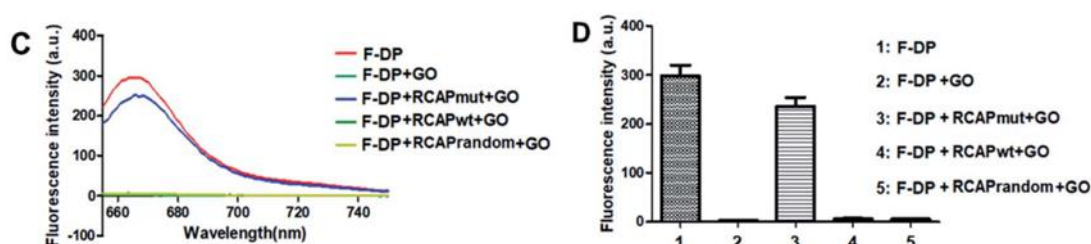


Figure 25 Scheme for specific detection of EGFR mutation using the RCA-based fluorogenic PNA probe based on the GO platform.



The assay was evaluated using a cy5-labeled PNA probe (F-DP) and RCAP corresponding to mutant, wildtype, and random DNA respectively. The results found that the fluorescence signal was obtained in the only presence of EGFR mutant-RCAP and slightly decreased when compared with F-DP alone. Meanwhile, the incubation of F-DP with EGFR wildtype- or random DNA-RCAP did not prevent the fluorescence quenching of F-DP by GO that indicated the specificity of this assay (**Figure 26**). Moreover, the sensitivity was also investigated using the EGFR mutant in the concentration range of 0 fM to 10 nM, displaying the limit of detection as 0.3 pM that evaluated by  $LOD = 3.3 \times SD_{blank}/Slope$  (**Figure 27**).



**Figure 26** The fluorescence signaling of specificity validation using F-DP in the presence of mutant, wildtype, or random DNA as RCAPs.

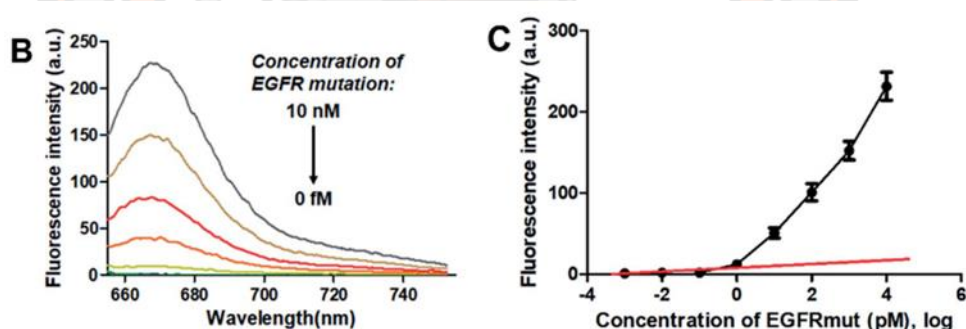


**Figure 27** The fluorescence signaling of sensitivity which was evaluated with various concentration of EGFR mutant DNA.

**The detection of *E. canis* DNA is based on isothermal amplification.**

In 2014, Chaumpluk and co-workers<sup>47</sup> reported the detection of *E. canis* based on the *p30* outer membrane protein gene by LAMP and nucleic acid hybridization in gold-nano colloids. When the oligonucleotide probe has been formed the DNA/DNA complex and induced aggregation of gold-nano colloids in solution, The color was changed from ruby red to purple. It could easily detect by the naked eyes immediately. This assay was performed on 90 minutes including DNA extraction step, high specificity, and high sensitivity that was detected less than 50 copies of DNA target. The steps of assay and color images as shown in **Figure 28**.

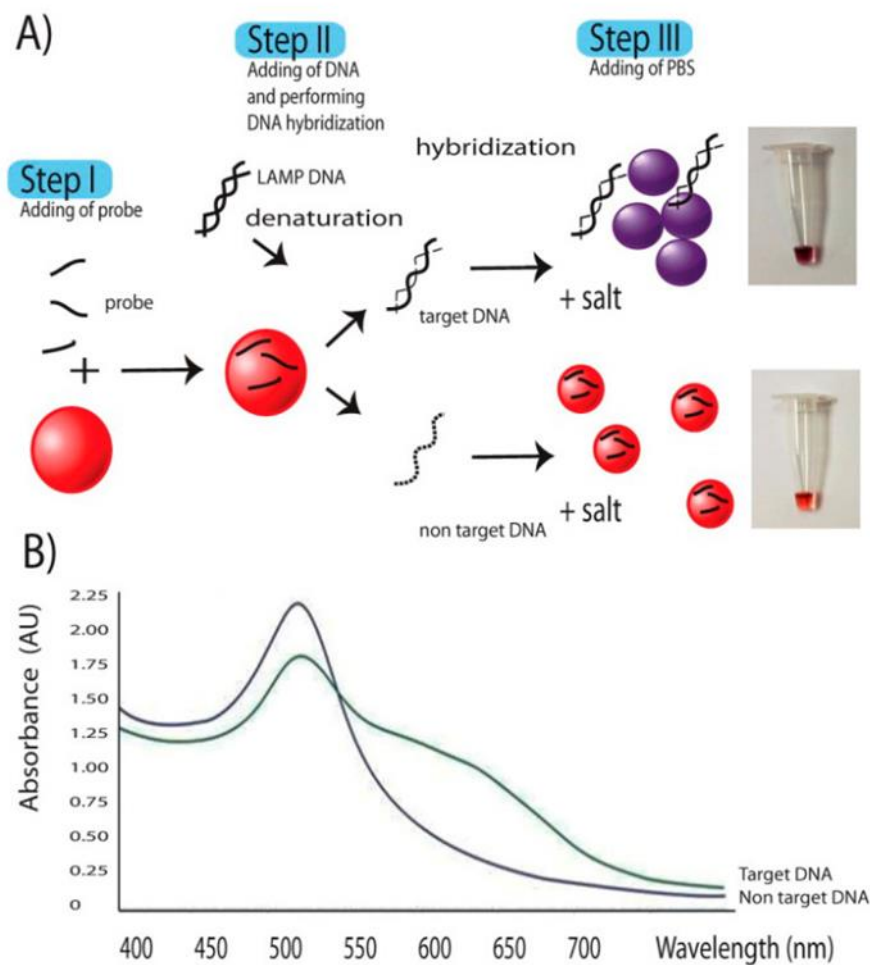


**Figure 28** The colorimetric DNA detection based on p30 DNA by gold nanoparticles and its corresponding change in the UV-Vis spectrum.

In 2015, Marins and co-workers<sup>48</sup> reported the detection of *E. canis* using *p30* gene amplification by LAMP. This assay was evaluated in comparison with conventional PCR technique and employing DNA extracted from *E. canis*-infected cultures of the macrophage cell line DH82 and positive *E. canis* DNA from dogs in Brazil confirmed by PCR. The sample was identified by LAMP to give 54.0% *E. canis*-DNA positive samples, whereas PCR could detect around 36.5% among the field samples. The LAMP products were visualized by gel electrophoretic analysis and gel-red dye straining (**Figure 29**), suggesting that the development of LAMP-based *E. canis* detection showed the maximized potential to use for nucleic acid testing and to improve the diagnosis of CME.

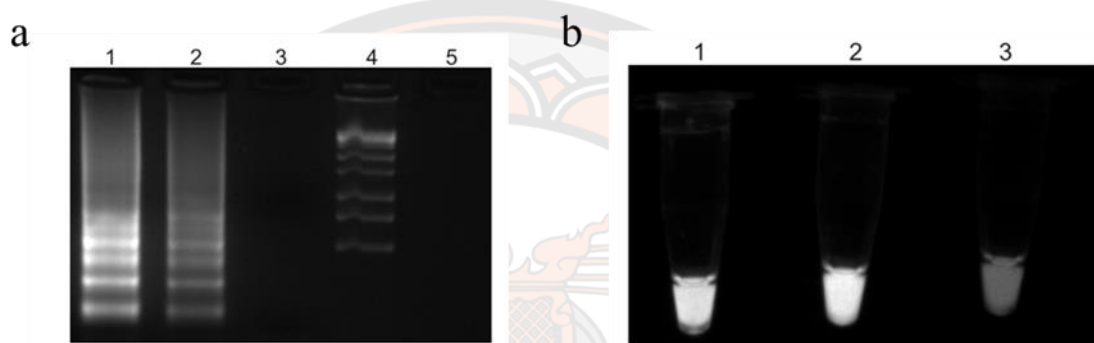


**Figure 29** The detection of *E. canis* based on the *p30* gene by LAMP. (a) Gel electrophoresis of amplified products: lane 1-2 indicate positive *E. canis* DNA, lane 3 indicate negative *E. canis* DNA, lane 4 1-kb DNA ladder, lane 5 empty. (b) The visual detection using gel red dye straining tube 1-2 and tube 3 corresponding to LAMP products that are positive and negative *E. canis* DNA, respectively.

## CHAPTER III

### RESEARCH METHODOLOGY

#### General procedure

##### 1. Instruments

All reactions were performed in glassware which was dried in an oven at 120°C at least 2 hours before used. The magnetic stirrer and heater of Heidolph are equipped with a magnetic bar. All chemical weights were determined by the Melder Toledo electrical balance and Sartorius electronic analytical balance. The solvent evaporation system was carried out by Büchi Rotavapor R-200 (Department of Chemistry, Faculty of Science, Naresuan University). The <sup>1</sup>H and <sup>13</sup>C NMR spectra were recorded on Bruker Avance 400 NMR spectrometer with operating 400 MHz and 100 MHz respectively. FT-IR spectra were recorded on the Perkin Elmer model spectrum GX FT-IR spectrometer operating by ATR mode. The fluorescence emission spectra were recorded on Synergy H1 Hybrid Multi-Mode Microplate Reader (Biotek) with 96-wells microplate for fluorescence-based assays (Science Lab Centre, Faculty of Science, Naresuan University). PCR and nested-PCR reactions were performed on a thermocycler (Bioer), whereas RPA was performed on a heating block (FOUR E'S scientific) using vortex and spin-down (FOUR E'S scientific) for mixing solution. The fluorescence intensity of pyrrolidinyl PNA in GO-based fluorogenic DNA detection was measured on the FAM channel of Bio-Rad CFX Connect real-time PCR and Bioer fluorescent quantitative detection system. The gel electrophoresis was performed by Bio-Rad real-time PCR and visualized by UV (256 nm) as well as LED transilluminator with maxima emission at 470 nm (GeneDireX) (Department of Biology, Faculty of Science, Naresuan University). The crude pyrrolidinyl PNAs were purified by reverse-phase HPLC which carried out by Water Delta 600 controller system equipped with a gradient pump and a Water 2996 photodiode array detector, column for separation: ACE 5 A71197, C18-AR, 150 x 4.6 mm, 5 µm particle size and analysis: UPS, 50 x 4.6 mm, 3 µm particle size. After the purification step, the collected fractions were characterized by Microflex MALDI-TOF mass spectrometry (Bruker Daltonik GmbH, Bremen, Germany). The identical fractions were freeze-dried and lyophilized on a Freeze dryer (Labconco). The optical density (OD) and melting temperature ( $T_m$ ) analysis were measured on 260 nm with a CARY 100 Bio UV-Visible spectrophotometer (Varian). Circular dichroism (CD) spectra were recorded on the JASCO J-815 CD spectrometer (Department of Chemistry, Faculty of Science, Chulalongkorn University).

## 2. Materials

All reagent grade chemicals which were used to synthesize pyrrolidinyl PNA monomers and spacers were purchased from the commercial supplier including Merck, Fluka, Acros Organics, TCI Chemicals, as well as Sigma-Aldrich. Graphene Oxide (10 mg/mL, Dispersion in Water) was purchased from TCI Chemicals. All oligonucleotides were purchased from Pacific Science (Bangkok, Thailand), Bio-Design Co., Ltd. (Bangkok, Thailand), or Macrogen (Seoul, Korea). Agarose A gel, acrylamide, and *N,N'*-methylene-bis-acrylamide, ammonium persulfate (APS), tetramethyl ethylenediamine (TEMED) were purchased from Sigma-Aldrich, whereas ethidium bromide was obtained from Bio basic Canada. The PCR reaction kits and 1 U/ $\mu$ L DNase I (1000 U) kits were obtained from Thermo Fisher Scientific Co. Ltd. The RPA liquid basic kit was purchased from TwistDx. All analytical grade solvents were purchased from RCI Labscan (Thailand) without other purification steps except THF which was distilled by Na(s) under inert gas using benzophenone as an indicator. The commercial-grade solvents were distilled before use. The silica gel 70-230 mesh was employed for the purification step. Thin-layer chromatography (TLC) was purchased from MERCK D.C. silica gel 60 F254 0.2 mm and visualized for monitoring reaction on a UV box equipped with UV light wavelength 254 nm. HPLC purification was carried out 0.1% TFA in methanol and 0.1% TFA in Milli-Q water that was purified *via* Ultrapure water system with Millpak® 40 filter unit 0.22  $\mu$ M, Millipore (USA) and filtered through a membrane filter (13mm  $\times$  0.45  $\mu$ M, Nylon). The solid-phase peptide synthesis was carried out TentaGel S-RAM resin as solid support (Novabiochem Co. Ltd.) and used coupling reagents including DMF (RCI Labscan), Fmoc-Lys(Boc)-OPfp (Novabiochem Co. Ltd.), piperidine, DBU, DIEA, 5(6)-carboxyfluorescein *N*-hydroxysuccinimide (Sigma-Aldrich), acetic anhydride (JDB), 98% trifluoroacetic acid (Fluka). Nitrogen gas was obtained from Thai Industrial Gas with 99.5% purity. The pyrrolidinyl PNA monomers (A, T, C, and G), ACPC and APC spacers were supported by Professor Dr. Tirayut Vilaivan or synthesized according to the previous report.<sup>49</sup>

## Experimental procedure

### 1. RPA primers and PNA probe designs

The 16S rRNA gene sequences for *Ehrlichia canis* (Eca), *Ehrlichia chaffeensis* (Ech), *Ehrlichia ewingii* (Eew), *Anaplasma platys* (Apl) and *Anaplasma phagocytophilum* (Aph), and *Canis lupus familiaris* (Clu) available in the GenBank nucleotide sequence database, were downloaded and aligned using the MultAlin (available in the website: <http://multalin.toulouse.inra.fr>) for designing specific region of primers and probe. The accession number of these sequences used for primer and probe designs as shown in **Table 1**. The pyrrolidinyl PNA probes were selected to recognize in antiparallel direction with specific-sequence of *E. canis* 16S rRNA gene within primers-based amplicons and using 5(6)-carboxyfluorescein (Flu) as a reporting unit. The pyrrolidinyl PNA probe sequence was *in silico* analyzed firstly to confirm the sequence-specificity by using Probe Match in Ribosomal Database Project Release 11 - Sequence Analysis Tools (available on <https://rdp.cme.msu.edu/>).

**Table 1 16S rRNA genes used for primer and probe designs**

Name	Accession number	Size (base pair)
<i>Ehrlichia canis</i>	EU106856.1	1,623
<i>Ehrlichia chaffeensis</i>	AF416764.1	2,056
<i>Ehrlichia ewingii</i>	M73227.1	1,435
<i>Anaplasma platys</i>	KX792089.2	1,431
<i>Anaplasma phagocytophilum</i>	DQ458805.2	1,442
<i>Canis lupus familiaris</i>	AB048590.1	6,120

### 2. Pyrrolidinyl PNA monomers and spacers

The pyrrolidinyl PNA monomers and spacers including *N*-Fmoc-A(Bz)-OPfp, *N*-Fmoc-C(Bz)-OPfp, *N*-Fmoc-T-OPfp, *N*-Fmoc-G-OH, *N*-Fmoc-ACPC-OPfp and *N*-Fmoc-APC(Tfa)-OPfp were supported by Professor Dr. Tirayut Vilaivan and synthesized following previous report.<sup>49</sup>

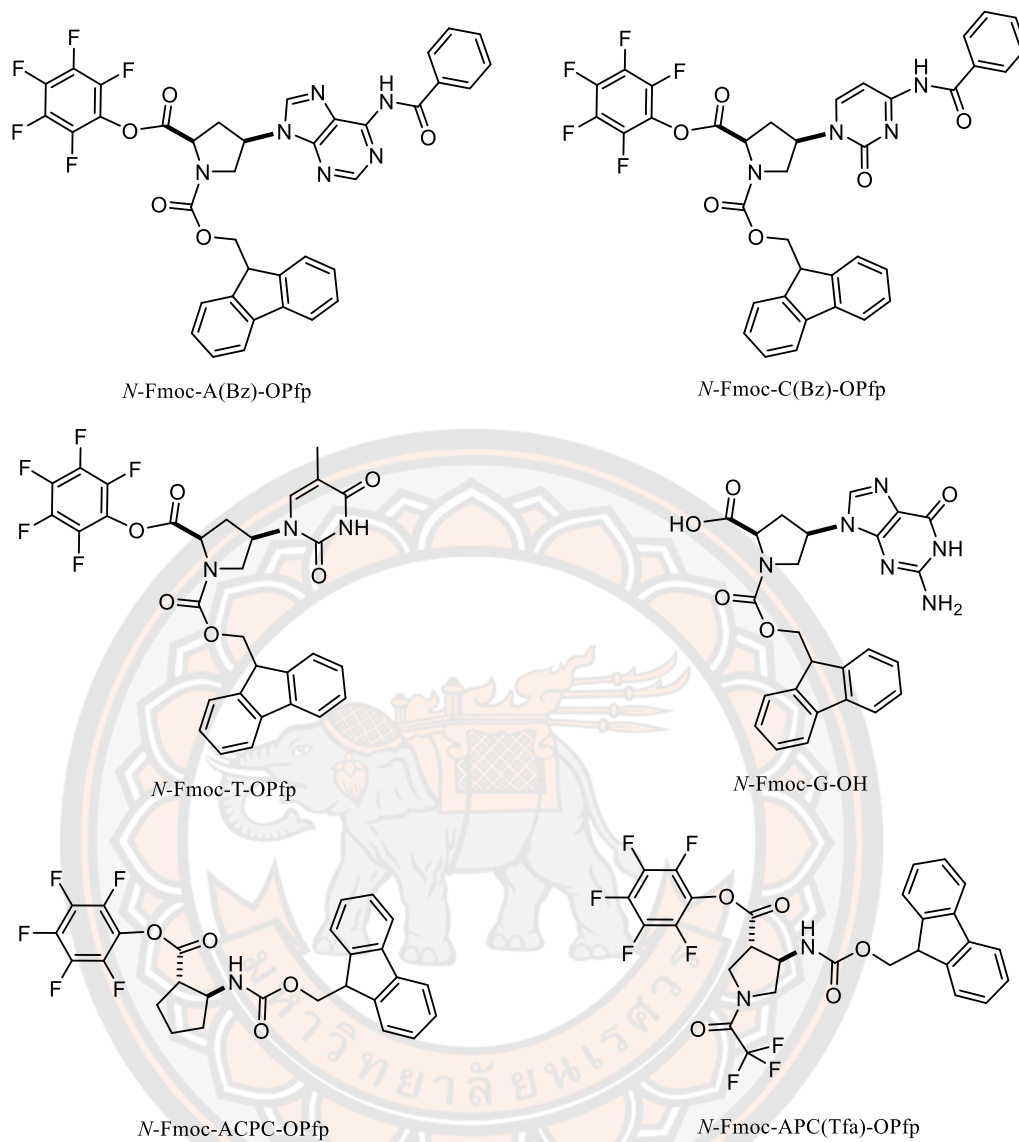
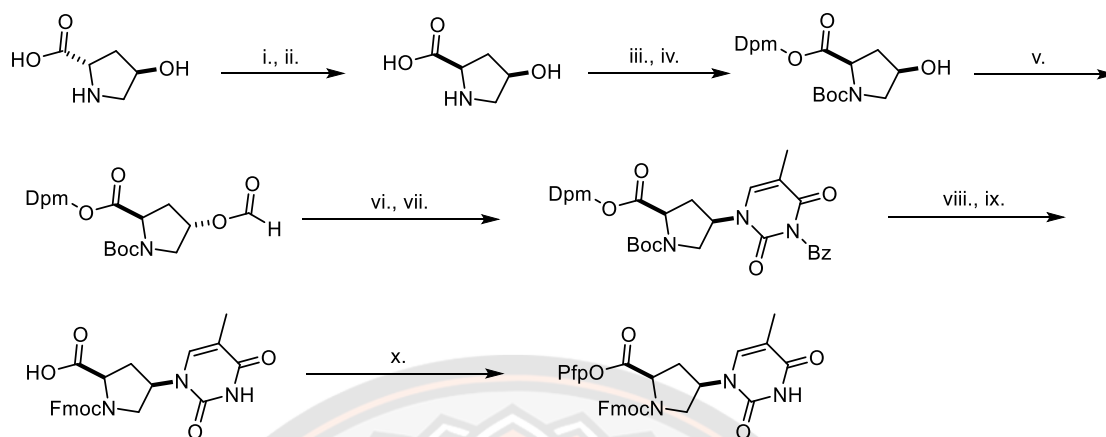


**Figure 30** The chemical structure of pyrrolidinyl PNA monomers and spacers.

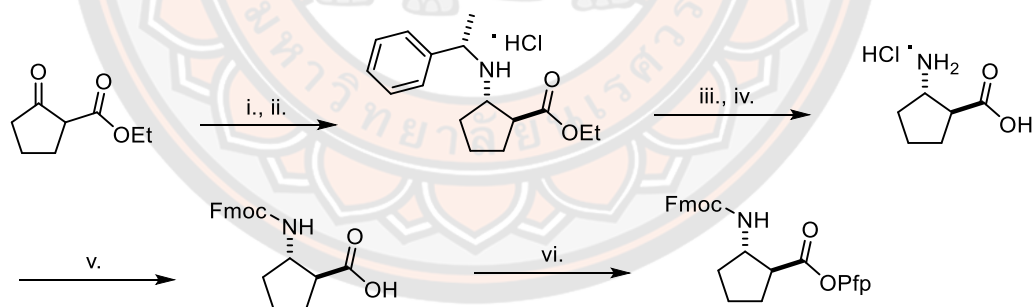
### 2.1 Synthesis of *N*-Fmoc-T-OPfp<sup>49</sup>



**i.** propionic anhydride, reflux, 3 h, **ii.** 2N HCl, reflux, 3h, **iii.** NaOH, Boc<sub>2</sub>O, H<sub>2</sub>O, <sup>t</sup>BuOH, 24 h, **iv.** (diazomethylene)dibenzene, EtOAc, 0°C, 24 h, **v.** HCOOH, PPh<sub>3</sub>, DIAD, THF, N<sub>2</sub>, 0°C – RT, 24 h, **vi.** NH<sub>3</sub>, CH<sub>3</sub>OH, 2 h, **vii.** (3*N*-benzoyl)-thymine, PPh<sub>3</sub>, DIAD, THF, N<sub>2</sub>, 0°C – RT, 24 h, **viii.** TFA, anisole, RT, 3h, **ix.** NaHCO<sub>3</sub> (pH = 8-9), Fmoc-OSu, CH<sub>3</sub>CN:H<sub>2</sub>O (1:1), **x.** DIEA, PfpOTfa, CH<sub>2</sub>Cl<sub>2</sub>, RT, 1 h.

**Figure 31** Schematic illustration for *N*-Fmoc-T-OPfp synthesis.

### 2.2 Synthesis of *N*-Fmoc-ACPC-OPfp<sup>5</sup>

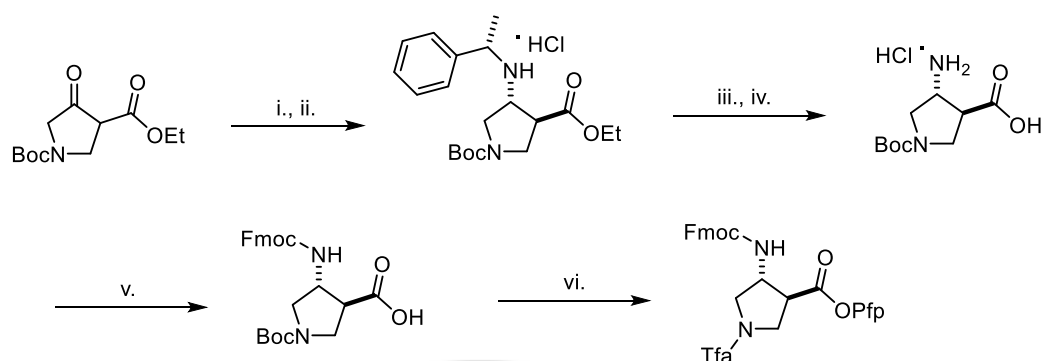


**i.** a) (*S*)-methylbenzylamine, AcOH, EtOH, RT, 2 h, b) NaBH<sub>3</sub>CN, 75°C, 16 h, **ii.** AcCl, EtOH, EtOAc, 0°C, recrystallization in CH<sub>3</sub>CN, **iii.** 10% w/w Pd(OH)<sub>2</sub>/C, H<sub>2</sub>, EtOH, 24 h, **iv.** 2N HCl, reflux, 3 h, **v.** NaHCO<sub>3</sub> (pH = 8-9), Fmoc-OSu, CH<sub>3</sub>CN:H<sub>2</sub>O (1:1), **vi.** DIEA, PfpOTfa, CH<sub>2</sub>Cl<sub>2</sub>, RT, 1 h.

**Figure 32** Schematic illustration of *N*-Fmoc-ACPC-OPfp synthesis.



### 2.3 Synthesis of *N*-Fmoc-APC(Tfa)-OPfp<sup>50</sup>



**i.** a) (*S*)-methylbenzylamine, AcOH, EtOH, RT, 2 h, b) NaBH<sub>3</sub>CN, 75°C, 16 h, **ii.** AcCl, EtOH, EtOAc, 0°C, recrystallization in CH<sub>3</sub>CN, **iii.** 10% w/w Pd(OH)<sub>2</sub>/C, H<sub>2</sub>, EtOH, 24 h, **iv.** LiOH, THF:CH<sub>3</sub>OH:H<sub>2</sub>O (6:3:1), 0°C, 3 h, **v.** NaHCO<sub>3</sub> (pH = 8-9), Fmoc-OSu, CH<sub>3</sub>CN:H<sub>2</sub>O (1:1), **vi.** DIEA, PfpOTfa, CH<sub>2</sub>Cl<sub>2</sub>, RT, 1 h.

**Figure 33 Schematic illustration of *N*-Fmoc-APC(Tfa)-OPfp synthesis.**

### 3. Synthesis of pyrrolidinyl PNA *via* solid-phase peptide synthesis<sup>49</sup>

The pyrrolidinyl PNA was manually synthesized on TentaGel S-RAM resin (0.24 mmol/g loading) at 1.5 μmol scale using Fmoc strategy following previously published protocol. The synthesis process was carried out the cycle of three steps including deprotection, anchoring or coupling, and capping. The used reagents of each step were freshly prepared as following:

**Table 2 The stock solutions and related reagents in SPPS.**

Lists	Materials and reagents
Solid support	7.1 mg of TentaGel S-RAM (1.5 $\mu\text{mol}$ , 1.0 eq.)
Stock #1	20%v/v of piperidine, 2%v/v of DBU in anh. DMF
Stock #2	7%v/v of DIEA in anh. DMF
Stock #3	5.5%w/v of HOAt in anh. DMF
Capping agent	Ac <sub>2</sub> O
Amino acid	4.80 mg of <i>N</i> -Fmoc-Lys(Boc)-OPfp (6 $\mu\text{mol}$ , 4 eq.)
Monomers	4.44 mg of <i>N</i> -Fmoc-A(Bz)-OPfp (6 $\mu\text{mol}$ , 4 eq.) 3.77 mg of <i>N</i> -Fmoc-T-OPfp (6 $\mu\text{mol}$ , 4 eq.)
Spacers	4.30 mg of <i>N</i> -Fmoc-C(Bz)-OPfp (6 $\mu\text{mol}$ , 4 eq.) 3.10 mg of <i>N</i> -Fmoc-ACPC-OPfp (6 $\mu\text{mol}$ , 4 eq.) 3.69 mg of <i>N</i> -Fmoc-APC(Tfa)-OPfp (6 $\mu\text{mol}$ , 4 eq.)
Dye labeling	4.26 mg of 5(6)-carboxyfluorescein-NHS (9 $\mu\text{mol}$ , 6 eq.)
Sidechain deprotection agents	NH <sub>3</sub> : Dioxane at ratio 1:1 by volume
Cleavage agent	TFA



### 3.2 General protocol of manual SPPS in PNA synthesis

Step 1 Deprotection: The Fmoc-protected at the amino group has been removed by using 100  $\mu\text{L}$  of **Stock #1** for 5 minutes, the deprotected solution was blown out, washed by three times of DMF by applying pressure to give dryness resin bearing free amino group as seen in **Figure 34**.

Step 2 Anchoring or Coupling: The free amino group was attended with an incoming carboxylic group by using 15  $\mu\text{L}$  of **Stock #2** and 15  $\mu\text{L}$  of **Stock #3** in the presence of 6  $\mu\text{mol}$  of *N*-Fmoc-Lys(Boc)-OPfp, or alternative pyrrolidinyl PNA monomers or spacers (4.0 eq.) for 40-60 min. After that, the coupling solution was blown out, washed, and dried.

Step 3 Capping: The unreacted amino group was capped acetyl group by employing 30  $\mu\text{L}$  of **Stock #2** with 5  $\mu\text{L}$  of  $\text{Ac}_2\text{O}$  for 5 min. The capping solution was blown out, washed many times with DMF, and dried. The process must be ended with this step.

Step 4 Dye labeling: When the SPPS process has been finished to give the desired oligonucleotide sequence, the Fmoc-protected *N*-terminus of oligonucleotide was deprotected by a solution of **Stock #1** for 5 min, blown out, washed, and dried. The deprotected resin was immersed in 10% v/v DIEA in anh. DMF in the presence of 5(6)-carboxyfluorescein *N*-succinimide ester (6 eq.) in dark for 4-5 days with periodical agitation.

### 3.3 The side chain deprotection

The solid support bearing Flu-labeled pyrrolidinyl PNA has been soaked in a solution of  $\text{NH}_3$  in dioxane at ratio 1:1 by volume at 65  $^\circ\text{C}$  for 18 hours and was washed several times with  $\text{CH}_3\text{OH}$  and dried by  $\text{N}_2$  streaming.

### 3.4 The cleavage of pyrrolidinyl PNA

1,500  $\mu\text{L}$  of TFA (3x500  $\mu\text{L}$ ) was employed for cleaving PNA from the resin by soaking PNA in TFA for 2 hours. The solution was carefully removed TFA by streaming  $\text{N}_2$  in the fume hood. The crude pyrrolidinyl PNA was washed and precipitated with diethyl ether to give a Flu-labeled pyrrolidinyl PNA crude as a yellow solid.

#### 4. The purification and characterization of pyrrolidinyl PNA

##### 4.1 PNA purification by using reverse-phase HPLC

The crude pyrrolidinyl PNA was dissolved by 10% v/v MeOH in Milli Q water making 120  $\mu$ L crude PNA solution. The PNA solution was purified on reverse-phase HPLC equipped with HPLC column type ACE 5 A71197, C18-AR, 150x4.6 mm with a gradient solvent system consisting 0.1% v/v TFA in Milli Q water and 0.1% v/v TFA in MeOH corresponding to solvent A and solvent B respectively (**Table 3**). The fractional solutions were collected manually monitoring absorbance at 310 nm and 260 nm. The aliquot collected fraction was confirmed by MALDI-TOF mass spectrometer with 90% purity. The identical fraction was diluted with Milli Q water making 8.0 mL aqueous solution in 15 mL plastic tube and freeze-dried respectively to give Flu-labeled pyrrolidinyl PNA product as a yellow solid.

**Table 3 Reverse-phase HPLC program.**

Modes	Times (min)	Solvent A (%)	Solvent B (%)
Hold	05	90	10
Linear gradient	10	10	90
Hold	05	10	90
Linear gradient	30	90	10

##### 4.2 The determination of PNA concentration and $T_m$ analysis

The crudely solid pyrrolidinyl PNA was dissolved in 200  $\mu$ L of Milli Q water within 1.5  $\mu$ L of microcentrifuge tube. 1  $\mu$ L of the aliquot solution was transferred into 1.0 mL of quartz UV cell containing 10 mM phosphate buffer pH 7.0, adjusting to 1,000  $\mu$ L by Milli Q water. The absorbance was measured at 260 nm and evaluating concentration by using the Beer-Lambert law equation.  $T_m$  experiment was obtained on 1.0  $\mu$ M of PNA-DNA in 10 mM phosphate buffer pH 7.0, and monitoring on OD<sub>260</sub> with different temperatures ranging from 25°C to 90°C at increasing rate 1°C/min. The received data was plotted and smoothed in Origin 8.0 (OriginLab Corporation). The corrected melting temperature was evaluated using equation (1)<sup>49</sup> as below:

**Equation (1)**

$$T_m = (0.9696 \times T_{block}) - 0.8396$$

## 5. The ssDNA detection by PNA probe in the GO platform

### 5.1 Fluorescence measurement

200  $\mu\text{L}$  of solutions (final volume) were mixed within a 96-well black plate and consequently measuring fluorescence emission spectra on a microplate reader with excitation wavelength at 460 nm and emission wavelength ranging from 500 to 700 nm. The received data was plotted and analyzed in Origin 8.0. The percentage of fluorescence quenching (%Q) was evaluated by equation (2), whereas the limit of detection (LOD) was evaluated by equation (3) following with literature review.<sup>20</sup>

#### Equation (2)

$$\%Q = \frac{F_{ssPNA} - F_{ssPNA+GO}}{F_{ssPNA}} \times 100\%$$

#### Equation (3)

$$LOD = \frac{3.3 \times SD}{S}$$

Where  $F_{ssPNA}$  and  $F_{ssPNA+GO}$  indicate the fluorescence intensity of the PNA probe in the absence and presence of GO.  $SD$ : standard deviation,  $S$ : the slope of a calibration curve.

### 5.2 The optimization of GO

The concentration of used GO was optimized by fixing the concentration of Flu-labeled pyrrolidinyl PNA at 200 nM (final concentration). Flu-labeled pyrrolidinyl PNA was added into Tris-HCl buffer (25 mM Tris-HCl buffer pH 8.0 and 50 mM NaCl) in the presence or absence of 240 nM complementary ssDNA (1.2 eq.) before incubating with GO (0 - 14  $\mu\text{g}/\text{mL}$  of final concentration).

### 5.3 Sequence selectivity

Flu-labeled pyrrolidinyl PNA (200 nM) was added into Tris-HCl buffer (25 mM Tris-HCl buffer pH 8.0 and 50 mM NaCl) containing various types of excess-ssDNA (240 nM, 1.2 eq.) which include complementary, single-mismatched, and double-mismatched DNA. Then, the PNA solution was mixed with 10  $\mu\text{g}/\text{mL}$  GO for 1 hour.

### 5.4 Sensitivity

Flu-labeled pyrrolidinyl PNA (200 nM) was added into Tris-HCl buffer (25 mM Tris-HCl buffer pH 8.0 and 50 mM NaCl) containing different concentration of **DNA1** ranging from 0 nM to 400 nM and consequently mixed with 10  $\mu\text{g}/\text{mL}$  GO for 1 hour.

## 6. The combination of a PNA/GO platform and PCR

In this study, PCR amplification was used to generate dsDNA as a PCR product. The DNA which was used as a DNA template in the PCR reaction was extracted from the dog's blood. The extracted DNA was received from an animal molecular diagnostic service, Chiangmai province, and confirmed infected parasites by conventional-standard PCR method and High-Resolution Melting Analysis (HRM) (supported by Dr. Kittisak Buddhachat research group).

### *6.1 Fluorescence measurement*

The solutions of PCR-based PNA/GO were mixed within 100  $\mu$ L real-time PCR tube strips in small-final volume (50  $\mu$ L). Before measuring the fluorescence, the GO-suspended solution was centrifuged to precipitate a large amount of GO. Then, the relative fluorescence intensity of the aliquot was recorded on the end-point mode in the FAM channel of the Bio-Rad real-time PCR machine. The received data was plotted and analyzed in Origin 8.0.

### *6.2 PCR and nested-PCR (nPCR) amplification*

The conventional PCR was performed on positive and negative samples (identified by HRM experiments) using only outer primers as **F1**: 5'-ATC ATG GCT CAG AAC GAA CG-3' and **R1**: 5'-GTG ACG GGC AGT GTG TAC AAG-3'. nPCR that was used to enhance sensitivity was performed by **F1-R1** firstly following with inner primers as **F2**: 5'-AAC GAA CGC TGG CGG CAA GCC-3' and **R2**: 5'-ACG AAT TTC ACC TCT ACA CTA GGA ATT CCG CTA-3', yielding dsDNA size ~1,380 bp and ~640 bp, respectively. The first round of PCR was carried on 25  $\mu$ L of the reaction mixture in containing 1 $\times$  PCR buffer, 0.2  $\mu$ M of each **F1** and **R1**, 0.2 mM dNTPs, and 1 U of *Taq* DNA polymerase. The master mix in PCR reaction was prepared to minimize handing in operation by mixing 1 $\times$  PCR buffer, PCR primers, and dNTPs firstly. Then, 23.8  $\mu$ L of master mix solution was transferred into a sterile-PCR tube following with the addition of 1  $\mu$ L of an extracted DNA, and 0.2  $\mu$ L of 5 units/ $\mu$ L *Taq* DNA polymerase. The thermal-cycling procedure was; 1 cycle of 5 minutes at 95°C, 40 cycles of 30 seconds at 95°C, 30 seconds at 58°C, 30 seconds at 72°C, and final cycle of 7 minutes at 72°C. Sterile Milli Q water was included as a negative control. nPCR was performed by using 1.0  $\mu$ L of 5-fold dilution of first-round PCR as template setting-up 30 seconds at 50°C for annealing temperature. The dsDNA products were visualized on EtBr-stained 2% agarose gel in TAE buffer after electrophoretic migration for 20 minutes at 400 mA, and 100 voltages. The gel images were obtained on a UV transilluminator at 256 nm.

### 6.3 Effect of PCR components to GO-based PNA probe

**PNA1** (200 nM) was added into the 20  $\mu\text{L}$  of 1 $\times$  PCR buffer solution in the absence or presence of different PCR compositions including 0.2 mM dNTPs, 0.2  $\mu\text{M}$  of each forward-reverse primers, and 0.24% v/v glycerol (as referred to the solution of Taq DNA polymerase in glycerol) within 100  $\mu\text{L}$  real-time PCR tube strips. Then, the PNA solution was mixed with 10  $\mu\text{g}/\text{mL}$  GO (final concentration) to making 50  $\mu\text{L}$  of total solution volume. The solution was vortexed, incubated for 1 hour, and centrifuged to precipitate heavily GO solids before measuring fluorescence intensity as described above.

### 6.4 The optimization of GO

**PNA1** (200 nM) was added into the 20  $\mu\text{L}$  of 1 $\times$  PCR buffer consisting of 10 mM of dNTPs, forward and reverse primers, as well as glycerol. The various concentrations of GO in the range of 0-50  $\mu\text{g}/\text{mL}$  were mixed for 1 hour and then measured fluorescence.

### 6.5 The fluorogenic detection for dsDNA of PCR reaction

To measure the fluorescence of dsDNA obtained from PCR, 1.0  $\mu\text{L}$  of 1.5  $\mu\text{M}$  **PNA1** (50 nM of final concentration) was added into the 20  $\mu\text{L}$  of PCR or nPCR products. The solution was heated up to 95 $^{\circ}\text{C}$  for 5 min, annealed at 50  $^{\circ}\text{C}$  for 30 minutes, and allowed to room temperature. 2.8  $\mu\text{L}$  of reaction buffer with  $\text{MgCl}_2$  (a buffer for DNase I) and 0.2  $\mu\text{L}$  of 1 U/ $\mu\text{L}$  DNase I (or Milli Q water) were added and incubating at 37  $^{\circ}\text{C}$  for 5 min in thermocycler following with the addition of 6.0  $\mu\text{L}$  of 125  $\mu\text{g}/\text{mL}$  GO (25  $\mu\text{g}/\text{mL}$  of final concentration). The relative fluorescence intensity of the aliquot solution was measured as described above.

## 7. The isothermal detection of dsDNA by RPA-DPG assay

In this study, plasmid DNAs (pUC57) harboring the 16S rRNA region for *E. canis*, *A. platys*, and 18S rRNA for *B. vogeli*, and *H. canis* were used as DNA template. The plasmid DNA was diluted into  $6.71 \times 10^8$  copies/reaction (approximately 1 ng/ $\mu\text{L}$ ) before used. The assay was performed in 200  $\mu\text{L}$  of PCR tube in the final volume of 15  $\mu\text{L}$ . The fluorescence intensity in a small volume was measured on the FAM channel of the Bioer fluorescent quantitative detection system. The fluorescence image was obtained on blue light LED transilluminator. The received data was plotted and analyzed in Origin 8.0 and %Q was evaluated by equation (2). The number of copies of a DNA template was evaluated by equation (4) with Avogadro constant  $NA = 6.022 \times 10^{23}$  copies/mol, assuming a molecular weight of 1 bp dsDNA approximately 650 g/mol.

### Equation (4)

$$\text{number of copies} = (ng \times 6.022 \times 10^{23}) / (\text{length} \times 1 \times 10^9 \times 650)$$



### 7.1 The optimization of RPA

TwistAmp™ Liquid Basic was used for RPA assay. The solution was carried on 25  $\mu\text{L}$  of reaction mixture consisting of 1X reaction buffer, 1.6 mM dNTPs, 0.48  $\mu\text{M}$  **F3** (5'-CGG CAA GCC TAA CAC ATG CAA GTC GAA CGG ACA AT-3'), 0.48  $\mu\text{M}$  **R2** (5'-ACG AAT TTC ACC TCT ACA CTA GGA ATT CCG CTA-3'), 1 $\times$  basic E-mix, 1X core reaction mix, and 14 mM  $\text{Mg}(\text{OAc})_2$ . All protein components required for RPA reaction (for example, recombinase, recombinase loading-factor, DNA polymerase, single-stranded binding protein, *etc.*) were included within the RPA kit. The master mix was prepared in the sterile-PCR tube firstly by mixing the 1 $\times$  of reaction buffer, basic E-mix, core reaction mix, 1.6 mM dNTPs, and 0.48  $\mu\text{M}$  of each **F3** and **R2**. The tube was flipped for 10X full-inversions and centrifuged, according to manual protocol. Then, the 23  $\mu\text{L}$  of the master-mix solution was transferred for each reaction with adding 1.25  $\mu\text{L}$  of 280 mM  $\text{Mg}(\text{OAc})_2$  and 1.0  $\mu\text{L}$  of DNA template inside the tube's lid carefully, mixing by 6X full-inversions, and consequently centrifuged. Sterile Milli Q water was included as a negative control. RPA reaction was optimized at 20-50°C for 40 min and 37°C for 5-40 min under a heating block. The amplification products obtained were analyzed by EtBr-staining agarose gel electrophoresis for 25 min at 100 V with visualizing under UV transilluminator (256 nm).

### 7.2 The determination of optimal GO

The solution was performed on 15.0  $\mu\text{L}$  of the reaction mixture. The PNA solution was prepared firstly to minimize the operation by mixing 1.0  $\mu\text{L}$  of 10  $\mu\text{M}$  **PNA1** (10 pmol PNA), 1.8  $\mu\text{L}$  of 10 $\times$  reaction buffer for DNase I (100 mM Tris-HCl, pH 7.5, 25 mM  $\text{MgCl}_2$ , 1 mM  $\text{CaCl}_2$ ), and 1.0  $\mu\text{L}$  of Milli Q water. 3.8  $\mu\text{L}$  of PNA solution was transferred into 5.0  $\mu\text{L}$  of RPA master mix (in absence of targeted DNA) following with the addition of 0.2  $\mu\text{L}$  of 1 U/ $\mu\text{L}$  DNase I. Then, 6.0  $\mu\text{L}$  of different GO concentrations (0 - 0.64  $\mu\text{g}/\mu\text{L}$ ) were mixed and incubated at room temperature for 10 min before measuring fluorescence.

### 7.3 The detection of dsDNA by RPA-DPG assay

The assay procedure was performed on 15.0  $\mu\text{L}$  of reaction mixture consisting of 3.8  $\mu\text{L}$  of PNA solution as described above and 5.0  $\mu\text{L}$  of each RPA product. The solution was incubated at 37°C for 5-30 min following with the addition of 0.2 U DNase I and continually performed for 5 min in a heating block. 6.0  $\mu\text{L}$  of 1.6  $\mu\text{g}/\mu\text{L}$  GO (9.6  $\mu\text{g}$ , 0.64  $\mu\text{g}/\mu\text{L}$ ) was mixed at RT for 10 min before precipitating GO suspension by centrifugation and measuring fluorescence respectively.

#### 7.4 Specific *E. canis* detection

The specificity of RPA-DPG assay for detecting *E. canis* was evaluated by using 1 ng/ $\mu$ L pUC57-plasmid DNA of related canine parasites including *E. canis*, *A. platys*, *B. vogeli*, and *H. canis*. Milli Q water was included as a negative control. The RPA assay was performed at 37°C for 40 min, whereas hybridization time was used for 20 min. The details of the process can see as described above.

#### 7.5 Sensitive detection for *E. canis*

1 ng/ $\mu$ L of *E. canis* plasmid DNA (1.11 pM,  $6.7 \times 10^8$  copies/ $\mu$ L) was diluted by 10-fold to preparing a concentration of standard template in the range of 1 fg - 1 ng/ $\mu$ L before used. The RPA reaction was performed at 37°C for 40 min and used Milli Q water as a negative control. The PNA-dsDNA<sub>target</sub> was hybridized for 20 min following with digestion and adsorption steps.

#### 7.6 PAGE analysis

The stock solution of 40% w/v polyacrylamide was manually prepared at ratio polyacrylamide: bis-acrylamide (29:1) by dissolving 38.67 g of polyacrylamide and 1.33 g of *N,N*-methylene-bis-acrylamide in DI water. Gel was set by immediately mixing 20% w/v native-PAGE with 0.1 % w/v APS and 0.1 % v/v TEMED in 1 $\times$  TBE. After that, 15  $\mu$ L of each solution was mixed with 30 % v/v glycerol (loading agent) and subjected to PAGE in 1 $\times$  TBE with migration at 230 V for 15 min. The image was obtained on blue light LED transilluminator.

#### 7.7 Clinical samples

All of the DNA samples extracted from whole blood were identified infected *E. canis* by conventional PCR method firstly by using RPA primers as **F3** and **R2**. The process was performed as the previous section with annealing temperature at 50°C for 40 cycles. The RPA process was obtained on 25  $\mu$ L of the reaction mixture as same as a specific and sensitive study. The amplified products were analyzed by agarose gel electrophoresis as well as RPA-DPG assay.

## CHAPTER IV

### RESULTS AND DISCUSSION

In this research, the application of pyrrolidinyl PNA for detecting the 16S rRNA of the *E. canis* gene was investigated. Firstly, a sequence-specifically 5(6)-carboxyfluorescein-labeled pyrrolidinyl PNA probe has been designed and synthesized by SPPS based-on Fmoc methodology. Second, the GO platform was employed for studying the fluorescence quenching of PNA. The fluorogenic pyrrolidinyl PNA probe in the GO platform was conceptually evaluated by synthetic single-stranded DNA including complementary, single-, and double-mismatched sequences. After that, this assay was applied to the PCR product for studying in preliminary of dsDNA detection. Finally, a recombinase polymerase amplification (RPA) technique was combined with DNase I-enhanced acpPNA probe-GO (so-called RPA-DPG assay) for increasing the efficacy of the detection. The details of results obtained from this study were described as following:

#### Design of primers and pyrrolidinyl PNA probe

The specific sequences of the RPA primer and pyrrolidinyl PNA probe were designed by multiple alignments of 16S rRNA genes that were downloaded from the NCBI database. The accession number of selected 16S rRNA gene comprising EU106856.1 for *E. canis* (Eca), AF416764.1 for *E. chaffeensis* (Ech), M73227.1 for *E. ewingii* (Eew), KX792089.2 for *A. platys* (Ap), DQ458805.2 for *A. phagocytophilum* (Aph), and AB048590.1 for *C. l. familiaris* (Clu) have the DNA length approximated 1,623 bp, 2,056 bp, 1,435 bp, 1,431 bp, 1,442 bp and 6,120 bp respectively. These bacteria were chosen because they are important agents causally tick-borne diseases in dogs. These sequences were aligned on MultAlin with a 90% high consensus level and a 50% low consensus level. The MultAlin sequence alignment was indicated in **Figure 35**. All designed sequences were concluded as shown in **Table 4**.

**Table 4 All sequences of primer and pyrrolidinyl PNA probe used in this study.**

Types	Sequences (5' → 3' or N' → C')	Lengths	Ref.
PNA probe	Fluorescein-ACAATTCCT-Lys-NH <sub>2</sub>	10 units	
<b>F1</b>	TCATGGCTACGAACGAACG	19 units	51
<b>F2</b>	AACGAACGCTGGCGGCAAGCC	21 units	
<b>F3</b>	CGGCAAGCCTAACACATGCAAGTCGAACGGACAAT	35 units	
<b>R1</b>	GTGACGGGCAGTGTGTACAAG	21 units	51
<b>R2</b>	ACGAATTCACCTCTACACTAGGAATTCCGCTA	33 units	

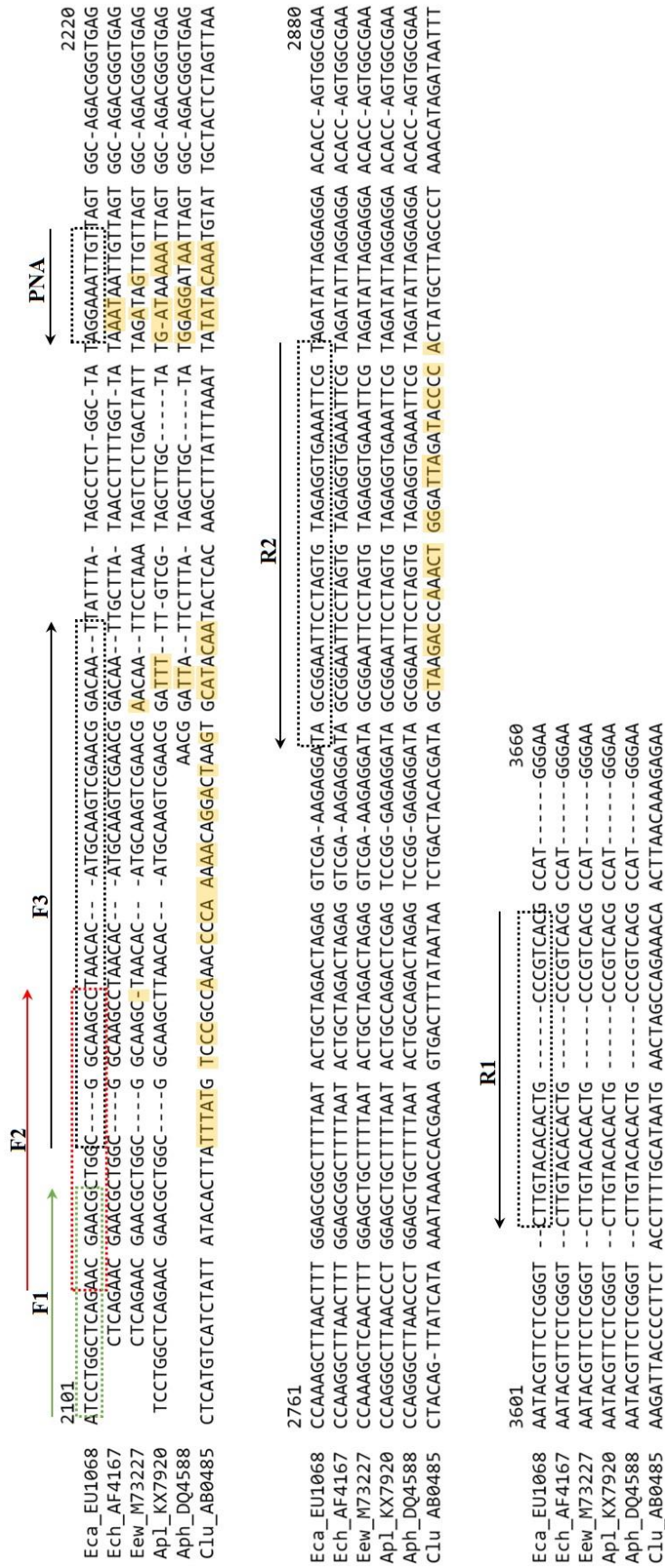


**Figure 35** The selected region of the 16S rRNA gene of *E. canis* for designing the sequences of primers and PNA probe. The base labeling is referred to the 16S rRNA gene of *C. l. familiaris* (Clu) (AB048590.1). Dash boxes indicate selected region. The yellow boxes show base-mismatched sequence.

The PNA sequences were investigated *in silico* for specificity by Probe Match software, available on RDP-Release 11. As shown in **Figure 36**, The designing probe sequence matched to *E. canis* in genus *Ehrlichia* >90%, and no cross-reaction to genus *Anaplasma* or *Neorickettsia* within the family Anaplasmataceae of order Rickettsiales.

**Probe Match Result** [ start over | help | options ]

Display depth:  Differences Allowed:  Probe: 5'ACAATTCCT 3'  
Target: 5'AGGAAATTGT 3'

Lineage (click node to return it to hierarchy view):  
Root (228/3482333) ; Bacteria (228/3196041) ; "Proteobacteria" (106/1088761) ; Alphaproteobacteria (89/270155)

Hierarchy View:  
order Rickettsiales (84/5748) (hits/total searched) [list results for this node]  
  family Anaplasmataceae (84/4608)  
    genus Anaplasma (0/3519)  
    ▶ genus Ehrlichia (84/332)  
      genus Neorickettsia (0/94)  
      unclassified\_Anaplasmataceae (0/663)  
      family Holosporaceae (0/0)  
      family Rickettsiaceae (0/1084)  
      family Rickettsiales\_incertae\_sedis (0/0)  
      unclassified\_Rickettsiales (0/56)

Data Set Options:

Strain:	<input type="radio"/> Type	<input type="radio"/> Non Type	<input checked="" type="radio"/> Both
Source:	<input type="radio"/> Uncultured	<input type="radio"/> Isolates	<input checked="" type="radio"/> Both
Size:	<input type="radio"/> >1200	<input type="radio"/> <1200	<input checked="" type="radio"/> Both
Quality:	<input type="radio"/> Good	<input type="radio"/> Suspect	<input checked="" type="radio"/> Both

---

▼ genus Ehrlichia (84/332)

S000001158 Ehrlichia canis; Florida; M73226  
S000003417 Ehrlichia canis; Gzh982; AF162860  
S000005995 Ehrlichia canis; VHE; AF373612  
S000007313 Ehrlichia canis; Oklahoma; M73221  
S000010972 Ehrlichia canis; VDE; AF373613  
S000143180 Ehrlichia canis; Kagoshima 1; AF536827  
S000391452 Ehrlichia ovina; Turkey; AF318946  
S000419421 Ehrlichia canis; Madrid; AY394465  
S000437402 Ehrlichia canis; 611; U26740  
S000437789 Ehrlichia sp.; Germishuys; U54805  
S000615392 Ehrlichia canis; TW1216; DQ228496  
S000615393 Ehrlichia canis; TW16113; DQ228497  
S000615394 Ehrlichia canis; TW16611; DQ228498  
S000615395 Ehrlichia canis; TW16659; DQ228499  
S000615396 Ehrlichia canis; TW16924; DQ228500  
S000615397 Ehrlichia canis; TW16927; DQ228501  
S000615398 Ehrlichia canis; TW16934; DQ228502  
S000615399 Ehrlichia canis; TW16945; DQ228503  
S000615400 Ehrlichia canis; TW16949; DQ228504  
S000615401 Ehrlichia canis; TW16977; DQ228505  
S000615402 Ehrlichia canis; TW16983; DQ228506  
S000615403 Ehrlichia canis; TW17122; DQ228507  
S000615404 Ehrlichia canis; TW17123; DQ228508  
S000615405 Ehrlichia canis; TW17124; DQ228509  
S000615406 Ehrlichia canis; TW17134; DQ228510  
S000615407 Ehrlichia canis; TW17146; DQ228511  
S000615409 Ehrlichia canis; TW17146; DQ228513  
S000615410 Ehrlichia canis; TW17146; DQ228514  
S000736193 Ehrlichia canis; DQ915970  
S000751005 Ehrlichia canis; GR21; EF011110  
S000751006 Ehrlichia canis; GR78; EF011111  
S000769746 Ehrlichia canis; EF139458  
S000805396 Ehrlichia canis; Brazil-CO1; EF195134  
S000805397 Ehrlichia canis; Brazil-CO2; EF195135  
S000927254 Ehrlichia canis; TWN1; EU106856  
S000927603 Ehrlichia canis; TWN2; EU123923  
S000942772 Ehrlichia canis; TWN3; EU143636  
S000942773 Ehrlichia canis; TWN4; EU143637  
S000968111 Ehrlichia canis; ECAN\_bkk\_07; EU263991  
S000979425 Ehrlichia canis; Kutahya; AY621071

**Figure 36** The snapshot for *in silico* sequence-specific analysis of the PNA probe.

## The detection of ssDNA by PNA probe in the GO platform

In recent years, the 2D and 3D carbon sheets, for example, GO, reduced GO, and carbon nanotubes become popular in DNA sensor applications towards quenching the fluorescence of light-up probe. The developed method has been established in successful detection for ssDNA in a homogenous solution.<sup>19,20,37,52,53</sup> The quenching mechanism is based on the strong adsorption of a single-stranded probe to the GO surface, causing fluorescence quenching of nearby organic dyes. When the hybrid had formed, the PNA-DNA duplex would desorb from GO surfaces because the nucleobases would now be concealed inside the double helix. So, the lower interaction of PNA-DNA/GO leads to restoring the fluorescence signals.<sup>54</sup> In this section, the ssDNA detection by pyrrolidinyl PNA probe in the GO platform was initially discussed as following:

### 1. Fluorescence stability of PNA probe in Tris-HCl buffer

Some of the known drawbacks for the use of a fluorescent-based PNA probe are that the diluted PNA easily loses its function, by adsorbing on vessel walls over time especially in the presence of GO, because PNA can interact readily with plastic surfaces or hydrophobic proteins.<sup>43</sup> To avoid non-specific adsorption of PNA and enhance PNA solubility, many approaches have been reported, for example, structural modifications,<sup>50,55,56</sup> or conjugating with solubility moieties (e.g. charged-amino acid,<sup>57</sup> cell-penetrated peptides<sup>58</sup> or hydrophilic linkers,<sup>13</sup> etc.). In the past of years, our groups reported an *apc* spacer instead of *acpc* spacer within the chain of acpcPNA as shown in **Figure 37**.<sup>50</sup>

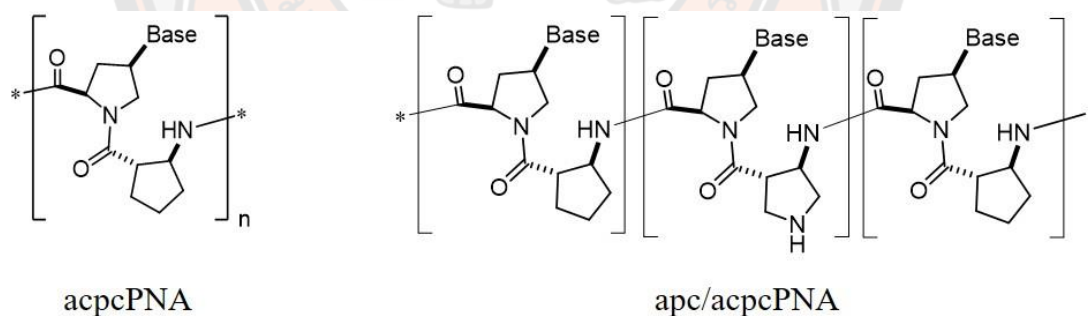


**Figure 37** The structure of acpcPNA and apc/acpcPNA probe.

In our previous study, the designing to have the pyrrolidine rings within the PNA chain will raise the partially positive-charges from *apc* spacers when it dissolves in an aqueous-based buffer solution. Moreover, the hybridization property to targeted complementary DNA, the apc/acpcPNA also displays a good affinity with high  $T_m$  likewise acpcPNA. Thus, to develop the pyrrolidinyl PNA probe in practical uses, the partially positive-charged apc/acpcPNA (**PNA2**) was utilized in a comparison with uncharged acpcPNA (**PNA1**) in the GO platform for ssDNA detection.

The expectation is that the partially positive-charged *apc/acpc*PNA should reduce the non-specific interaction from hydrophobic PNA to plastic surfaces used in this study (**Figure 38**). So, The Flu-labeled *apc*PNA (**PNA1**) and *apc/acpc*PNA (**PNA2**) were consequently synthesized by manual SPPS methodology corresponding to the previously published method,<sup>49</sup> giving 25% yield for **PNA1** and 12% yield for **PNA2** in high purity (>90%). HPLC results as shown in an appendix (**Figure 63-64**), the two peaks of each product were observed due to the presence of 5(6)-isomers of fluorescein tagged dye. Then, these synthesized pyrrolidinyl PNA probes were identified by MALDI-TOF mass spectroscopy; **PNA1** (calculated  $[M+H]^+$  3810.064, found 3811.282) and **PNA2** (calculated  $[M+H]^+$  3813.028, found 3812.985). Finally, the binding property of probes to targeted complementary ssDNA by the  $T_m$  experiment was confirmed, showing that both PNA can stably bind with a target in a sequence-specific manner ( $T_m = 59^\circ\text{C}$  for **PNA1** and  $T_m = 55^\circ\text{C}$  **PNA1**) as see in an appendix (**Figure 65-68**).

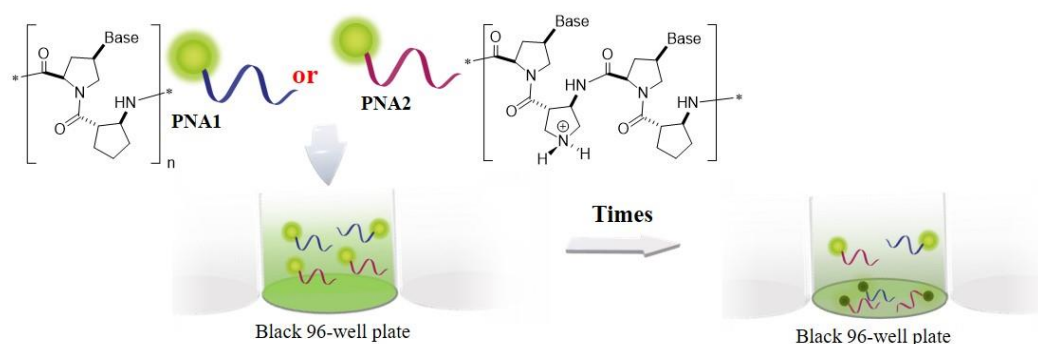


**Figure 38 Schematic illustration of possibly non-specific adsorption occurred between PNA and hydrophobic 96-well plate.**

Before adopting the PNA/GO system as a fluorogenic DNA sensor, an aliquot PNA (200 nM) was transferred to 25 mM Tris-HCl buffer pH 8.0 and 50 mM NaCl in the absence of DNA within a 96-well plate following with scanning the fluorescence emission on the microplate reader over 60 min periods. The excitation wavelength was set at 460 nm, whereas emission spectra were recorded in a range of 500 – 700 nm. As displayed in **Figure 39**, The maximum emission wavelength of both was obtained at 530 nm. the initial relative fluorescence intensity of **PNA1** was higher than **PNA2** ~1.4 folds (black lines). Meanwhile, the relative fluorescence intensities from the recording were gradually decreased with exponential over time since Flu-labeled PNA was slowly adsorbed on a plate's surface. This phenomenon denoted that non-specific fluorescent quenching of PNA could have occurred corresponding to a recently published report by Min and co-worker.<sup>43</sup> Upon evaluating the loss fluorescence in percentage scale compared with initial signals (black lines), the results found that fluorescence intensities at 530 nm of **PNA1** and **PNA2** were decreased around 51% and 58% after 1 h (orange lines), respectively. The fluorescence obtained from this study hypothesized that the electronic interaction between dissolved ions (Tris-HCl, salts) and partially positive-charged *apc* constituents of **PNA2** affords to nearby organic dyes, introducing quenching behavior. These results suggested that

**PNA2** bearing partially positive-charges relieves sufficiently unable to reduce the hydrophobic adsorption between PNA and the plastic surface of 96-well plate with loss fluorescent signal over time.

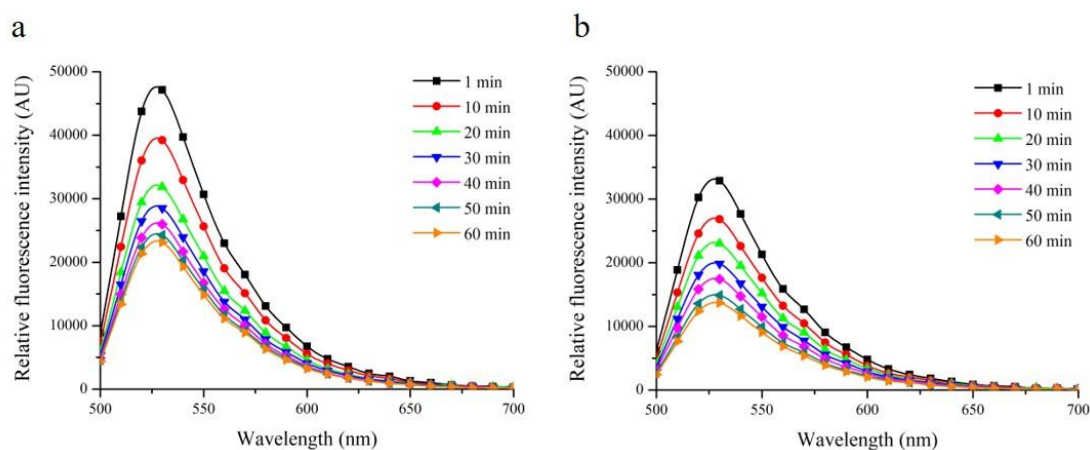


**Figure 39** The decreasing of fluorescence signals of (a) PNA1 and (b) PNA2 in Tris-HCl buffer over 1 h period.

The fluorescence spectra were measured in 25 mM Tris-HCl pH 8.0 and 50 mM NaCl, [PNA] = 200 nM, total volume = 200  $\mu$ L, excitation at 460 nm.

## 2. Fluorescence quenching ability of GO to Flu-labeled pyrrolidinyl PNA

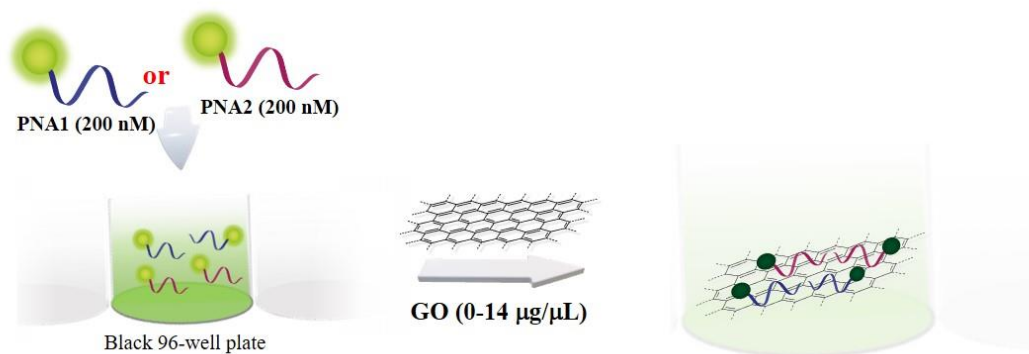


**Figure 40** Schematic illustration for studying fluorescence quenching of GO to Flu-labeled pyrrolidinyl PNA.



For detection of ssDNA by the PNA/GO system, the optimal GO used for quenching to PNA (200 nM) was firstly determined by adding the various concentrations of GO (0 - 14  $\mu\text{g}/\text{mL}$ ) into Tris-HCl buffer containing PNA suddenly and then, measuring fluorescence as same as previous protocol (as seen in **Figure 40**). The fluorescence emission spectra of PNA/GO-mixed solutions were recorded on a microplate reader every 10 min until the 1 h period. The results founded that the relative fluorescence intensity of both **PNA1** and **PNA2** was decreased obviously according to the increasing of GO and disappeared completely upon using 10  $\mu\text{g}/\text{mL}$  GO (dark-green lines in **Figure 41a** and **41b**). Then, the relative fluorescence intensity ( $F$ ) obtained at 530 nm was evaluated to be a percentage of fluorescence quenching (%Q) by using equation (2).

$$\%Q = (F_{ssPNA} - F_{ssPNA+GO} / F_{ssPNA}) \times 100\%$$

As seen in **Figure 41c**, at a low concentration of GO (2  $\mu\text{g}/\text{mL}$ ), the fluorescence signal of **PNA1** was quenched moderately around 70% and remained slightly lower than **PNA2** upon increasing the GO (black-line compared with red-line). Meanwhile, at a higher GO concentration (10  $\mu\text{g}/\text{mL}$ ), the highest fluorescent quenching ability to both Flu-labeled pyrrolidiny PNA was observed up to 96-97%. **Figure 41d**, the kinetic studies of each PNA with 10  $\mu\text{g}/\text{mL}$  GO were showing that **PNA2** was quenched rapidly around 79% (1 min) and slightly more than **PNA1** (~74%). The adsorption of the PNA/GO complex has proceeded completely after 10 min. These results obtained from this optimizing implied that unpaired nucleobases and hydrophobic backbones of PNA were considerably adsorbed on the GO surface *via* strongly  $\pi$ - $\pi$  stacking interaction, hydrophobic driving force, and occurring hydrogen bonding between exocyclic amino groups and carboxyl- and epoxy on GO layer.<sup>15</sup> In particular, the partially positive-charged moieties of **PNA2** were greatly undergone to electrostatically interact with GO, leading to quenching fluorescence of nearby tagged-dyes consequently.<sup>59,60</sup> The comparison of the **PNA1** and **PNA2** in the GO platform was examined towards ssDNA detection.

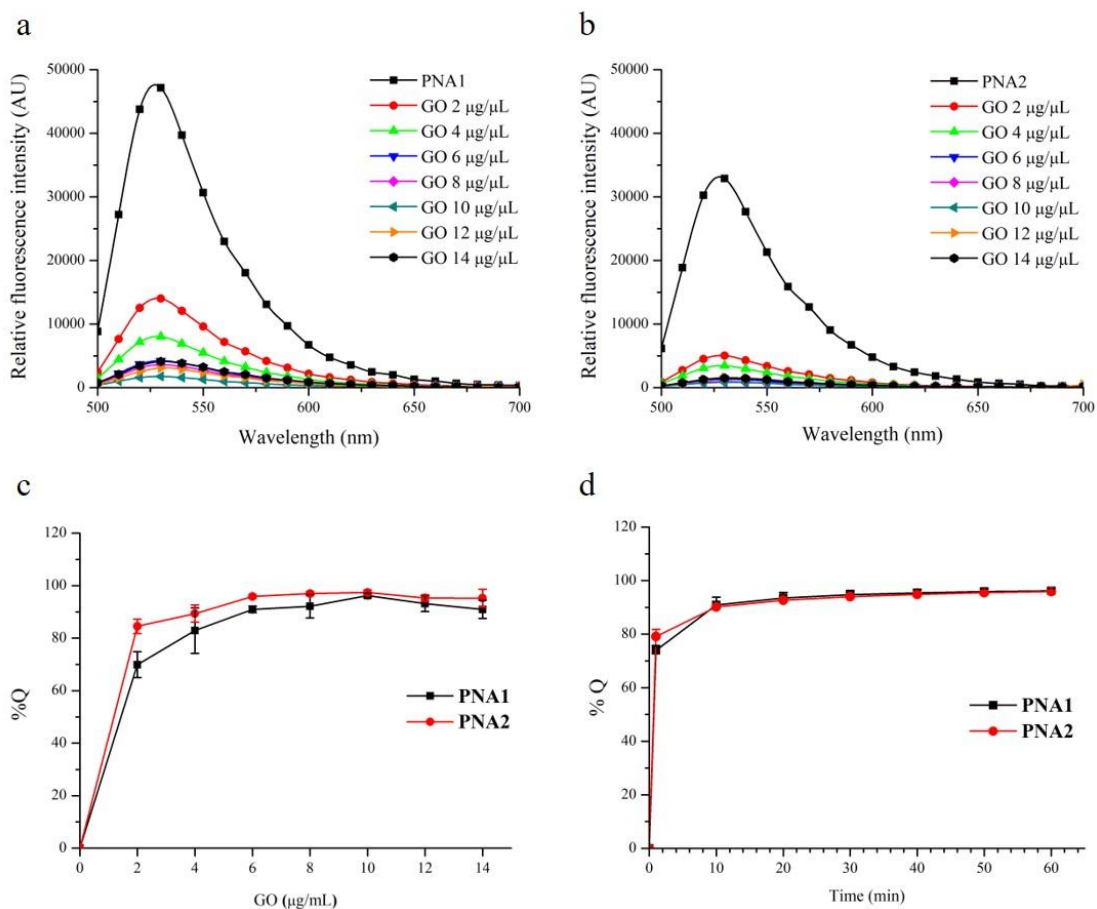


**Figure 41** The study of GO-quenching PNA1 and PNA2.

The fluorescence emission spectra of (a) PNA1 (b) PNA2 in the presence of different GO concentration (0 - 14 µg/mL). (c) %Q of PNA1 and PNA2. (d) Kinetics of PNA1 and PNA2 with 10 µg/mL GO in Tris-HCl buffer. The error bars indicate triplicated measurement. Conditions; the spectra were recorded in 25 mM Tris-HCl pH 8.0 and 50 mM NaCl, [PNA] = 200 nM, [GO] = 0-14 µg/mL, total volume = 200 µL, excitation at 460 nm.

### 3. The sequence specificity of PNA probe in the GO platform

The specificity of PNA probes was demonstrated by using ssDNA comprising complementary, single-, and double-mismatched sequences as **DNA1-5** (sequences as shown in **Table 5**) and dividing the study into 2 parts. **Route A** or **DNA Pre-mixing**, the PNA has been mixed with ssDNA to preparing PNA-DNA hybrid before, then solution was added by GO and incubated at RT for 1 hour. Another **Route B** or **DNA Post-mixing**, the PNA solution was saturated onto GO firstly and incubated with various types of ssDNA for 1 h subsequently (**Figure 42**).

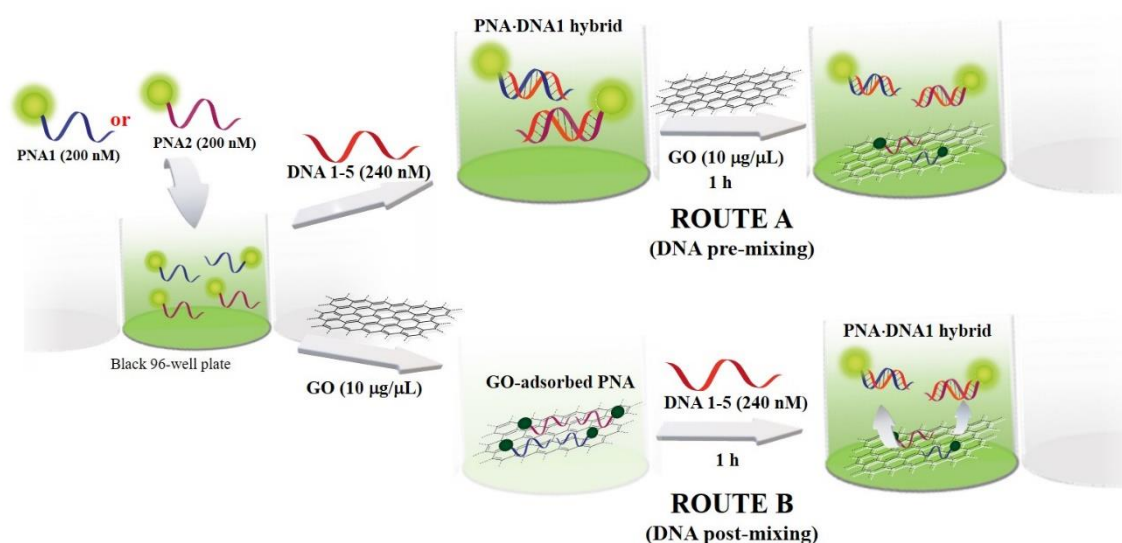


**Figure 42 Schematic illustration of specific ssDNA detection.** The study was divided into 2 parts including (a) DNA Pre-mix; mixing ssDNA with PNA before adding GO, or (b) DNA Post-mix; saturating PNA on GO before adding ssDNA.

**Table 5 PNA and Oligonucleotide sequences in the sequence-specific study.**

Oligonucleotides	Sequences (5'→3' or N'→C') <sup>b</sup>	Notes
Pyrrolidiny PNA <sup>a</sup>	Flu- <u>ACAATTTCT</u> -Lys-NH <sub>2</sub>	(PNA1 and PNA2)
DNA1	AGGAAATTGT	Complementary DNA
DNA2	AGGATATTGT	Single-mismatched T
DNA3	AGGAGATTGT	Single-mismatched G
DNA4	AGGACATTGT	Single-mismatched C
DNA5	AGGTTAATTGT	Double-mismatched T, A

<sup>a</sup>the underlines indicate the use of APC spacers instead of ACPC spacers. <sup>b</sup>the yellow boxes imply the base-mismatched positions.

The fluorescence emission spectra were recorded on the microplate reader as same as the previous section. The slight blue shift was observed upon forming PNA·DNA hybrid as presented in **Figure 43**. For **Route A; DNA pre-mixing**, the fluorescence emission of **PNA1·DNA1/GO** complex obtained from red-line in **Figure 43a** was remained and given a value higher than other ssDNA (**DNA2-5**) around 9-11 folds. The same manner was observed in **PNA2** (**PNA2·DNA1/GO** complex) except in the case of a single-mismatched T sequence (**DNA2**). The fluorescence of target binding was presented higher than the binding for single-mismatched T ~2.6 folds. Besides, the fluorescence of **PNA2·DNA2/GO** obtained from the blue-line in **Figure 43b** was given rather than other **DNA3-5** around 6-8 folds (pink, green, orange lines in **Figure 43b**). Based on these findings, it could preliminarily summarize that **PNA2** could bind with non-targeted DNA (single-mismatched T) and remain fluorescence signal in GO solution. When **PNA2** dissolved in the Tris-HCl buffer (pH ~8), the pyrrolidine-nitrogen ( $pK_a \sim 8.75$ ) was in the protonated form. It is possible that the non-targeted binding of **PNA2** to **DNA2** (single-mismatched T) would be occurred by the favorable electrostatic attraction between the positively charged *apc* spacers and the negatively charged phosphate-backbone of DNA.<sup>50</sup>

In the fluorescent restoration potency study of the PNA/GO system towards DNA detection, the PNA was saturated onto GO firstly to quenching the fluorescence of the light-up probe and incubated subsequently with incoming DNA for 1 h (**Route B; DNA Post-mixing**). The fluorescence emission spectrum of each experiment was recorded on a microplate reader as same as **Route A**. As the results shown in **Figure 43c-d**, the fluorescence emission of both **PNA1** and **PNA2** in case of mixing with the targeted sequence was poorly recovered by restoring signals higher than the background (PNA/GO complex) only 2-fold (red lines in **Figure 43c** and **43d**) which no different from mismatched sequences. The hypothesis is that hydrophobicity of PNA's backbone extremely adsorb on the GO with great affinity, so PNA·DNA could not easily release into the solution. Even through, the fluorescent recovering potency can be enhanced by taking long periods (more than 1 hour) together with the elevated temperature (less than  $T_m$ ) for targeted hybridization,<sup>20,37</sup> but the requirement of times becomes the limitation of the method. Therefore, the order of addition is an important role in adopting the PNA/GO system towards DNA detection. Moreover, **PNA1** is chosen for next experiment because its high sequence-specificity rather than **PNA2**.

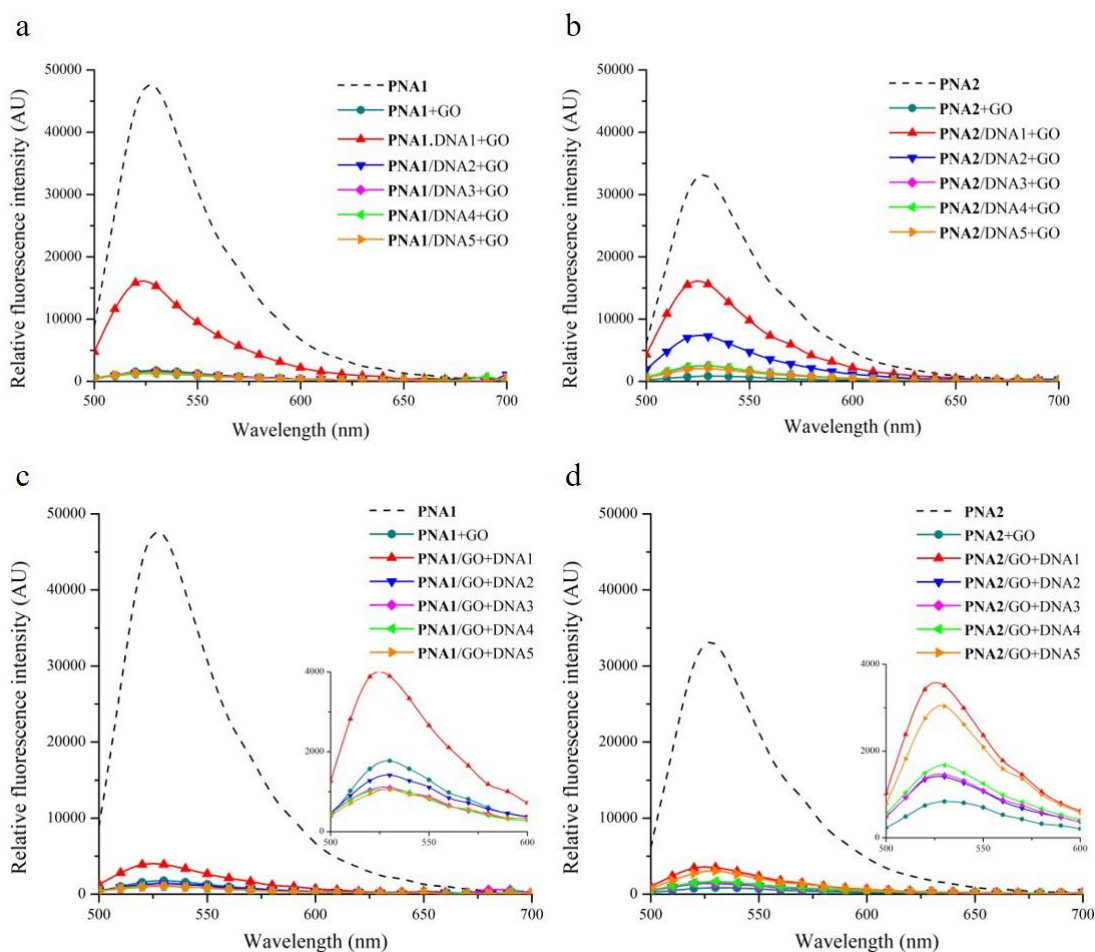


**Figure 43** The fluorescence emission spectra of specific ssDNA detection by Route A; DNA pre-mixing of (a) PNA1 and (b) PNA2, and Route B; DNA post-mixing of (a) PNA1 and (b) PNA2 in GO platform.

Route A; each of ssDNA (240 nM) was mixed with PNA1 or PNA2 (200 nM) in 25 mM Tris-HCl pH 8.0 and 50 mM NaCl before adding 10  $\mu\text{g/mL}$  GO. Route B; PNA1 or PNA2 (200 nM) in 25 mM Tris-HCl pH 8.0 and 50 mM NaCl was saturated on 10  $\mu\text{g/mL}$  GO following with incubating ssDNA (240 nM) at RT for 1 h. Total volume = 200  $\mu\text{L}$ , excitation at 460 nm.

#### 4. The sensitivity DNA detection by PNA probe in the GO platform

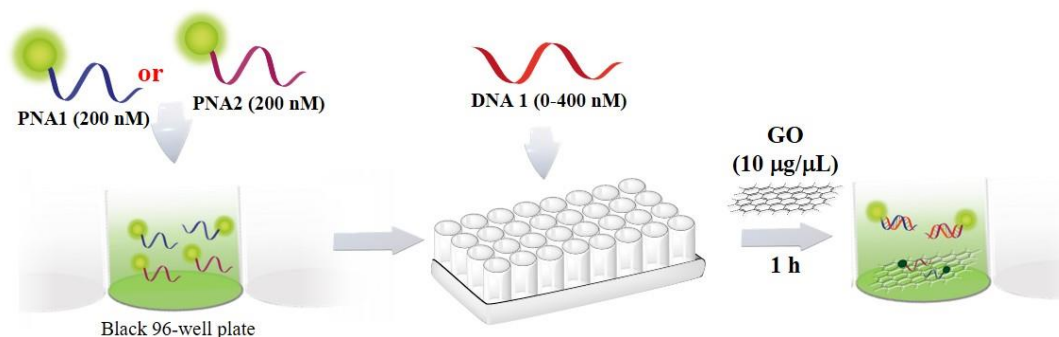


**Figure 44** Schematic illustration for sensitivity ssDNA detection by PNA/GO system.

In this study, the sensitivity of the detection was demonstrated with various concentrations of **DNA1** ranging from 0 nM to 400 nM. The PNA was hybridized with complementary DNA before incubating with 10 µg/mL GO (**Figure 44**). After 1 hour, fluorescence emission spectra were recorded on the microplate reader. The results showed that the fluorescence of both **PNA1** and **PNA2** was increased according to the increasing amount of **DNA1** (**Figure 45a** and **45b**). Additionally, this assay indicated good linear relationship between relative fluorescence intensity of PNA at 530 nm (y) and concentration of **DNA1** (x) in range of 0-160 nM with good linearity,  $R^2 = 0.9892$  for **PNA1** (**Figure 45c**), and  $R^2 = 0.9703$  for **PNA2** (**Figure 45d**). The limit of detection (LOD) was evaluated using equation (3);<sup>20</sup>  $LOD = 3.3 \times (SD/S)$ . Where  $SD$  is standard deviation of each PNA-GO complex (283.89 for **PNA1** and 186.56 for **PNA2**) and  $S$  is a slope of the calibration curve. It was indicated that these PNA probe in GO platform have a good limit of detection at 8.84 nM and 7.38 nM for **PNA1** and **PNA2** respectively. This can be concluded that the targeted complementary ssDNA was successfully detected by GO-based PNA probe with high sequence specificity and high sensitivity. Based on all results mentioned above, the concept of the acpcPNA probe (**PNA1**) in the GO platform would capably use for DNA detection. With amplification assays such as PCR or RPA, this platform is simple and rapid for DNA target detection

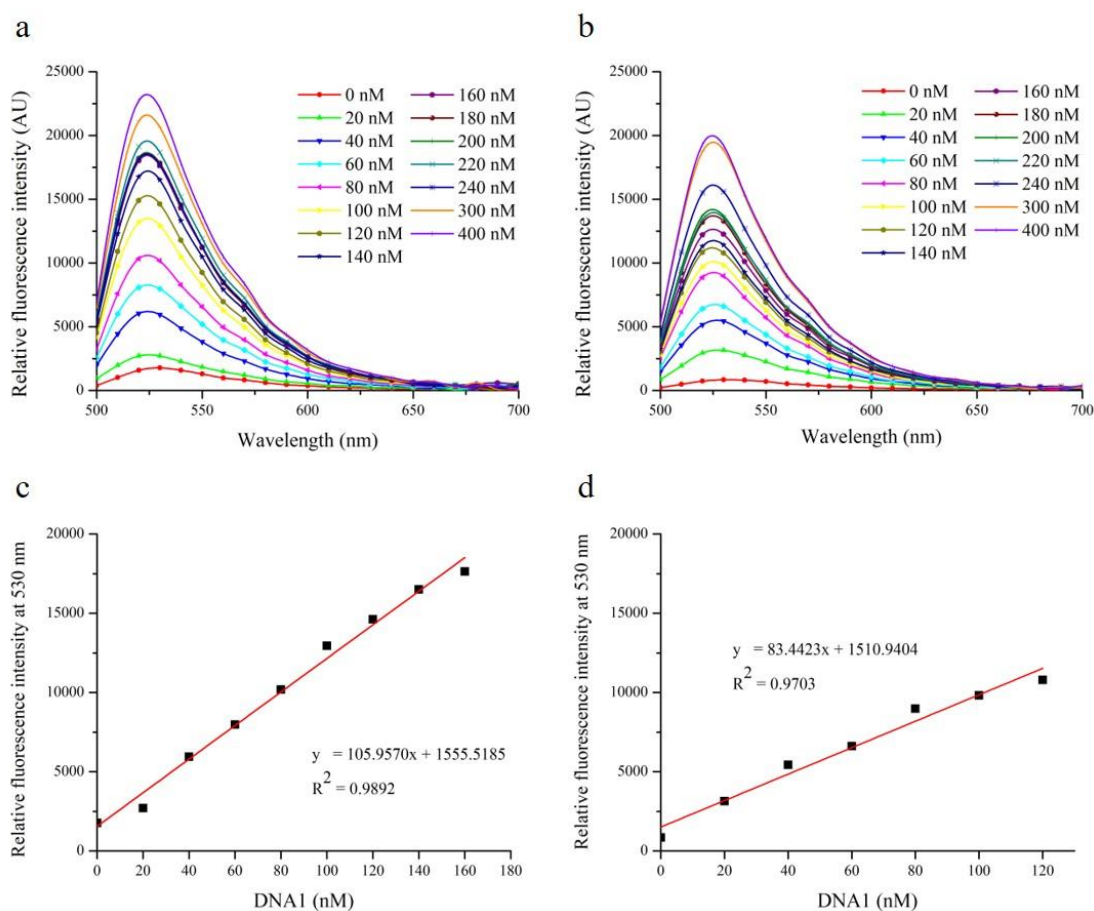


**Figure 45** The fluorescence emission spectra of (a) PNA1 and (b) PNA2 upon the increasing concentration of DNA1. The linear calibration curve plots between relative fluorescence intensity at 530 nm of (c) PNA1 and (d) PNA2 with different concentrations of DNA1.

**Condition;** [PNA] = 200 nM, [DNA1] = 0-400 nM, [GO] = 10  $\mu\text{g/mL}$  in 25 mM Tris-HCl pH 8.0 and 50 mM NaCl, total volume = 200  $\mu\text{L}$ . Measurement; microplate reader, excitation at 460 nm and emission in range of 500-700 nm.

## The preliminary study for dsDNA detection

### 1. Effect of PCR components

The attempt to use PNA/GO system for straightforward detecting dsDNA obtained from PCR was investigated, firstly the **PNA1** (200 nM) was added into PCR reaction-solution (in the absence of dsDNA), following with the addition of GO (10  $\mu\text{g}/\mu\text{L}$ ). As a result, the fluorescent background signal (PNA-GO complex) was not quenched as obvious presenting (data not shown). The hypothesis for this phenomenon is that PNA cannot interact well with the GO surface in this condition (as shown in the scheme of **Figure 46**). In the presence of some chemical reagents in the PCR reaction-solution, for example, detergents, formamide, DMSO, betaine, dNTPs, unused primers, glycerol, polyethylene glycol (PEG) as well as *Taq* DNA polymerase, could disrupt to PNA adsorption on the GO, leading to giving a high signal's background. As previously reported by Giuliadori and coworkers,<sup>23</sup> the DNA probe in the GO platform was developed as a *cspC* DNA sensor by using unlabeled primers for PCR amplification and DNA probe for fluorescence-based amplified DNA detection. The results from their experiments showed that dNTPs were affected for GO-based PNA·DNA<sub>target</sub> complex, whereas unrelated DNA primers could introduce the non-specific fluorescence by non-specific replacement mechanism. To find what are PCR components affecting to PNA/GO adsorption, the experiment were designed and tested by measuring the fluorescence of PNA and PNA/GO complex in the presence of PCR buffer (bearing detergents, formamide, DMSO, betaine, BSA, salts, PEG, *etc.*), dNTPs, primers, and glycerol (glycerol refers to *Taq* DNA polymerase solution) as depicted in **Table 6**.

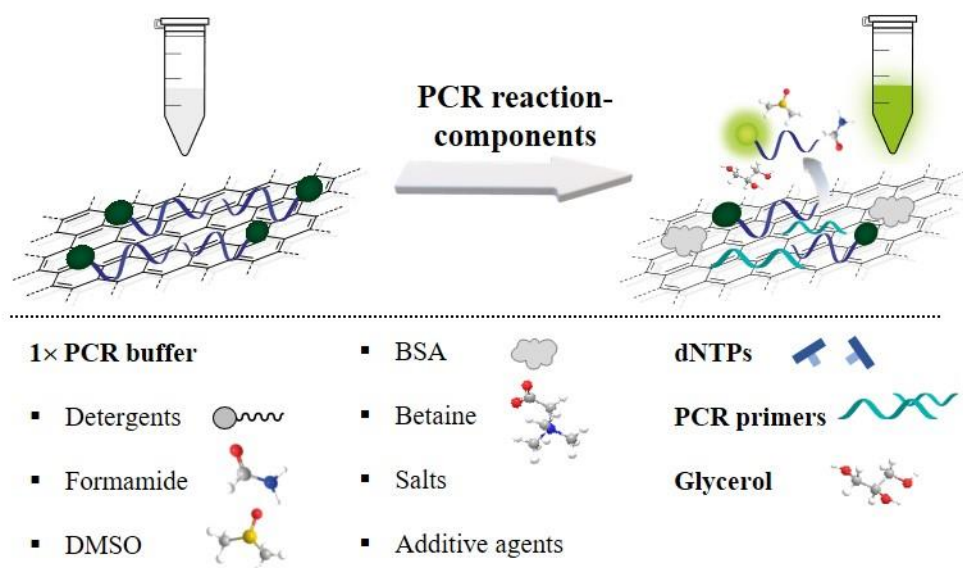


**Figure 46** Schematic illustration of the effect of PCR reagents to PNA/GO complex.



**Table 6 The experiment setup for studying of PCR reagent-induced PNA desorption.**

Experiment (EX)	PNA1/GO system (200 nM : 10 µg/mL) in buffer
1	25 mM Tris-HCl pH 8.0 and 50 mM NaCl
2	1× PCR buffer
3	1× PCR buffer, 200 nM of dNTPs
4	1× PCR buffer, 200 nM of each primer
5	1× PCR buffer, 0.24% v/v glycerol

The PCR reaction-reagents in each experiment were prepared before used on 20 µL of volume. Then, **PNA1** (200 nM) was added into an aliquot and adjusted to 50 µL of the final volume by 20 µL of Milli Q or aqueous GO to making 10 µg/mL of the final concentration. The GO-suspended solution was kept at RT for 1 h and then centrifuged. Relative fluorescence intensity was measured subsequently on the end-point mode in the FAM channel of Bio-rad real-time PCR. In the absence of GO, the fluorescences of **PNA1** achieved from PCR-based solution were slighter than **PNA1** in Tris-HCl as experiment 1 (EX1) as shown in dark bars, **Figure 47a**. Meanwhile, in the presence of GO, the fluorescences of the PNA/GO complex were quenched as fluorescent background. When compared the ratio between the fluorescence of **PNA1** in the absence ( $F_1$ ) and presence of GO ( $F_0$ ), the result found that the difference of fluorescence signal was considerable decreased (**Figure 47b**). These results suggested that the chemical reagents in PCR reaction-buffer comprising DMSO, formamide, surfactants, proteins, dNTPs, DNA primers, glycerol can interrupt the PNA adsorption process, resulting in presented fluorescence as background. DMSO and formamide which are the denaturing agents in PCR can form the hydrogen bonding with nucleobases or carboxyl as well as epoxy groups of GO. Additionally, glycerol used for dissolving and stabilizing *Taq* DNA polymerase can stabilize the PNA molecule by surrounding it into a solution phase as shown in **Figure 48**. Hence, the optimal GO concentration used for the quenching **PNA1** was re-determined. The result found that **PNA1** in the presence of PCR reagents requires a GO content at 40 µg/mL to quenching **PNA1** in the final volume of 50 µL (**Figure 49a**) with 94% quenching (**Figure 49b**), respectively.

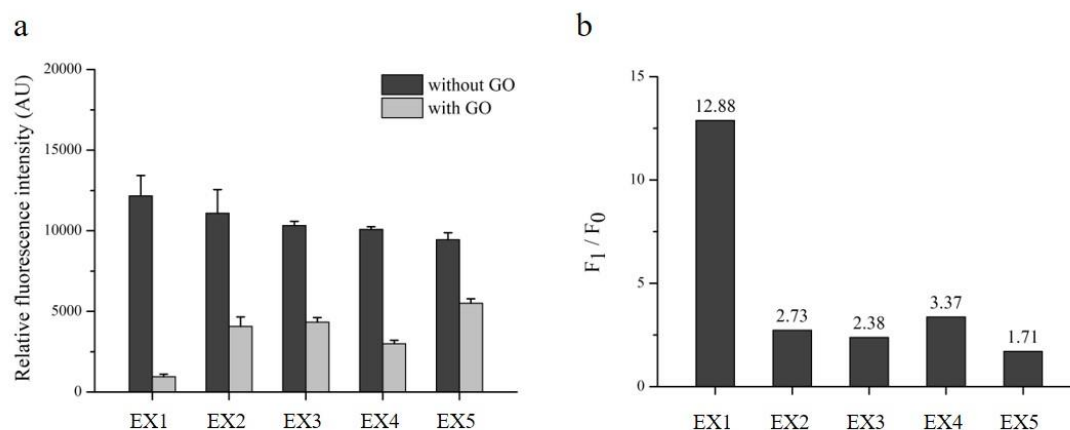


**Figure 47 (a) Relative fluorescence intensity of PNA with and without GO in the presence of different PCR reagents and (b) their  $F_1/F_0$  values. Conditions; [PNA1] = 200 nM in 1× PCR buffer, [dNTP] = 200 nM, [each primer] = 200 nM, [glycerol] = 0.24% v/v, [GO] = (10  $\mu\text{g/mL}$ ), volume = 50  $\mu\text{L}$ , time = 1 h.**

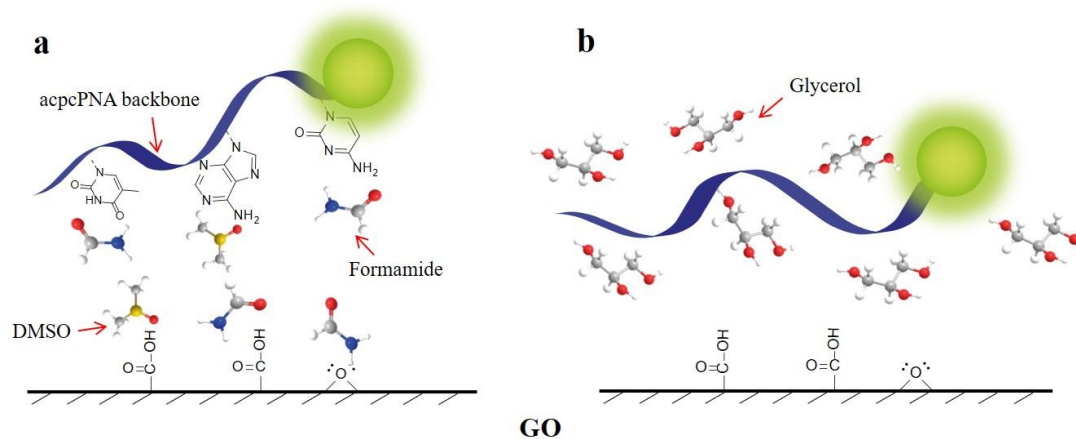


**Figure 48 Schematic illustration of PCR reagents induce the release of PNA from the GO surface. (a) The PNA desorbed from GO by forming a hydrogen bonding with formamide or DMSO. (b) The PNA was stabilized into the solution phase by glycerol.**

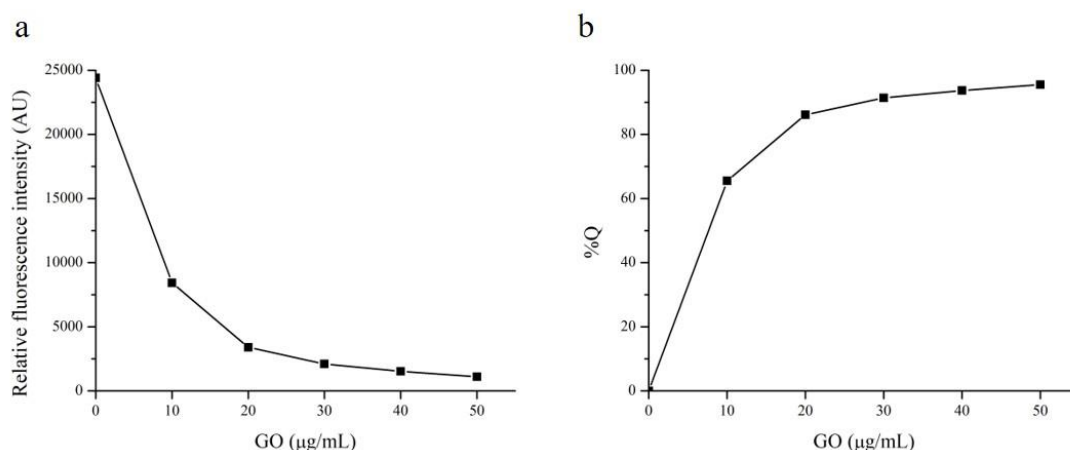


**Figure 49** The re-determination of optimal GO for quenching PNA1 in presence of PCR reaction-components. (a) The relative fluorescence intensities of PNA1 and (b) their %Q upon increasing GO.

Conditions; [PNA1] = (200 nM) in 20 µL of PCR reaction-buffer, [GO] = 0 - 50 µg/mL, volume = 50 µL.

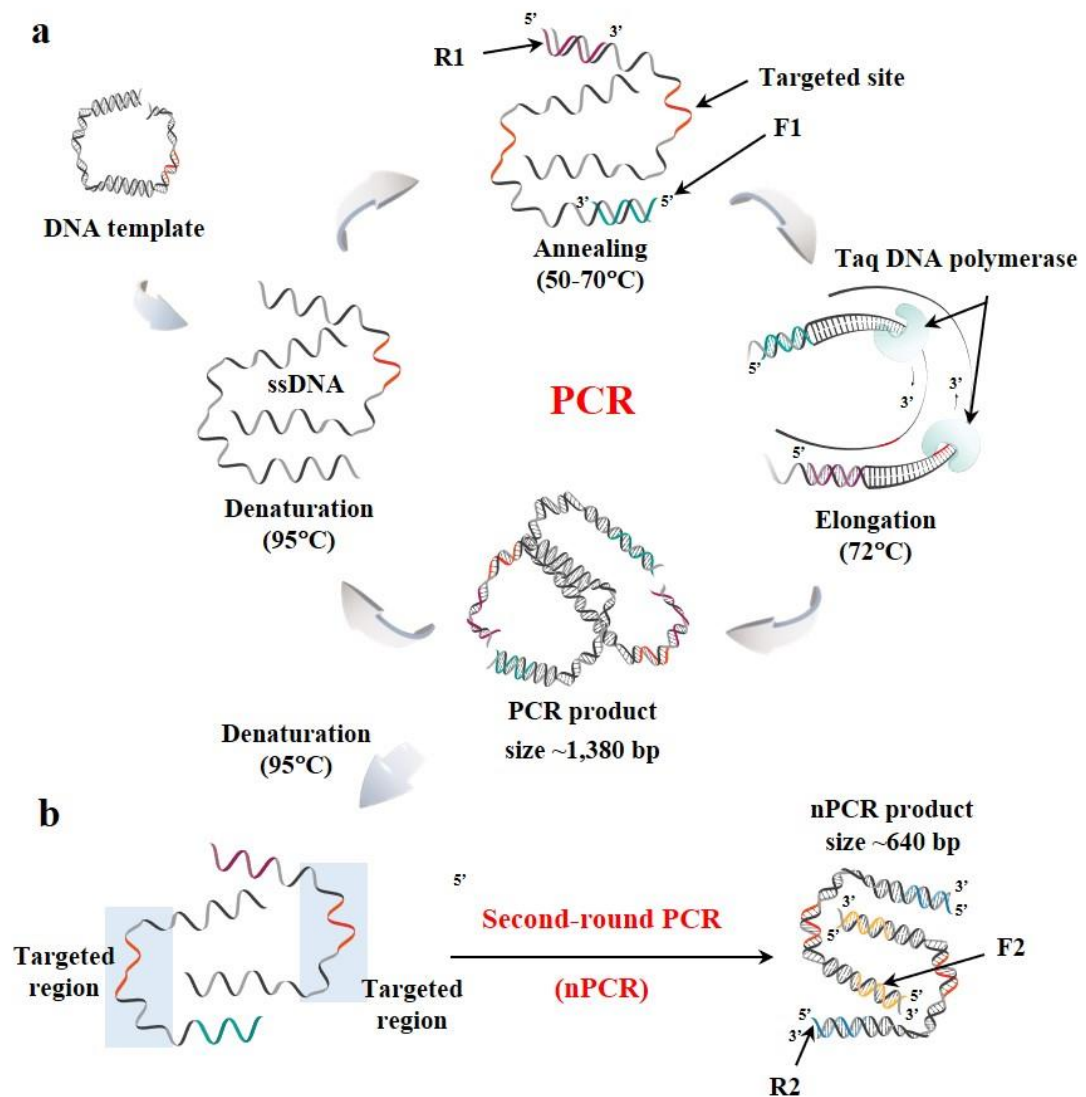
## 2. The detection of dsDNA (PCR product) by PNA probe in the GO platform

### 2.1 Specificity of primers

In this section, the DNA used for PCR and nPCR was extracted from dogs' blood which was received from an Animal Molecular Diagnostic Service, Chiangmai province, Thailand. The DNA samples have been confirmed to identify infected parasites by conventional PCR and High-Resolution Melting Analysis (HRM), supported by Assistant Professor Dr. Kittisak Buddhachat (Department of Biology, Faculty of Science, Naresuan University). PCR is a sensitive method for detecting and characterizing monocytic ehrlichiosis in dogs.<sup>32,51,61,62</sup> Several methods are based on different targets, for example, *16S rRNA*, *p28*, *p30*, *dsb*, *VirB9* genes.<sup>26</sup> As shown in **Figure 50**, the basic steps of PCR include cycles of DNA denaturation, annealing, and elongation which generates million to billion copies of a target gene. Meanwhile, nPCR is a modification of PCR for enhancing the sensitivity and specificity by using two sets of primers comprising outer (**F1**, **R1**) and inner (**F2**, **R2**) primers (sequences showed in **Table 7**). The first-round PCR was carried out **F1** and **R1** to generating PCR product with a size of ~1,380 bp. Subsequently, the second round was performed by **F2** and **R2** to amplifying the secondary target within 1<sup>st</sup> dsDNA, in size ~640 bp.

**Table 7 DNA primers in PCR and nPCR amplification.**

Primers	Sequences (5'-3')	Product sizes	Ref.
<b>F1</b>	ATCATGGCTCAGAACGAACG	1,380 bp	51
<b>R1</b>	GTGACGGGCAGTGTGTACAAG		
<b>F2</b>	AACGAACGCTGGCGGCAAGCC	640 bp	
<b>R2</b>	ACGAATTTACCTCTACACTAGGAATTCCGCTA		



In this study, the *E. canis* 16S rRNA gene was used as a target. Firstly, the inner primers (**F2** and **R2**) were initially demonstrated by using positive *E. canis* samples (confirmed by PCR and HRM) with annealing at 50°C for 40 cycles. PCR products were analyzed on EtBr-stained agarose gel electrophoresis as indicated in **Figure 51**. The DNA targets (~640 bp length) were present in all samples (lane 1-8), suggesting that these primers could successfully amplified DNA samples from the whole blood. Notably, the non-targeted bands were also found because it has various types of DNA within the DNA pool.

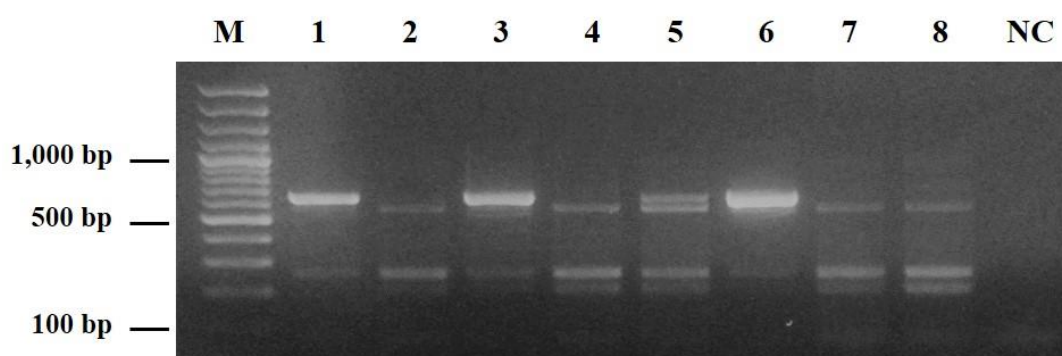


**Figure 51** Gel electrophoretic analysis of PCR products that used **F2** and **R2** as DNA primers.

**M** and **NC** indicate the DNA ladder and negative control. Conditions; an aliquot PCR product was subjected in 2%w/v agarose A gel in TAE buffer, and running at 100 V, 400 mA for 25 min. The gel was visualized under UV transilluminator (254 nm) by EtBr-straining.

### 2.2 Detection of dsDNA obtained from PCR

At the end of the PCR process, **PNA1** (200 nM) was added into 20  $\mu$ L of the PCR product and subsequently heated up to 95°C for 5 min. Then, the solution was annealed at 50°C for 30 min and cooled down to room temperature.<sup>23</sup> When GO (40  $\mu$ g/mL) was added into the solution, the visual fluorescence was not observed in all cases (data not shown). The hypothesis is that fluorescence might be quenched by long-chain dsDNA upon forming PNA·dsDNA strand-invasion complex, or non-specific adsorption of PNA·dsDNA might occur at high GO concentration (**Figure 52**). It is known that dsDNA can behave as a quencher *via* the transmission of photo-induced electron transfer along dsDNA.<sup>63</sup> Although, the ratio of GO and PNA was reduced by 4-fold corresponding to 10  $\mu$ g/mL GO and 50 nM PNA in final concentration, but fluorescence signal still not presented (**Figure 53**, tube 3).

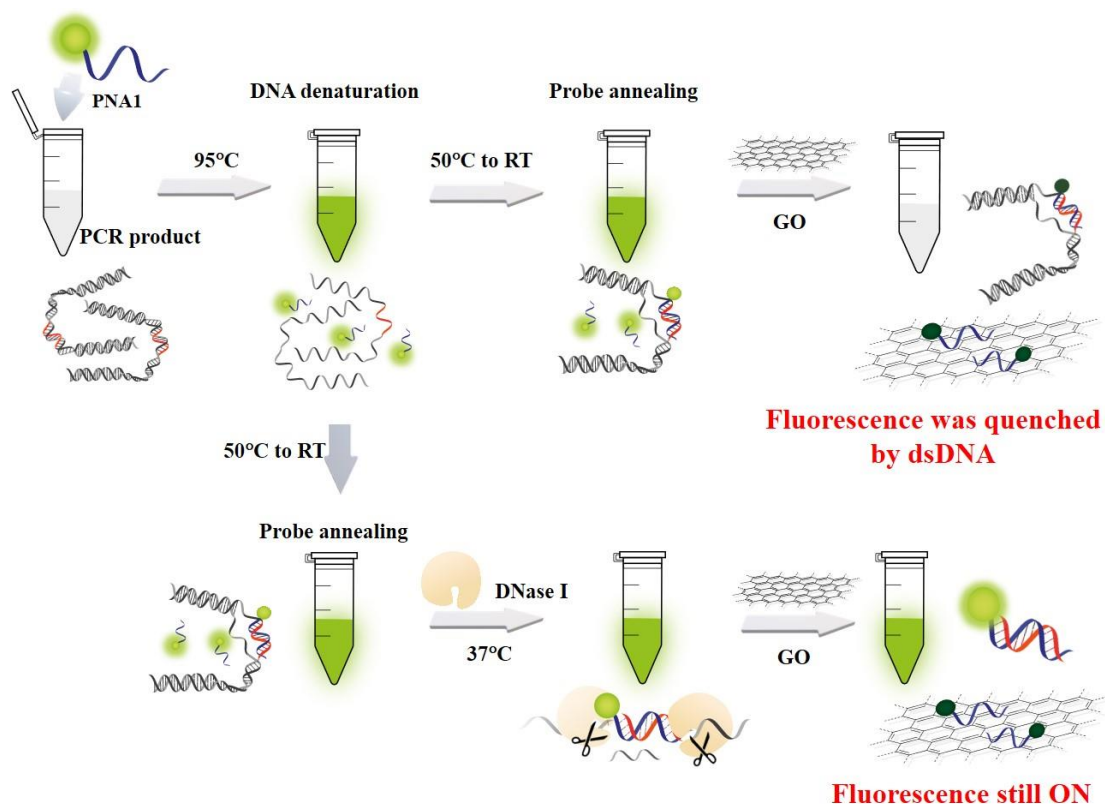


**Figure 52 Schematic illustration of GO quenching-based fluorogenic detection of dsDNA obtained from PCR.**

With this hypothesis in mind, the enzymatic digestion was next applied to treat PNA-dsDNA strand for eliminating dsDNA-induced quenching. The DNase I is one type of nuclease that cleaves DNA at the phosphodiester linkages to providing short DNA fragments. PNA·DNA<sub>target</sub> hybrid should remain in the enzymatic solution when dsDNA's specific region was invaded by the PNA probe (**Figure 52**). Hence, 1 U of DNase I was therefore added into PNA-dsDNA solution and incubated at 37°C for 10 min before adding 40 µg/mL GO. LED-based visualization of this experiment was shown in **Figure 53**. As a preliminary results, the fluorescence signal was only slightly presented in the presence of targeted dsDNA (tube 5), whereas the fluorescent signal of the non-amplified DNA sample was not observed (tube 6). Notably that PNA1·DNA<sub>target</sub> hybrid survived from the degradation process and remained in GO solution, resulting in the fluorescence signal recovering.

Tube	1	2	3	4	5	6
PNA1	+	+	+	+	+	+
target DNA	-	-	+	-	+	-
non-target DNA	-	-	-	+	-	+
DNase I	-	-	-	-	+	+
GO	-	+	+	+	+	+

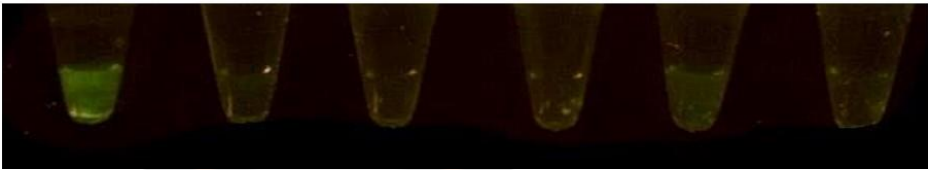


**Figure 53** The visual image of GO quenching-based fluorogenic detection of PCR product by the combination of GO-based PNA probe and DNase I treatment. **tube 1: PNA1 only, tube 2: PNA1-GO complex, tube 3: PNA1+dsDNA<sub>target</sub>+GO, tube 4: PNA1+dsDNA<sub>non-target</sub>+GO, tube 5: PNA1+dsDNA<sub>target</sub>+DNase I+GO, and tube 6: PNA1+dsDNA<sub>non-target</sub>+DNase I+GO.**

However, the visual fluorescence was still unclear enough due to the low concentration of targeted DNA amplicons. Hence, the assay volume was decreased subsequently from 50  $\mu\text{L}$  to 30  $\mu\text{L}$  by fixing PNA1 and GO at a ratio of 50 nM PNA1: 25  $\mu\text{g}/\mu\text{L}$  GO. Moreover, nPCR was attempted to enhance the targeted amplicons. The first-round PCR was carried out by outer primers (F1 and R1) that have been reported towards amplification of nearly full-length *E. canis* 16S rRNA.<sup>51</sup> The second-round PCR was performed on inner primers (F2 and R2) with annealing 10, 20, 30, and 40 cycles. A negative *E. canis* sample (as a positive *A. platys*) obtained from PCR (data supported from KB research group) and Milli Q water were included as a negative control (40 cycles).

Gel electrophoretic analysis showed that targeted bands (~640 bp) were clearly observed from the amplification of positive samples (lane 1-4) obtained from HRM, whereas a negative *E. canis* sample (as a positive *A. platys*) was also amplified (Figure 54a; lane 5). This result indicated that nPCR has a high performance enough for detecting a low copy of *E. canis* DNA within the DNA pool extracted from the whole blood with sensitive and specific rather than PCR. When applied DNase I-treated PNA/GO system into nPCR product, the visual fluorescence was obviously presented in only positive samples (Figure 54b). These results suggested that the specificity and sensitivity of this assay were enhanced upon using nPCR as an amplification method and depending on the degree of targeted amplicons. However, the determination of final DNA concentration was not demonstrated because it requires additional DNA purification kits and loss of times.

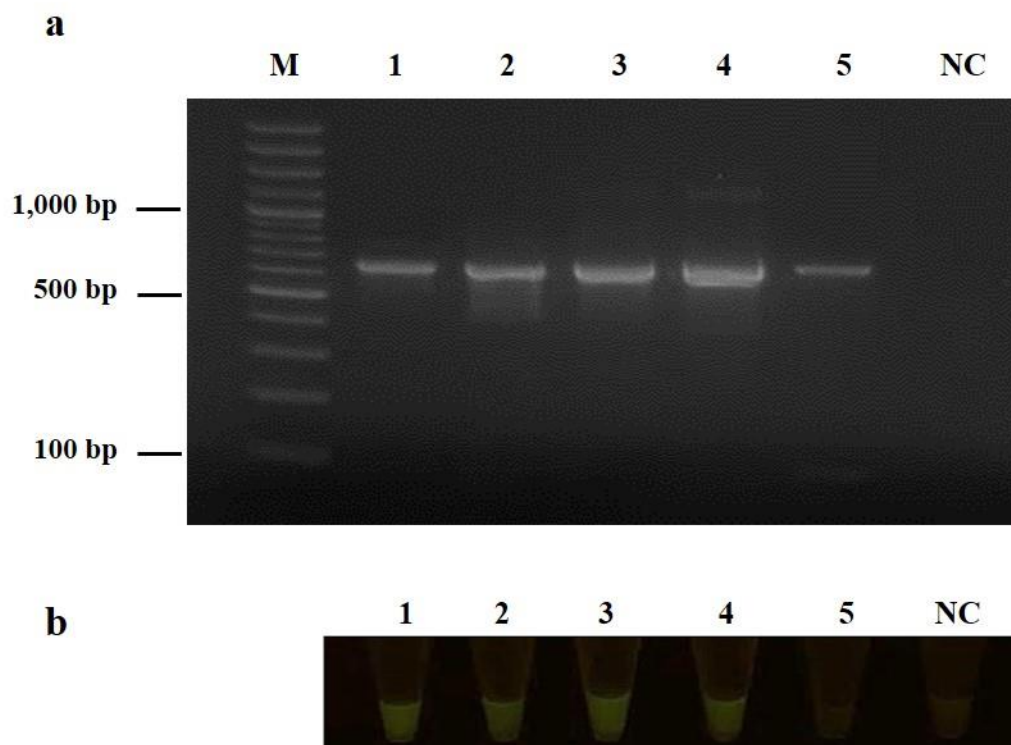


**Figure 54 (a) Gel electrophoresis of nPCR products and (b) fluorescence images based on DNase I-treated PNA/GO system.**

**M = DNA ladder, lane 1-4 = positive *E. canis* samples (10-40 cycles), lane 5 = negative *E. canis* sample (positive *A. platys* obtained from PCR), NC = negative control. Conditions; each of the nPCR product was subjected in 2%w/v agarose A gel in TAE buffer, and running at 100 V, 400 mA for 25 min. The gel was visualized under UV transilluminator (254 nm) by EtBr-straining.**

#### **Isothermal detection for dsDNA by RPA-DPG assay**

In recent years, RPA has been reported towards the identification of canine blood parasites, for example, *A. phagocytophilum*,<sup>64,65</sup> *B. gibsoni*,<sup>66</sup> and *Rickettsia rickettsii*.<sup>67</sup> Meanwhile, the detection of *E. canis* by using RPA assay has not been reported yet. RPA is one of the isothermal amplification techniques that use to generate multiple-copied genes of interest. The standard RPA assay comprises three key proteins as recombinase, recombinase loading factor, and single-stranded binding protein (SSB) in co-operation with ancillary components such as DNA polymerase, crowding agent, ATPs, and salts to perform the RPA reaction mechanism.<sup>68</sup> In principle, recombinase protein firstly binds together with primers to making a recombinase-primers complex. Then, the specific region within dsDNA is invaded by the recombinase-primers complex in the D-looped structure that the separately single-stranded DNA is stabilized by SSB protein. Second, the parental strand is separated and the new DNA strand is synthesized by DNA polymerase, providing two new DNA strands as RPA product harboring a specific site for PNA binding (**Figure 4, CHAPTER I**).



## 1. The optimization of the RPA reaction process

In this section, the plasmid DNA used as a template was cloned on the pUC57 vector by inserting 1 copy of the 16S rRNA genes of *E. canis* or *A. platys* and 18S rRNA genes of *B. vogeli* or *H. canis* into the genome of the vector. All processes in DNA cloning, extraction, and purification were supported by the KB research group. The pUC57-plasmid DNA of each was diluted into 1 ng/ $\mu$ L before used as a standard template, whereas the 1 ng/ $\mu$ L of pUC57-plasmid DNA of *E. canis* was calculated by equation (4) to give  $6.71 \times 10^8$  copies/ $\mu$ L as 1.11 pM. In optimization of RPA to amplifying targeted DNA, RPA assay was carried out using 1 ng/ $\mu$ L of pUC57-plasmid DNAs including *E. canis*, *A. platys*, *B. vogeli*, and *H. canis* which Milli Q water was used as a negative control (NC). Forward and reverse primers in this study are **F3** (5'-CGG CAA GCC TAA CAC ATG CAA GTC GAA CGG ACA AT-3') and **R2** (5'-ACG AAT TTC ACC TCT ACA CTA GGA ATT CCG CTA-3'). The selected RPA primer was referred to criteria suggested in the TwistAmp<sup>TM</sup> assay design manual (<https://www.twistdx.co.uk/>). Briefly, the GC content of the targeted region should be between 40 and 60%, and the selected primer should be 30-36 bp with GC content in the range of 20-70%.

The RPA reaction was optimized in factor of temperature, time, and specificity of primers. Firstly, the incubation temperature was optimized for 40 min by using temperature in the range of 20-50°C and subsequent analysis on EtBr-gel electrophoresis. As shown in **Figure 55a**, RPA product (size of ~628 bp) occurred in the temperature range of 20-40°C (lane 2-4). The optimal time for the RPA process was evaluated at 37°C for 5, 10, 20, 30, and 40 min. As shown in **Figure 55b**, agarose gel electrophoresis showed the appearance of a targeted band that was initially observed at 20 min and successfully amplified at 40 min, according to the manufactory protocol (available on <https://www.twistdx.co.uk/>). Finally, the specificity of RPA was performed at 37°C for 40 min by using pUC57-plasmid DNA including *E. canis*, *A. platys*, *B. vogeli*, and *H. canis* as DNA templates. As shown in **Figure 55c**, the targeted DNA was observed only in the presence of *E. canis* 16S rRNA (lane 1), suggesting that the RPA reaction was successfully amplified *E. canis* plasmid DNA in a short time as 20 min by these specific primers with incubating temperature in a range of 30-40°C.

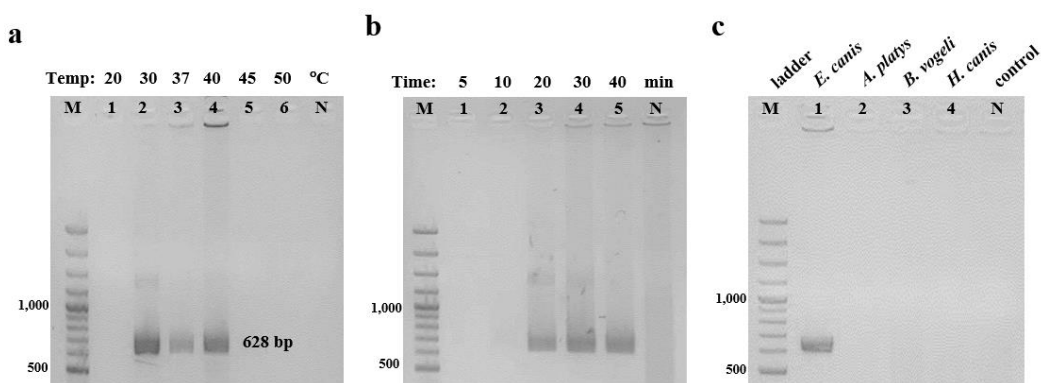


**Figure 55** The gel electrophoresis for the optimization of RPA conditions. The optimization (a) over a temperature range of 20-50°C (40 min) and (b) incubation periods of 5-40 min (37°C) using 1 ng pUC57-plasmid DNA of *E. canis* as DNA template. (c) The specificity test of RPA primers by incubating at 37°C for 40 min and using 1 ng pUC57-plasmid DNA of *E. canis*, *A. platys*, *B. vogeli*, *H. canis* as DNA template. M = DNA ladder, N = negative control. Conditions; each of RPA product was subjected in 2%w/v agarose A gel in TAE buffer, and running at 100 V, 400 mA for 25 min. The gel was visualized under UV transilluminator (254 nm) by EtBr-staining.

## 2. dsDNA detection by RPA-DPG assay

In a previously published report,<sup>38</sup> the D-loop formation in PNA·dsDNA strand-invasion complex at isothermal process could be stabilized by SSB proteins. Notably, SSB is presented in a common RPA reaction-kit, thus contributing to the advantage for dsDNA detection based on the PNA probe in GO platform when used in combination with DNase I digestion. As represented in **Figure 56**, the targeted dsDNA obtained from the RPA product was incubated with PNA1 to provide the strand invasion before the digestion and quenching steps. On the other hand, the non-targeted dsDNA that has not been hybridized with the PNA probe would be degraded under enzymatic hydrolysis and yielding DNA fragment. All processes were performed under isothermal incubation with a simple heating block, and the fluorescence intensity could be measured on the FAM channel of Bioer real-time PCR as well as visualizing fluorescence on blue-light LED transilluminator.

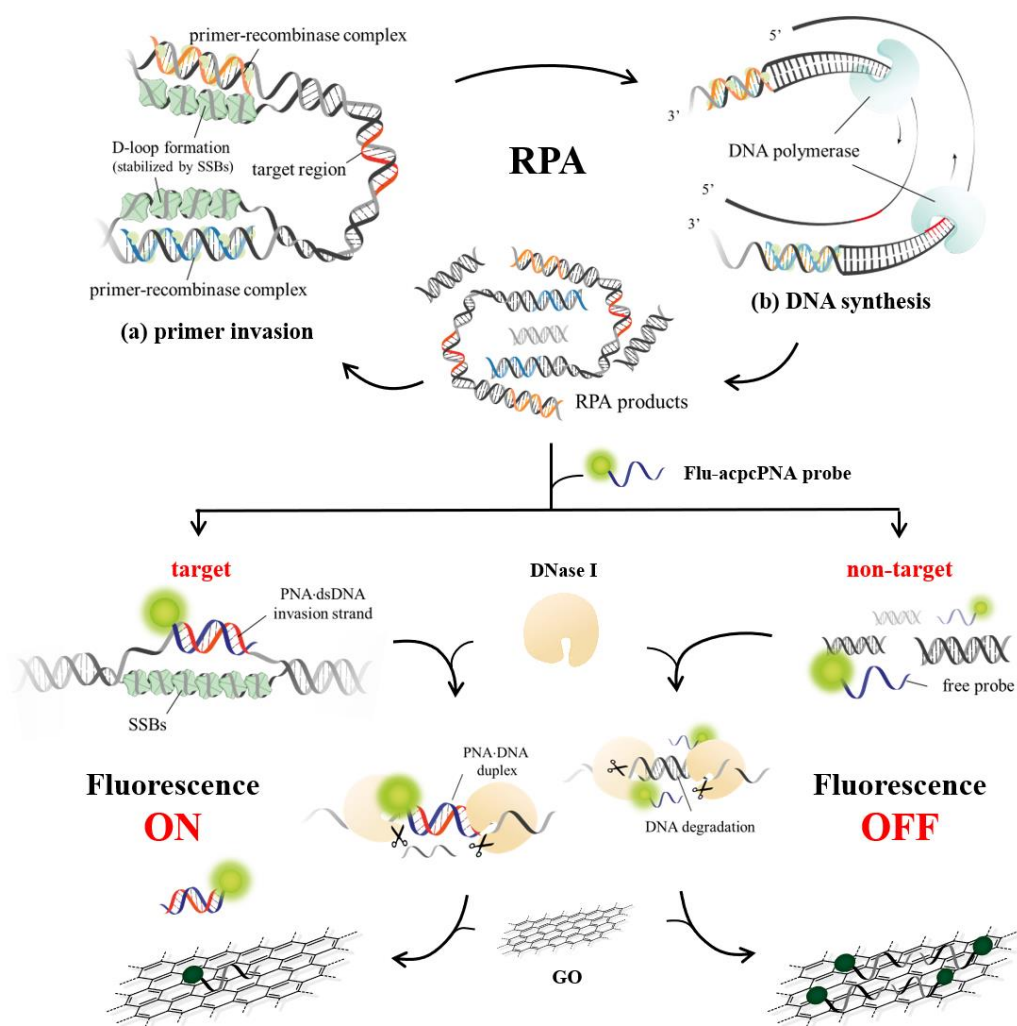
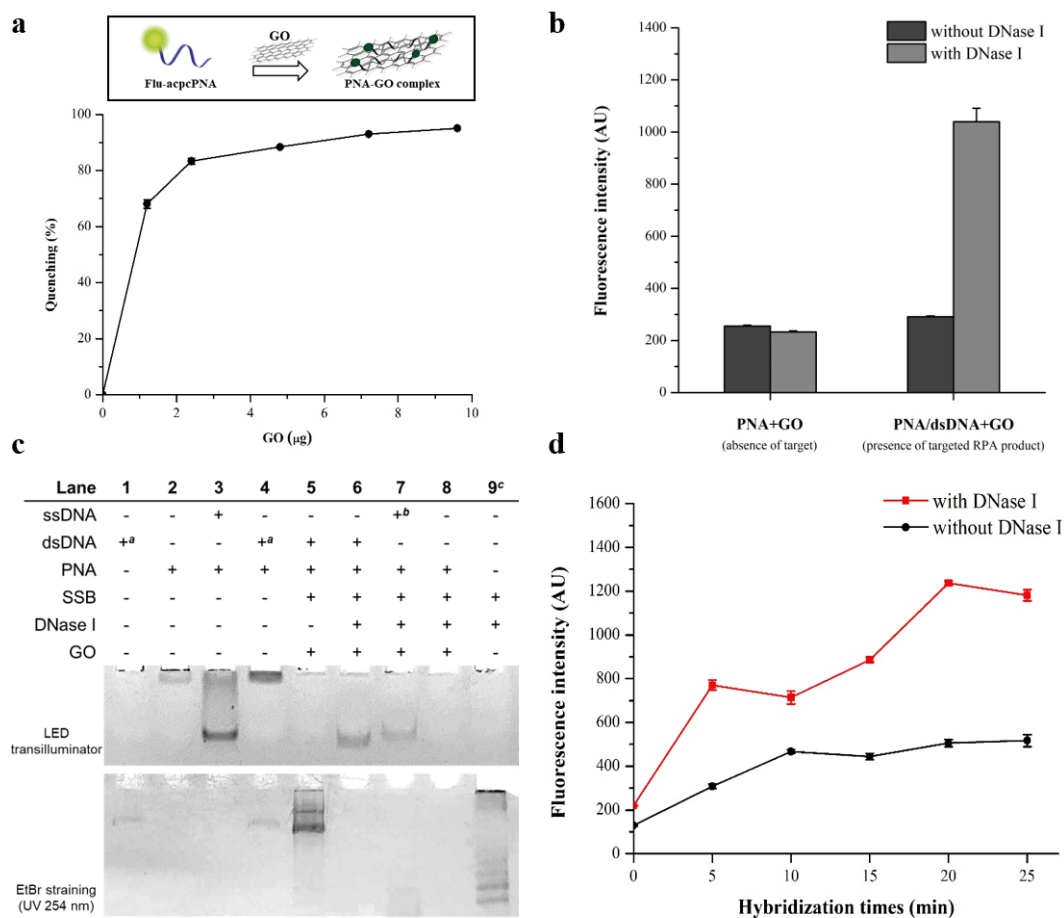


**Figure 56** Schematic illustration for *E. canis* dsDNA detection by RPA-DPG assay in this research.

### 2.1 The optimization for the DNase I-treatment

The concentration of GO used for quenching PNA was firstly optimized. 1  $\mu\text{L}$  of 10  $\mu\text{M}$  PNA1 (10 pmol, 667 nM) was added into 5  $\mu\text{L}$  of the RPA reaction-solution (in the absence of targeted dsDNA) and adjusted to 15  $\mu\text{L}$  by different GO concentrations (0 - 9.6  $\mu\text{g}$ , 0 - 640  $\mu\text{g}/\text{mL}$  of final concentration). The GO-suspended solution was kept at RT for 10 min followed by centrifuge step. Then, the relative fluorescence intensity was recorded on the FAM channel of the Bioer fluorescent quantitative detection system. The result showed that the relative fluorescence intensity of 10 pmol PNA1 was quenched by large amounts of GO at 9.6  $\mu\text{g}$  (640  $\mu\text{g}/\text{mL}$ ) with 96% quenching as shown in **Figure 57a**. Because of RPA solution comprising of several chemical components could affect to adsorption efficiency of PNA with GO molecule. In particular, crowding agents (a high molecular weight

polyethylene glycol, PEG) which was used to mimic the real biomacromolecules condition and enhancing catalytic activity could interfere the interaction between PNA and GO. To generating targeted DNA, the RPA was performed at 37°C for 40 min by using 1 ng pUC57-plasmid DNA as a standard template. After that, the PNA solution (10 pmol) was added into 5.0  $\mu$ L of RPA product and incubated with an isothermal setup for 15 min. Then, 0.2 U DNase I or Milli Q water were added subsequently with continue incubating for 5 min before adding 9.6  $\mu$ g GO (final volume of 15.0  $\mu$ L). As shown in **Figure 57b**, the fluorescence of **PNA1**·dsDNA<sub>target</sub> in GO without enzymatic treatment was not different from the signal of **PNA1** with GO. These results indicated that long-chain dsDNA bearing purine and pyrimidine bases behaves fluorescence quenching *via* transferring excited electron (by LED light) between fluorophore and purine bases which lead to strong fluorescence quenching.<sup>63</sup> Meanwhile, in the case of using DNase I treatment, the fluorescence of **PNA1**·dsDNA<sub>target</sub> in GO platform was significantly enhanced up to ~3.6 folds. Based on these findings, it can conclude that the **PNA1**·dsDNA<sub>target</sub> strand was degraded to yielding small DNA fragment and **PNA1**·DNA<sub>target</sub> hybrid proportion, leading to the remaining of fluorescence signal in GO solution. This hypothesis was confirmed by 20% native-PAGE analysis as shown in **Figure 57c**. The fluorescence band of **PNA1**·DNA<sub>1</sub> was presented with moving faster than **PNA1**. Meanwhile, the incubating **PNA1** with dsDNA<sub>target</sub> at 37°C for 20 min without SSB, DNase I, and GO (purified DNA from RPA reaction), **PNA1**·dsDNA<sub>target</sub> was not observed. In the case of **PNA1**/GO/RPA product without DNase I, the new band was presented which moved slower than dsDNA (visualizing under UV 254 nm with EtBr staining). This result implied that SSB protein within the RPA reaction-buffer facilitates the PNA-mediated invasion strand and consequently local DNA unwinding.<sup>69</sup> On the other hand, in the case of using GO quenching PNA as RPA-DPG assay, the band of **PNA1**·ssDNA<sub>target</sub> was observed as same as in the case of spiked **DNA1** into RPA reaction-buffer, suggesting that proteins could be removed by precipitating of the protein-GO complex. The optimal time for probe invasion to a specific region of *E. canis* DNA (RPA product) was next demonstrated. The process was performed at isothermal setting-up by using 10 pmol of **PNA1** and RPA products harboring targeted dsDNA with incubating for 0 - 25 min following with DNase I treatment (0.2 U, 5 min) and GO quenching steps (9.6  $\mu$ g GO, 10 min). **Figure 57d**, the highest fluorescence was increased according to increasing hybridization time and achieving the highest signal at 20 min.



Note: <sup>a</sup> purified RPA product (628 bp), <sup>b</sup> 4-equiv. ssDNA, <sup>c</sup> RPA reaction-buffer (in the absence of DNA template)

**Figure 57** The optimization for dsDNA detection based on RPA-DPG assay. (a) %Quenching of 10 pmol PNA1 in RPA reaction-solution upon increasing GO (0-9.6 µg). (b) Fluorescence intensity of GO-quenching PNA1 towards RPA product detection with and without DNase I treatment. (c) 20%-native PAGE, the study of PNA·DNA<sub>target</sub> yielding, was performed at 120 V for 1 h 30 min and visualized under blue light LED transilluminator and EtBr straining. (d) Fluorescence intensity of RPA-DPG assay upon increasing hybridization time. The error bars are the standard deviation of triplicated measurements. Conditions; PNA1 solution (10 pmol) was added to RPA solution in the presence and absence of targeted dsDNA following with incubation for hybridization, DNase I treatment, GO-adsorption, and fluorescence measurement.

## 2.2 Specificity

The specificity of GO-based fluorometric assay was evaluated by using pUC57-plasmid DNA that related to tick-carrier parasites including *E. canis*, *A. platys*, *B. vogeli*, and *H. canis*, whereas Milli Q water was used as a negative control. The RPA process was performed on a heating block at 37°C for 40 min. After that, RPA products were incubated with PNA1 for 20 min before the digestion and adsorption steps. As shown in **Figure 58a**, the strong fluorescence signal was only achieved in the case of targeted *E. canis*. Meanwhile, the signals were not observed from other related canine parasites, suggesting that this DNA sensor provided a highly specific detection for the target *E. canis* and can distinguish *E. canis* from other parasites. Furthermore, the fluorescence signal was strongly presented in only *E. canis* which was simply and rapidly visualized under a LED transilluminator (**Figure 58b**).

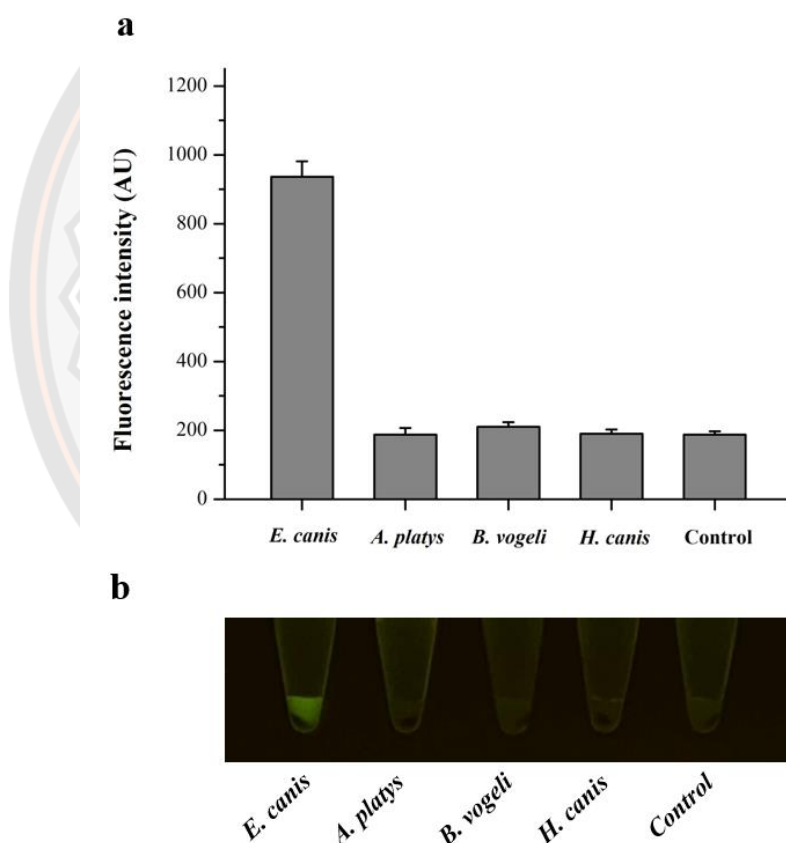


**Figure 58** The specificity of RPA-DPG assay for *E. canis* detection.

(a) Fluorescence intensities of RPA-DPG assay towards *E. canis* pUC57-plasmid DNA detection and (b) its images were obtained under LED transilluminator. The error bars are the standard deviation of triplicated measurements. 10 pmol PNA1 was added to 5  $\mu$ L of RPA products, and incubating at 25 min before digested with 0.2 U DNase I (5 min) following with adsorbing excess-PNA by 9.6  $\mu$ g GO (10 min).

### 2.3 Sensitivity

The sensitivity study was evaluated using the pUC57-plasmid DNA of *E. canis*. The different concentrations of DNA were prepared before used by 10-fold serial dilution to give DNA solutions in a range of 1 fg/ $\mu$ L - 1 ng/ $\mu$ L as  $6.7 \times (10^2 - 10^8)$  copies/ $\mu$ L. The process was performed as same as described in the topic of a specific study. As shown in **Figure 59a**, the fluorescence intensity of supernatant (y) was plotted with a concentration of the DNA template in the logarithmic scale (x), indicating that this assay is sensitive to target *E. canis* DNA concentration and increases upon increasing DNA template. Notably, the fluorescence image was visualized at least 10 pg DNA template. The linear relationship between the fluorescence intensity and  $\log_{10}$  [dsDNA template] gave a linear equation  $y = 40.575x + 348.640$  with regression coefficient  $R^2 = 0.966$ , and displaying limit of detection (LOD) at 2.22 fg/ $\mu$ L (**Table 8**), that accords to equation (3);  $LOD = 3.3 \times (SD/S)$ .<sup>20</sup>

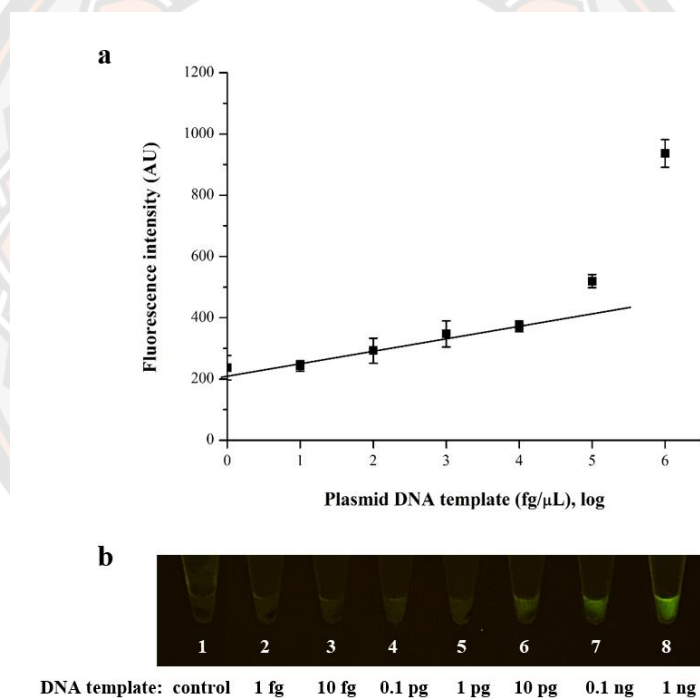


**Figure 59 Sensitivity of RPA-DPG assay for *E. canis* detection.**

(a) The linear relationship range between fluorescence intensity (y) and logarithms concentration of *E. canis* pUC57-plasmid DNA (x) in the range of 1 fg/ $\mu$ L - 10 pg/ $\mu$ L. (b) Fluorescence images of sensitivity study obtained by LED transilluminator. The error bars are the standard deviation of triplicated measurements. 10 pmol PNA1 was added to 5  $\mu$ L of RPA products, and incubating at 25 min before digested with 0.2 U DNase I (5 min) following with adsorbing excess-PNA by 9.6  $\mu$ g GO (10 min).

**Table 8 Several methods for DNA detection by fluorogenic nucleic acid-GO system**

DNA sensing platform	Target/oligonucleotides (length)	Conditions/Equipment	Sensitivity	Ref.
PNA-assembled GO	ssDNA (22-mer)	40°C, 40 min/fluorescence spectrophotometer	800 pM	37
PNA-GO	dsDNA (21-mer)	RT, 1 h/microplate reader	260 pM	20
RCA/PNA-GO	RCA product/ssDNA	Ligation; 85°C for 3 min, RT for 15 min, 25°C for 1 h. Amplification; 30°C for 90 min, 60°C for 10 min/thermocycler PNA-GO; 25°C for 20 min/microplate reader	0.4 pM	24
PCR/DNA-GO	PCR product/dsDNA	PCR; N/A/thermocycler DNA-GO; 95°C for 3 min, 25°C (10°C/min), 25°C for 10 min/thermocycler and microplate reader	N/A	23
RPA-DPG	RPA product/dsDNA	Amplification; 37°C for 40 min/heating block DNase I-enhanced PNA-GO; 37°C for 35 min/heating block, LED transilluminator (visualization)	2.26 fM, 11.1 pM (visualization)	In this study

LOD = limit of detection, N/A = not available



### 2.4 Clinical samples

All 28 samples of extracted DNA were initially identified infected *E. canis* by conventional PCR in using these specific RPA primers (**F3** and **R2**) and annealing temperature at 50°C for 40 cycles. As shown in **Figure 60**, agarose gel electrophoretic analysis implied that the DNA product band was presented in samples 1-5, 7, 9, 14-16, 19, 20, 22-25, 28, whereas samples 8 and 10, the DNA band slightly presented in unclear observation.

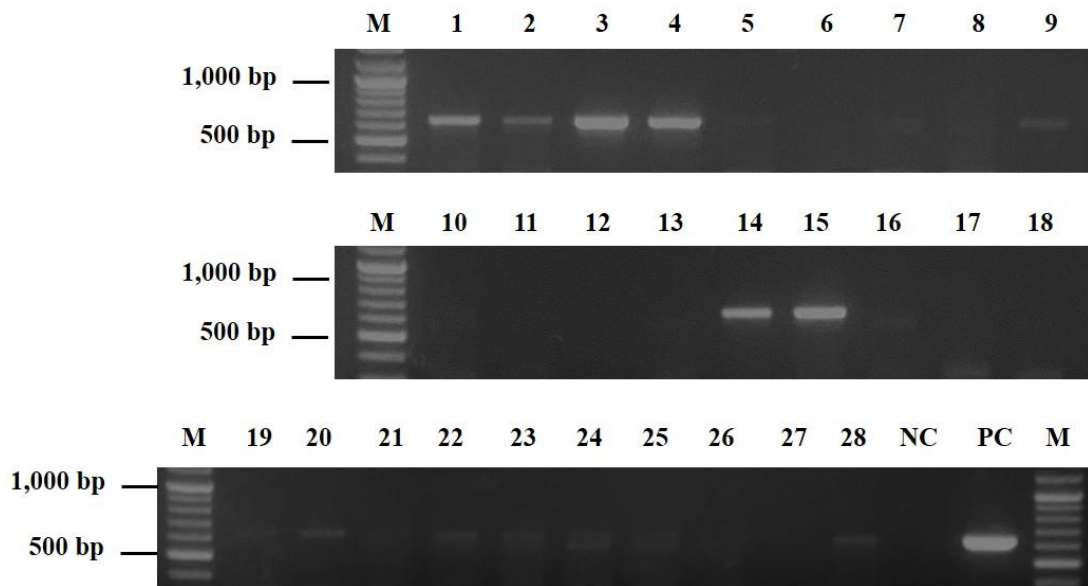


**Figure 60** Agarose gel electrophoresis of PCR products using extracted DNA from whole blood as a DNA template.

The aliquot DNA sample was amplified by annealing at 50°C for 40 cycles using RPA primers (**F3** and **R2**) before subjected in 2%w/v agarose A gel in TAE buffer, and running at 100 V, 400 mA for 25 min. The gel was visualized under UV transilluminator (254 nm) by EtBr-staining. M = DNA ladder, NC = negative control, PC = positive control.

Although conventional PCR was also identified infected *E. canis*, the DNA samples which has been extracted from dogs' blood containing the many factors could inhibit the RPA process, resulting in giving very low target dsDNA<sup>70</sup> as shown in **Figure 61**. Based on gel electrophoresis, the DNA band was not observed in all RPA products. However, in a previous study, The RPA-DPG assay was successfully performed with pUC57-plasmid DNA in the highly specific and sensitive tests by rapid fluorescence visualization, suggesting that this developed assay is promising tools for DNA detection in the field. When applied RPA-DPG assay for clinical samples, the fluorescence was presented in samples 2, 4, 5, 15, and 28 (**Figure 62a**) but the visual fluorescence still un-cleared yet (**Figure 62b**).

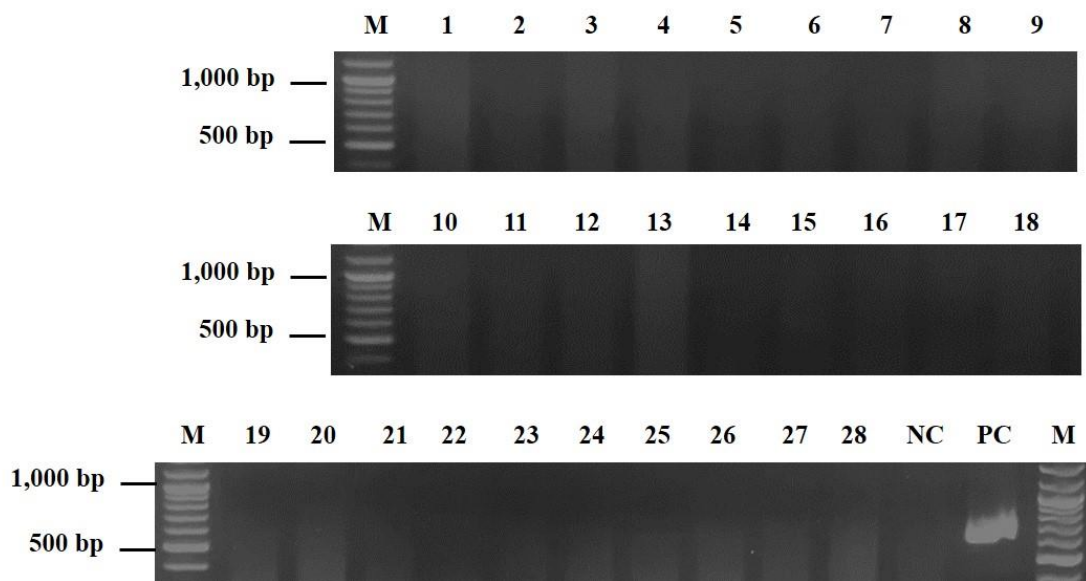


**Figure 61** Agarose gel electrophoresis of RPA products using extracted DNA from whole blood as a DNA template.

The aliquot DNA sample which was used as a template was processed at 37°C for 40 min under heating block using RPA primers (F3 and R2) before subjected in 2%w/v agarose A gel in TAE buffer, and running at 100 V, 400 mA for 25 min. The gel was visualized under UV transilluminator (254 nm) by EtBr-staining. M = DNA ladder, N = negative control, PC = positive control obtained from amplifying pUC57-plasmid DNA.

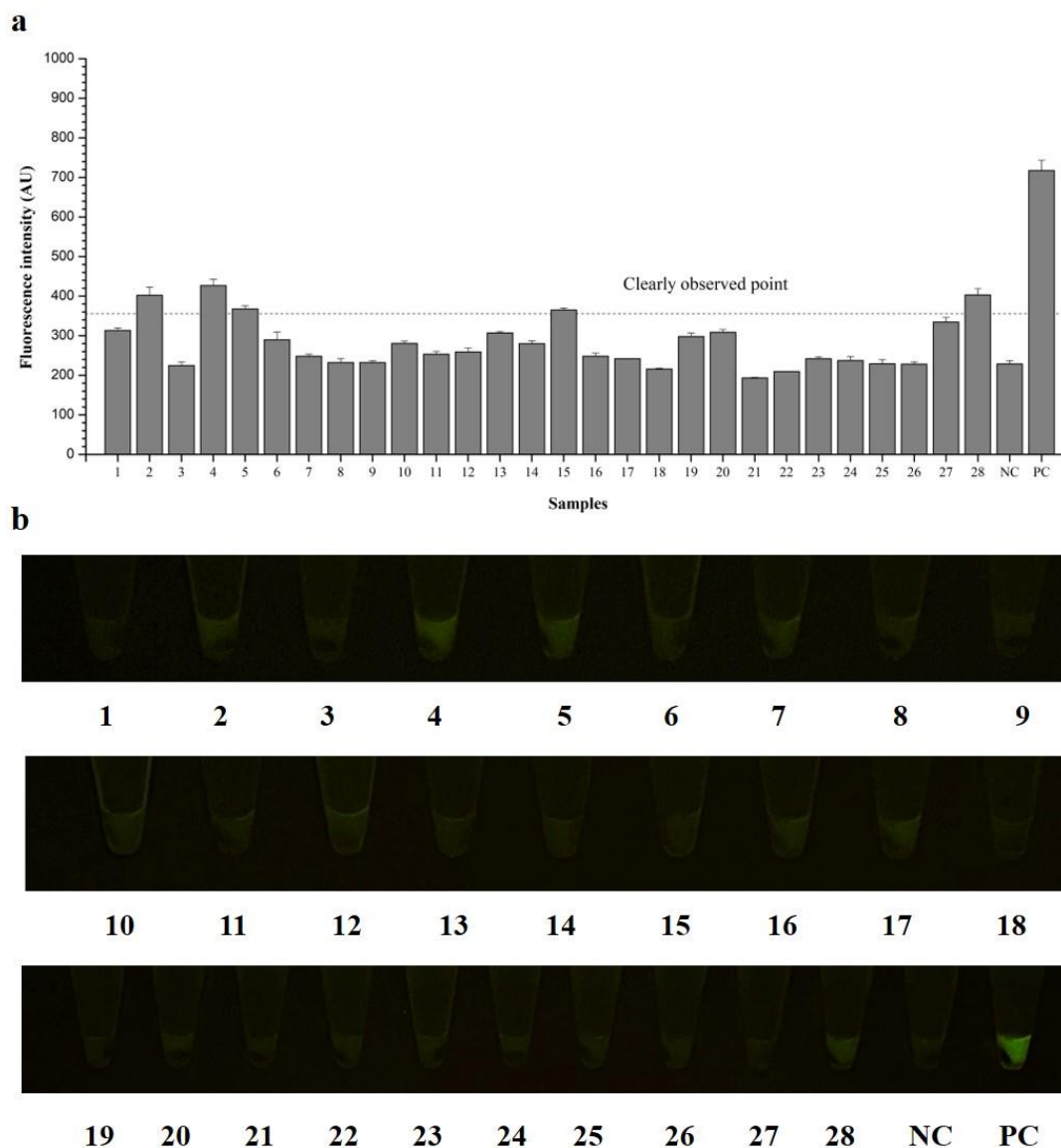


**Figure 62 (a) Fluorescence intensity of RPA-DPG assay for the detection of *E. canis* DNA samples from dogs' blood and (b) fluorescence images obtained by LED transilluminator.**

The observed point refers to the detection of using 10 pg/ $\mu$ L pUC57-plasmid DNA of *E. canis* as a DNA template. 10 pmol PNA1 was added to 5  $\mu$ L of each RPA product, and incubating at 25 min before digested with 0.2 U DNase I (5 min) following with adsorbing excess-PNA by 9.6  $\mu$ g GO (10 min).

## CHAPTER V

### CONCLUSION

The DNA sensor based on conformational-constrained pyrrolidinyl PNA probe in the GO platform was successfully established by using a specific-sequence of the *E. canis* 16S rRNA gene as a target. The concept of this assay is that shining ssPNA probe bearing nucleobases is greatly adsorbed on GO surface (PNA-GO complex) *via* hydrophobic driving force and hydrogen bond interaction, introducing to quenching of nearby tagged fluorescent dye (Fluorescence-OFF). Contrarily, the pairing of nucleobases inside the helix structure of PNA-DNA<sub>target</sub> hybrid introduces the releasing duplex molecule in GO solution, brightening fluorescence signal (Fluorescence-ON). The non-specific adsorption between the acpcPNA probe (**PNA1**) and the microplate's surface leads to quenching fluorescent signals over time, and remaining fluorescence ~51% from the initial signal for 1 hour. The partially positive-charged skeleton (apc/acpcPNA, **PNA2**) used for reducing non-specific adsorption cannot encourage the fluorescent stability of the ssPNA probe. For ssDNA detection, the various types of ssDNA in Tris-HCl buffer were employed and indicating that **PNA1** is high sequence-selectivity rather than **PNA2**. These results contribute the possibility to use this platform in other DNA detection especially in combination with the amplification technique.

Towards dsDNA detection based on isothermal setting-up, the specific-primers were successfully amplified only pUC57-based *E. canis* plasmid DNA within 40 min at 37°C, yielding DNA product approximately 628 bp. Furthermore, in the presence of SSB proteins within the RPA reaction buffer could be stabilized D-loop formation which was promoted PNA invasion to the specific binding sites of dsDNA at low temperature. In this finding, the DNase I treatment for PNA-dsDNA<sub>target</sub> strand is a simple and useful technique to eliminate fluorescent quenching phenomenon from long-chain dsDNA in DNA detection especially by PNA/GO platform. Moreover, this developed RPA-DPG assay was successfully established towards *E. canis* detection, preferring greatly specific detection and high sensitivity with LOD = 2.22 fg/μL (2.46 fM) upon using pUC57-plasmid DNA as a DNA template. Notably that the developed assay was simply visualized under blue light LED transilluminator with clear observation upon DNA template  $>6.7 \times 10^6$  copies/μL as 10 pg/μL or 11.1 pM.

In clinical sample detection, although these primers were successfully amplified only infected *E. canis* by PCR technique, RPA also challenged because the extracted DNA bearing many influences particularly RPA inhibitor could restrict to amplification process (gel electrophoresis is undetectable). However, the fluorescence visualization for RPA product detection was slightly presented in some positive samples, indicating that this technique is a promising tool for detecting *E. canis* by isothermal setting-up particularly in resource limiting fields.

## REFERENCES

- (1) Nielsen PE, Egholm M, Berg RH, Buchardt O. (1991). Sequence-selective recognition of DNA by strand displacement with a thymine-substituted polyamide. *Science*. 254(5037):1497–1500.
- (2) Chakrabarti MC, Schwarz FP. (1999). Thermal stability of PNA/DNA and DNA/DNA duplexes by differential scanning calorimetry. *Nucleic Acids Res*. 27(24):4801–4806.
- (3) Nielsen PE, Egholm M. (1999). An introduction to peptide nucleic acid. *Curr Issues Mol Biol*. 1(1–2):89–104.
- (4) Vilaivan T, Suparpprom C, Lowe G. (2001). Synthesis and properties of novel pyrrolidinyl PNA carrying  $\beta$ -amino acid spacers. *Tetrahedron Lett*. 42(32):5533–5536.
- (5) Suparpprom C, Srisuwannaket C, Sangvanich P, Vilaivan T. (2005). Synthesis and oligodeoxynucleotide binding properties of pyrrolidinyl peptide nucleic acids bearing prolyl-2-aminocyclopentanecarboxylic acid (ACPC) backbones. *Tetrahedron Lett*. 46(16):2833–2837.
- (6) Vilaivan T, Srisuwannaket C. (2006). Hybridization of pyrrolidinyl peptide nucleic acids and DNA: Selectivity, base-pairing specificity, and direction of binding. *Org Lett*. 8(9):1897–1900.
- (7) Vilaivan T. (2015). Pyrrolidinyl PNA with  $\alpha/\beta$ -Dipeptide Backbone: From Development to Applications. *Acc Chem Res*. 48(6):1645–1656.
- (8) Boontha B, Nakkuntod J, Hirankarn N, Chaumpluk P, Vilaivan T. (2008). Multiplex mass spectrometric genotyping of single nucleotide polymorphisms employing pyrrolidinyl peptide nucleic acid in combination with ion-exchange capture. *Anal Chem*. 80(21):8178–8186.
- (9) Maneelun N, Vilaivan T. (2013). Dual pyrene-labeled pyrrolidinyl peptide nucleic acid as an excimer-to-monomer switching probe for DNA sequence detection. *Tetrahedron*. 69(51):10805–10810.
- (10) Yotapan N, Nim-anussornkul D, Vilaivan T. (2016). Pyrrolidinyl peptide nucleic acid terminally labeled with fluorophore and end-stacking quencher as a probe for highly specific DNA sequence discrimination. *Tetrahedron*. 72(49):7992–7999.
- (11) Jirakittiwut N, Panyain N, Nuanyai T, Vilaivan T, Praneenararat T. (2015). Pyrrolidinyl peptide nucleic acids immobilized on cellulose paper as a DNA sensor. *RSC Adv*. 5(31):24110–24114.
- (12) Teengam P, Siangproh W, Tuantranont A, Vilaivan T, Chailapakul O, Henry CS. (2017). Multiplex Paper-Based Colorimetric DNA Sensor Using Pyrrolidinyl Peptide Nucleic Acid-Induced AgNPs Aggregation for Detecting MERS-CoV, MTB, and HPV Oligonucleotides. *Anal Chem*. 89(10):5428–5435.
- (13) Pansuwan H, Ditmangklo B, Vilaivan C, Jiangchareon B, Pan-In P, Wanichwecharungruang S, et al. (2017). Hydrophilic and Cell-Penetrable Pyrrolidinyl Peptide Nucleic Acid via Post-synthetic Modification with Hydrophilic Side Chains. *Bioconjug Chem*. 28(9):2284–2292.
- (14) Arthi G PB, BD L. (2015). A Simple Approach to Stepwise Synthesis of Graphene Oxide Nanomaterial. *J Nanomed Nanotechnol*. 06(01):1–4.
- (15) Chung C, Kim YK, Shin D, Ryoo SR, Hong BH, Min DH. (2013). Biomedical

- applications of graphene and graphene oxide. *Acc Chem Res.* 46(10):2211–2224.
- (16) Cinti S, Scognamiglio V, Moscone D, Arduini F. (2017). Efforts, Challenges, and Future Perspectives of Graphene-Based Biosensors for Biomedical Applications [Internet]. *Graphene Bioelectronics.* Elsevier Inc.; 133–150.
- (17) Swathi RS, Sebastian KL. (2009). Long range resonance energy transfer from a dye molecule to graphene has (distance)<sup>-4</sup> dependence. *J Chem Phys.* 130(8):128–131.
- (18) Liu B, Sun Z, Zhang X, Liu J. (2013). Mechanisms of DNA sensing on graphene oxide. *Anal Chem.* 85(16):7987–7993.
- (19) He S, Song B, Li D, Zhu C, Qi W, Wen Y, et al. (2010). A graphene nanoprobe for rapid, sensitive, and multicolor fluorescent DNA analysis. *Adv Funct Mater.* 20(3):453–459.
- (20) Lee J, Park IS, Jung E, Lee Y, Min DH. (2014). Direct, sequence-specific detection of dsDNA based on peptide nucleic acid and graphene oxide without requiring denaturation. *Biosens Bioelectron.* 62:140–144.
- (21) Park JS, Baek A, Park IS, Jun BH, Kim DE. (2013). A graphene oxide-based platform for the assay of RNA synthesis by RNA polymerase using a fluorescent peptide nucleic acid probe. *Chem Commun.* 49(80):9203–9205.
- (22) Ning Y, Zou L, Gao Q, Hu J, Lu F. (2018). Graphene oxide-based fluorometric determination of methicillin-resistant *Staphylococcus aureus* by using target-triggered chain reaction and deoxyribonuclease-assisted recycling. *Microchim Acta.* 185(3):1–8.
- (23) Giuliadori AM, Brandi A, Kotla S, Perrozzi F, Gunnella R, Ottaviano L, et al. (2017). Development of a graphene oxide-based assay for the sequence-specific detection of double-stranded DNA molecules. *PLoS One.* 12(8):1–17.
- (24) Hong C, Baek A, Hah SS, Jung W, Kim DE. (2016). Fluorometric Detection of MicroRNA Using Isothermal Gene Amplification and Graphene Oxide. *Anal Chem.* 88(6):2999–3003.
- (25) Dantas-Torres F. (2008). The brown dog tick, *Rhipicephalus sanguineus* (Latreille, 1806) (Acari: Ixodidae): From taxonomy to control. *Vet Parasitol.* 152(3–4):173–185.
- (26) Harrus S, Waner T. (2011). Diagnosis of canine monocytotropic ehrlichiosis (*Ehrlichia canis*): An overview. *Vet J.* 187(3):292–296.
- (27) Sykes JE, Sykes JE. (2014). Chapter 28 – Ehrlichiosis [Internet]. *Canine and Feline Infectious Diseases.* Elsevier Inc.; 278–289.
- (28) Mylonakis ME, Harrus S, Breitschwerdt EB. (2019). An update on the treatment of canine monocytic ehrlichiosis (*Ehrlichia canis*). *Vet J.* 246:45–53.
- (29) Almazán C, González-Álvarez VH, Fernández de Mera IG, Cabezas-Cruz A, Rodríguez-Martínez R, de la Fuente J. (2016). Molecular identification and characterization of *Anaplasma platys* and *Ehrlichia canis* in dogs in Mexico. *Ticks Tick Borne Dis.* 7(2):276–283.
- (30) Kaewmongkol G, Lukkana N, Yangtara S, Kaewmongkol S, Thengchaisri N, Sirinarumitr T, et al. (2017). Association of *Ehrlichia canis*, Hemotropic *Mycoplasma* spp. and *Anaplasma platys* and severe anemia in dogs in Thailand. *Vet Microbiol.* 201:195–200.
- (31) Liu M, Ruttayaporn N, Saechan V, Jirapattharasate C, Vudriko P, Moumouni PFA, et al. (2016). Molecular survey of canine vector-borne diseases in stray

- dogs in Thailand. *Parasitol Int.* 65(4):357–361.
- (32) Nazari M, Lim SY, Watanabe M, Sharma RSK, Cheng NABY, Watanabe M. (2013). Molecular Detection of *Ehrlichia canis* in Dogs in Malaysia. *PLoS Negl Trop Dis.* 7(1):7–10.
- (33) Pinyoowong D, Jittapalapong S, Suksawat F, Stich RW, Thamchaipenet A. (2008). Molecular characterization of Thai *Ehrlichia canis* and *Anaplasma platys* strains detected in dogs. *Infect Genet Evol.* 8(4):433–438.
- (34) Daher RK, Stewart G, Boissinot M, Bergeron MG. (2016). Recombinase polymerase amplification for diagnostic applications. *Clin Chem.* 62(7):947–958.
- (35) Moore MD, Jaykus LA. (2017). Recombinase polymerase amplification: A promising point-of-care detection method for enteric viruses. *Future Virol.* 12(8):421–429.
- (36) Li J, Macdonald J, Von Stetten F. (2019). Review: a comprehensive summary of a decade development of the recombinase polymerase amplification. *Analyst.* 144(1):31–67.
- (37) Guo S, Du D, Tang L, Ning Y, Yao Q, Zhang GJ. (2013). PNA-assembled graphene oxide for sensitive and selective detection of DNA. *Analyst.* 138(11):3216–3220.
- (38) Ishizuka T, Otani K, Sumaoka J, Komiyama M. (2009). Strand invasion of conventional PNA to arbitrary sequence in DNA assisted by single-stranded DNA binding protein. *Chem Commun.* (10):1225–1227.
- (39) Zhao Y, Sarkar A, Wang X. (2020). Peptide nucleic acid based tension sensor for cellular force imaging with strong DNase resistance. *Biosens Bioelectron.* 150:111959.
- (40) Jimenez-Cervantes E, López-Barroso J, Martínez-Hernández AL, Velasco-Santos C. (2016). Graphene-Based Materials Functionalization with Natural Polymeric Biomolecules. *Recent Adv Graphene Res.* Pramoda Kumar Nayak, IntechOpen. Available: <https://www.intechopen.com/books/recent-advances-in-graphene-research/graphene-based-materials-functionalization-with-natural-polymeric-biomolecules>.
- (41) Wu M, Kempaiah R, Huang PJJ, Maheshwari V, Liu J. (2011). Adsorption and desorption of DNA on graphene oxide studied by fluorescently labeled oligonucleotides. *Langmuir.* 27(6):2731–2738.
- (42) Park JS, Goo NI, Kim DE. (2014). Mechanism of DNA adsorption and desorption on graphene oxide. *Langmuir.* 30(42):12587–12595.
- (43) Lee J, Park I, Kim H, Woo J, Choi B, Min D. (2015). BSA as additive: A simple strategy for practical applications of PNA in bioanalysis. *Biosens Bioelectron.* 69:167–173.
- (44) Lu CH, Yang HH, Zhu CL, Chen X, Chen GN. (2009). A graphene platform for sensing biomolecules. *Angew Chemie - Int Ed.* 48(26):4785–4787.
- (45) Kotikam V, Fernandes M, Kumar VA. (2012). Comparing the interactions of DNA, polyamide (PNA) and polycarbamate nucleic acid (PCNA) oligomers with graphene oxide (GO). *Phys Chem Chem Phys.* 14(43):15003–15006.
- (46) Xu X, Xing S, Xu M, Fu P, Gao T, Zhang X, et al. (2019). Highly sensitive and specific screening of EGFR mutation using a PNA microarray-based fluorometric assay based on rolling circle amplification and graphene oxide. *RSC Adv.* 9(66):38298–38308.
- (47) Muangchuen A, Chaumpluk P, Suriyasomboon A, Ekgasit S. (2014).

- Colorimetric detection of *Ehrlichia canis* via nucleic acid hybridization in gold nano-colloids. *Sensors*. 14(8):14472–14487.
- (48) Pinhanelli VC, Costa PNM, Silva G, Aguiar DM, Silva CML, Fachin AL, et al. (2015). Development and evaluation of a loop-mediated isothermal amplification assay for detection of *Ehrlichia canis* DNA in naturally infected dogs using the *p30* gene. *Genet Mol Res*. 14(4):17885–17892.
- (49) Lowe G, Vilaivan T. (1997). Amino acids bearing nucleobases for the synthesis of novel peptide nucleic acids. *J Chem Soc Perkin Trans*. 1:539–546.
- (50) Reenabthue N, Boonlua C, Vilaivan C, Vilaivan T, Suparpprom C. (2011). 3-Aminopyrrolidine-4-carboxylic acid as versatile handle for internal labeling of pyrrolidiny PNA. *Bioorganic Med Chem Lett*. 21(21):6465–6469.
- (51) Liu Z, Liu B, Ding J, Liu J. (2014). Fluorescent sensors using DNA-functionalized graphene oxide. *Anal Bioanal Chem*. 406(27):6885–6902.
- (52) Baek A, Baek YM, Kim HM, Jun BH, Kim DE. (2018). Polyethylene Glycol-Engrafted Graphene Oxide as Biocompatible Materials for Peptide Nucleic Acid Delivery into Cells. *Bioconjug Chem*. 29(2):528–537.
- (53) Lee J, Kim J, Kim S, Min DH. (2016). Biosensors based on graphene oxide and its biomedical application. *Adv Drug Deliv Rev*. 105:275–287.
- (54) Dragulescu-Andrasi A, Rapireddy S, Frezza BM, Gayathri C, Gil RR, Ly DH. (2006). A simple  $\gamma$ -backbone modification preorganizes peptide nucleic acid into a helical structure. *J Am Chem Soc*. 128(31):10258–10267.
- (55) Bonora GM, Drioli S, Ballico M, Faccini A, Corradini R, Cogoi S, et al. (2007). PNA conjugated to high-molecular weight poly(ethylene glycol): Synthesis and properties. *Nucleosides Nucleotides Nucleic Acids*. 26(6–7):661–664.
- (56) Hu J, Corey DR. (2007). Inhibiting Gene Expression with Peptide Nucleic Acid (PNA)–Peptide Conjugates that Target Chromosomal DNA. *Biochemistry*. 46(25):7581–7589.
- (57) Shiraishi T, Nielsen PE. (2011). Peptide nucleic acid (PNA) cell penetrating peptide (CPP) conjugates as carriers for cellular delivery of antisense oligomers Takehiko. *Artif DNA PNA XNA*. 2(3):90–99.
- (58) Pandit S, De M. (2017). Interaction of amino acids and graphene oxide: Trends in thermodynamic properties. *J Phys Chem C*. 121(1):600–608.
- (59) Rossi-Fernández AC, Villegas-Escobar N, Guzmán-Angel D, Gutiérrez-Oliva S, Ferullo RM, Castellani NJ, et al. (2020). Theoretical study of glycine amino acid adsorption on graphene oxide. *J Mol Model*. 26(2):33.
- (60) Vinasco J, Li O, Alvarado A, Diaz D, Hoyos L, Tabachi L, et al. (2007). Molecular evidence of a new strain of *Ehrlichia canis* from South America. *J Clin Microbiol*. 45(8):2716–2719.
- (61) Kaewmongkol G, Maneesaay P, Suwanna N, Tiraphut B, Krajarngjang T, Chouybumrung A, et al. (2016). First Detection of *Ehrlichia canis* in Cerebrospinal Fluid from a Nonthrombocytopenic Dog with Meningoencephalitis By Broad-Range PCR. *J Vet Intern Med*. 30(1):255–2559.
- (62) Qiu H, Kelly PJ, Zhang J, Luo Q, Yang Y, Mao Y, et al. (2016). Molecular detection of *anaplasma* spp. and *ehrlichia* spp. in ruminants from twelve provinces of China. *Can J Infect Dis Med Microbiol*. 2016(5):1-9.
- (63) Mao H, Luo G, Zhan Y, Zhang J, Yao S, Yu Y. (2018). The mechanism and regularity of quenching the effect of bases on fluorophores: The base-quenched



- probe method. *Analyst*. 143(14):3292–3301.
- (64) Zhao S, Cui Y, Jing J, Yan Y, Peng Y, Shi K, et al. (2019). Rapid and sensitive detection of *Anaplasma phagocytophilum* using a newly developed recombinase polymerase amplification assay. *Exp Parasitol*. 201:21–25.
- (65) Jiang L, Ching P, Chao C-C, Dumler JS, Ching W-M. (2020). Development of a Sensitive and Rapid Recombinase Polymerase Amplification Assay for the Detection of *Anaplasma phagocytophilum*. *J Clin Microbiol*. 58(5):1–9.
- (66) Cui J, Zhao Y, Sun Y, Yu L, Liu Q, Zhan X, et al. (2018). Detection of *Babesia gibsoni* in dogs by combining recombinase polymerase amplification (RPA) with lateral flow (LF) dipstick. *Parasitol Res*. 117(12):3945–3951.
- (67) Qi Y, Shao Y, Rao J, Shen W, Yin Q, Li X, et al. (2018). Development of a rapid and visual detection method for *Rickettsia rickettsii* combining recombinase polymerase assay with lateral flow test. *PLoS One*. 13(11): e0207811.
- (68) Lobato IM, O’Sullivan CK. (2018). Recombinase polymerase amplification: Basics, applications and recent advances. *TrAC - Trends Anal Chem*. 98:19–35.
- (69) Machnik G, Bułdak Ł, Ruczyński J, Gašior T, Huzarska M, Belowski D, et al. (2017). The application of strand invasion phenomenon, directed by peptide nucleic acid (PNA) and single-stranded DNA binding protein (SSB) for the recognition of specific sequences of human endogenous retroviral HERV-W family. *J Mol Recognit*. 30(5):1–9.
- (70) Kersting S, Rausch V, Bier FF, Nickisch-Roseneck M von. (2014). Rapid detection of *Plasmodium falciparum* with isothermal recombinase polymerase amplification and lateral flow analysis. *Malar J*. 13(99):3–9.



**APPENDIX**

มหาวิทยาลัยนครสวรรค์



**Figure 63 RP-HPLC chromatogram of PNA1. The product was observed at 31.9 min with the presence of two peaks corresponding to the 5(6)-isomers of fluorescein.**

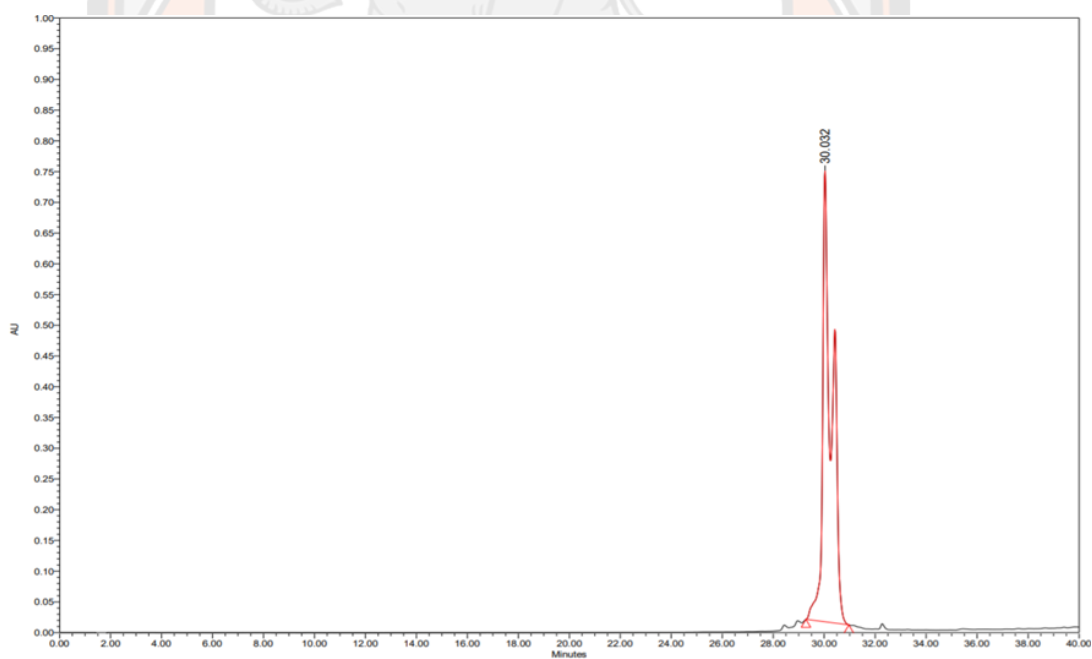


**Figure 64 RP-HPLC chromatogram of PNA2. The product was observed at 30.0 min with the presence of two peaks corresponding to the 5(6)-isomers of fluorescein.**

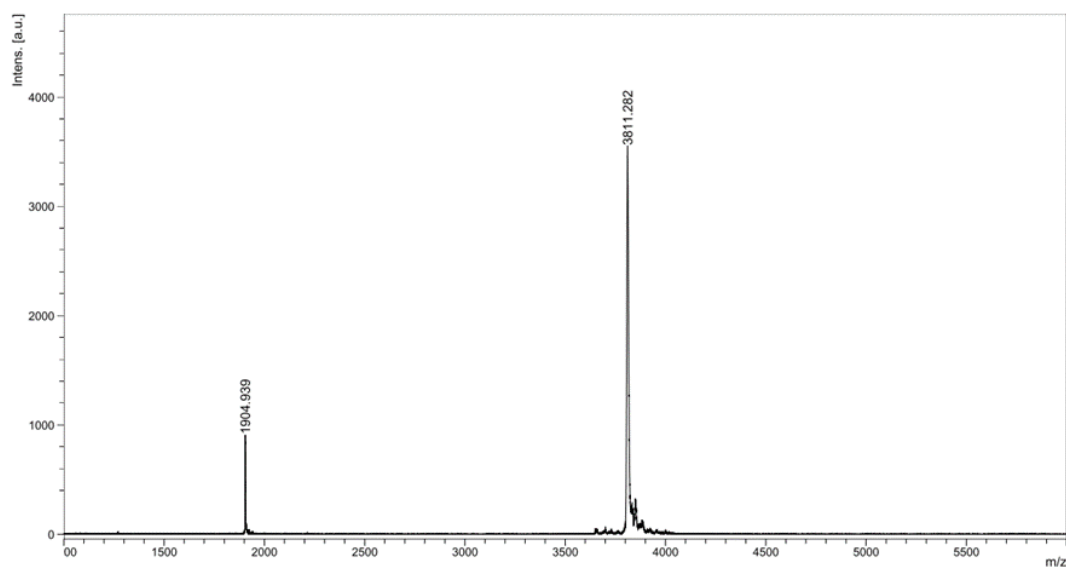


**Figure 65 MALDI-TOF spectrum of PNA1. (calculated  $[M+H]^+$  3810.064, found 3811.282).**

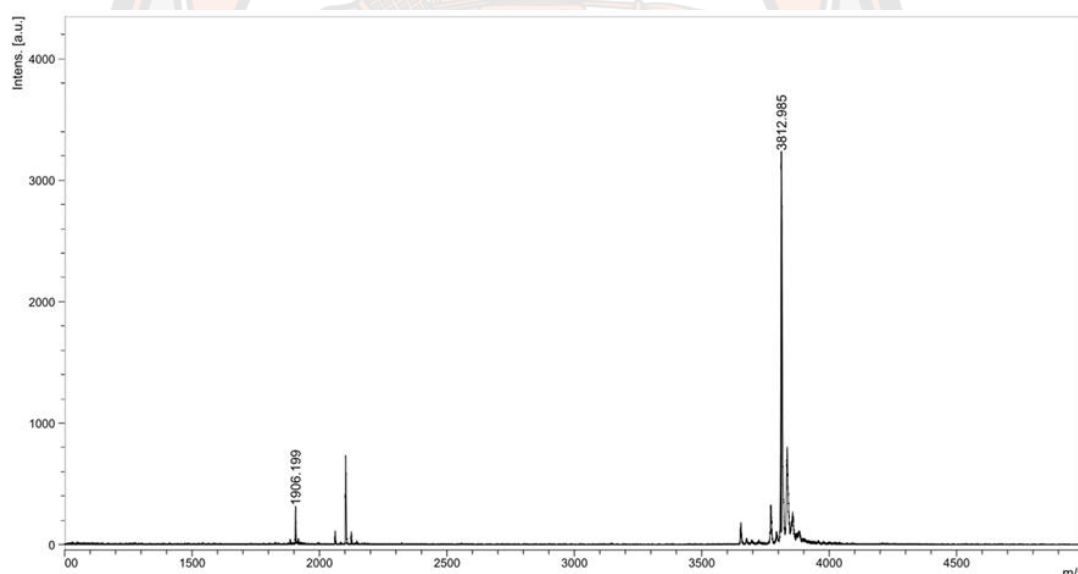


**Figure 66 MALDI-TOF spectrum of PNA2. (calculated  $[M+H]^+$  3813.028, found 3812.985).**

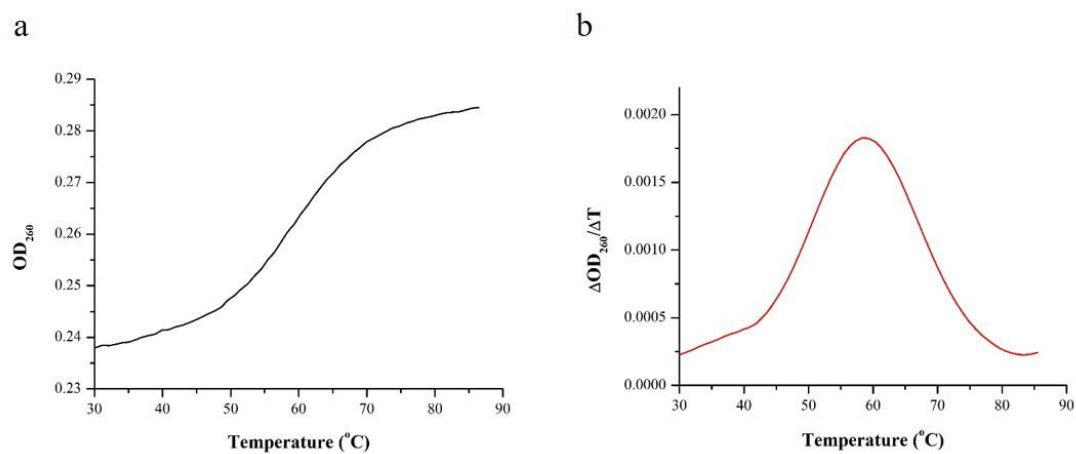


**Figure 67 (a)  $T_m$  analysis of PNA1-DNA1 (targeted DNA) in 0.1 M phosphate buffer pH 7.0 and (b) first-derivative curve showed  $T_m = 59^{\circ}C$ .**

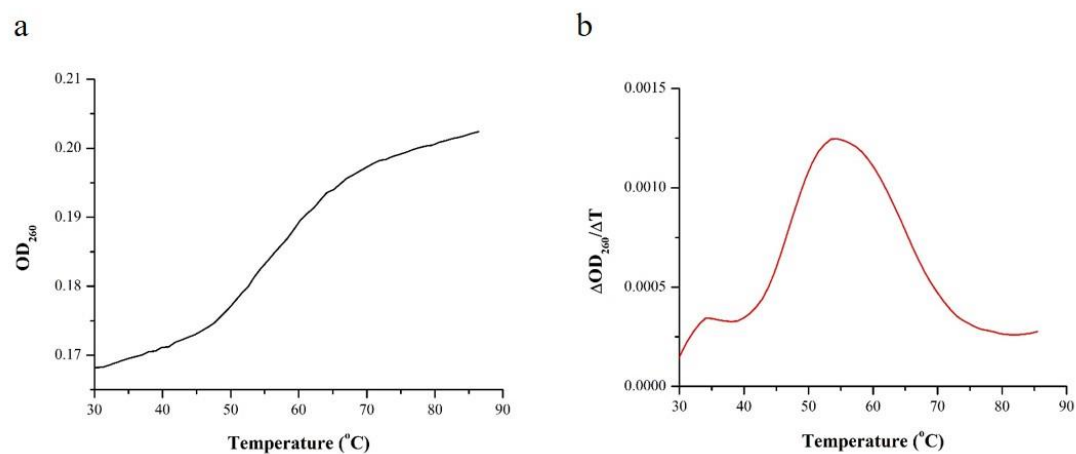


**Figure 68 (a)  $T_m$  analysis of PNA2-DNA1 (targeted DNA) in 0.1 M phosphate buffer pH 7.0 and (b) first-derivative curve showed  $T_m = 55^{\circ}C$ .**



**Table 10 Fluorescence emission data of PNA in Tris-HCl buffer with different concentration of GO (Figure 41a-b).**

nm	PNA1 (200 nM) with GO ( $\mu\text{g/mL}$ )										PNA1 (200 nM) with GO ( $\mu\text{g/mL}$ )													
	0	2	4	6	8	10	12	14	0	2	4	6	8	10	12	14	0	2	4	6	8	10	12	14
500	8850	2481	1462	756	671	386	529	751	6153	885	643	285	227	234	302	313								
510	27218	7624	4424	2264	1878	1023	1498	2088	18878	2746	1897	710	545	494	790	777								
520	43765	12529	7190	3702	3110	1576	2526	3439	30230	4507	3076	1166	842	746	1305	1254								
530	47152	13999	8020	4238	3623	1773	3089	4127	32875	5045	3445	1343	985	844	1570	1508								
540	39722	12091	6895	3832	3319	1577	2872	3851	27684	4297	2972	1268	885	809	1530	1459								
550	30679	9621	5477	3165	2748	1299	2374	3236	21302	3387	2357	1030	747	701	1290	1250								
560	22978	7194	4162	2418	2116	983	1864	2498	15896	2558	1806	783	563	535	982	950								
570	18061	5716	3255	1951	1725	819	1554	2082	12669	2070	1406	654	458	435	827	787								
580	13089	4182	2385	1414	1268	609	1113	1507	9041	1480	1036	504	337	328	624	594								
590	9728	3145	1819	1099	1016	456	911	1209	6714	1147	810	387	296	285	507	480								
600	6736	2200	1288	796	701	368	653	894	4776	794	574	263	219	210	380	388								
610	4760	1611	912	601	543	278	469	674	3320	545	419	233	175	181	295	293								
620	3545	1216	677	459	400	231	401	520	2433	437	303	182	153	147	241	224								
630	2462	869	527	319	303	191	272	381	1820	297	227	162	109	128	198	197								
640	1997	676	395	274	256	138	246	353	1338	235	147	117	129	145	179	169								
650	1310	480	292	199	222	118	192	223	898	193	113	104	80	78	146	133								
660	1027	352	243	172	182	144	149	149	671	128	130	95	76	83	148	170								
670	661	246	172	96	134	81	156	166	527	131	136	122	77	96	58	102								
680	487	102	122	77	100	90	183	24	299	137	124	61	76	82	49	172								
690	409	216	165	206	128	100	160	25	285	64	109	87	142	58	148	117								
700	368	158	116	134	222	164	143	96	166	7	96	41	87	275	480	177								

**Table 11 Average percentage of fluorescence quenching (%Q) of PNA in Tris-HCl buffer with different concentrations of GO for 1 hour (Figure 41c).**

GO ( $\mu\text{g/mL}$ )	PNA1 (200 nM)		PNA2 (200 nM)	
	%Q(average)	SD	%Q(average)	SD
0	0	0	0	0
2	69.90	4.91	84.51	2.74
4	82.88	8.69	89.36	3.31
6	90.95	1.24	95.88	0.71
8	92.15	4.46	96.96	0.86
10	96.21	0.80	97.39	0.94
12	93.19	3.05	95.29	1.31
14	90.96	3.44	95.24	3.34

**Table 12 Average percentage of fluorescence quenching (%Q) of PNA-GO complex (200 nM: 10  $\mu\text{g/mL}$ ) in Tris-HCl buffer decreased over time (Figure 41c).**

Time (min)	PNA1/GO (200 nM : 10 $\mu\text{g/mL}$ )		PNA2/GO (200 nM : 10 $\mu\text{g/mL}$ )	
	%Q(average)	SD	%Q(average)	SD
1	73.92	1.88	79.12	2.64
10	90.94	2.85	90.11	0.75
20	93.52	2.05	92.67	0.58
30	94.73	1.58	93.98	0.57
40	95.38	1.31	94.86	0.61
50	95.92	0.98	95.50	0.60
60	96.21	0.80	95.88	0.58



**Table 13 Fluorescence emission data for specific ssDNA detection by pre-mixing DNA with PNA before adding GO (Figure 43a-b).**

nm	PNA1-ssDNA (1.2 equiv.-excess)										PNA2-ssDNA (1.2 equiv.-excess)										
	PNA	PNA/GO	DNA1	DNA2	DNA3	DNA4	DNA5	PNA	PNA/GO	DNA1	DNA2	DNA3	DNA4	DNA5	PNA	PNA/GO	DNA1	DNA2	DNA3	DNA4	DNA5
500	8850	386	4745	519	511	485	511	1269	473	467	442	396	8850	386	1269	473	467	442	396	8850	386
510	27218	1023	11621	963	879	887	1040	2821	907	805	794	713	27218	1023	2821	907	805	794	713	27218	1023
520	43765	1576	15816	1383	1253	1188	1390	3884	1281	1052	1018	950	43765	1576	3884	1281	1052	1018	950	43765	1576
530	47152	1773	15289	1581	1380	1273	1470	3899	1420	1112	1058	1069	47152	1773	3899	1420	1112	1058	1069	47152	1773
540	39722	1577	12210	1378	1169	1148	1344	3338	1280	983	986	933	39722	1577	3338	1280	983	986	933	39722	1577
550	30679	1299	9517	1127	965	955	1081	2660	1114	873	818	848	30679	1299	2660	1114	873	818	848	30679	1299
560	22978	983	7351	967	789	791	833	2112	848	666	636	644	22978	983	2112	848	666	636	644	22978	983
570	18061	819	5663	812	640	693	655	1658	724	523	535	567	18061	819	1658	724	523	535	567	18061	819
580	13089	609	4271	647	538	554	551	1188	570	458	403	432	13089	609	1188	570	458	403	432	13089	609
590	9728	456	3125	572	446	449	442	1006	464	340	320	345	9728	456	1006	464	340	320	345	9728	456
600	6736	368	2218	398	345	331	403	723	380	334	276	328	6736	368	723	380	334	276	328	6736	368
610	4760	278	1585	383	306	297	310	557	342	268	230	284	4760	278	557	342	268	230	284	4760	278
620	3545	231	1186	259	218	253	244	355	299	269	186	231	3545	231	355	299	269	186	231	3545	231
630	2462	191	917	262	243	216	225	257	199	137	127	170	2462	191	257	199	137	127	170	2462	191
640	1997	138	768	175	164	215	208	228	120	117	113	158	1997	138	228	120	117	113	158	1997	138
650	1310	118	389	148	204	206	322	353	96	202	240	226	1310	118	353	96	202	240	226	1310	118
660	1027	144	481	29	88	198	133	202	227	78	96	16	1027	144	202	227	78	96	16	1027	144
670	661	81	348	279	0	224	18	0	90	206	162	0	661	81	0	90	206	162	0	661	81
680	487	90	547	187	2	270	49	238	316	549	29	163	487	90	238	316	549	29	163	487	90
690	409	100	544	0	127	711	0	0	0	549	331	77	409	100	0	0	549	331	77	409	100
700	368	164	0	1127	278	0	626	0	23	164	0	178	368	164	0	23	164	0	178	368	164

**Table 14 Fluorescence emission data for specific ssDNA detection by post-mixing DNA with PNA-GO complex (Figure 43c-d).**

nm	PNA1-ssDNA (1.2 equiv.-excess)										PNA2-ssDNA (1.2 equiv.-excess)																	
	PNA	PNA/GO	DNA1	DNA2	DNA3	DNA4	DNA5	PNA	PNA/GO	DNA1	DNA2	DNA3	DNA4	DNA5	PNA	PNA/GO	DNA1	DNA2	DNA3	DNA4	DNA5							
500	6153	234	4308	1979	674	701	609	1031	501	492	557	782	6153	234	6153	234	4308	1979	674	701	609	1031	501	492	557	782	6153	234
510	18878	494	10839	4806	1526	1569	1282	2386	928	929	1045	1819	18878	494	18878	494	10839	4806	1526	1569	1282	2386	928	929	1045	1819	18878	494
520	30230	746	15506	6995	2267	2343	1887	3426	1340	1374	1493	2750	30230	746	30230	746	15506	6995	2267	2343	1887	3426	1340	1374	1493	2750	30230	746
530	32875	844	15591	7236	2481	2515	2028	3510	1409	1456	1675	3035	32875	844	32875	844	15591	7236	2481	2515	2028	3510	1409	1456	1675	3035	32875	844
540	27684	809	12701	6099	2137	2208	1804	2993	1263	1316	1496	2620	27684	809	27684	809	12701	6099	2137	2208	1804	2993	1263	1316	1496	2620	27684	809
550	21302	701	9806	4761	1692	1730	1486	2365	1072	1094	1255	2094	21302	701	21302	701	9806	4761	1692	1730	1486	2365	1072	1094	1255	2094	21302	701
560	15896	535	7334	3575	1323	1338	1160	1785	841	880	990	1591	15896	535	15896	535	7334	3575	1323	1338	1160	1785	841	880	990	1591	15896	535
570	12669	435	5910	2834	1077	1066	954	1458	683	749	831	1367	12669	435	12669	435	5910	2834	1077	1066	954	1458	683	749	831	1367	12669	435
580	9041	328	4188	2151	828	814	748	1069	568	596	670	999	9041	328	9041	328	4188	2151	828	814	748	1069	568	596	670	999	9041	328
590	6714	285	3164	1614	664	669	596	804	475	476	533	767	6714	285	6714	285	3164	1614	664	669	596	804	475	476	533	767	6714	285
600	4776	210	2225	1171	485	514	445	622	376	374	425	583	4776	210	4776	210	2225	1171	485	514	445	622	376	374	425	583	4776	210
610	3320	181	1596	900	386	396	380	479	306	308	334	459	3320	181	3320	181	1596	900	386	396	380	479	306	308	334	459	3320	181
620	2433	147	1226	666	297	347	264	393	240	231	308	379	2433	147	2433	147	1226	666	297	347	264	393	240	231	308	379	2433	147
630	1820	128	904	486	263	263	259	312	208	226	246	321	1820	128	1820	128	904	486	263	263	259	312	208	226	246	321	1820	128
640	1338	145	725	405	229	208	205	282	163	189	184	237	1338	145	1338	145	725	405	229	208	205	282	163	189	184	237	1338	145
650	898	78	532	352	179	196	195	214	151	143	195	200	898	78	898	78	532	352	179	196	195	214	151	143	195	200	898	78
660	671	83	356	277	154	187	124	205	132	105	144	187	671	83	671	83	356	277	154	187	124	205	132	105	144	187	671	83
670	527	96	264	187	121	142	161	150	90	142	111	130	527	96	527	96	264	187	121	142	161	150	90	142	111	130	527	96
680	299	82	294	154	90	155	191	124	120	117	146	36	299	82	299	82	294	154	90	155	191	124	120	117	146	36	299	82
690	285	58	337	314	259	150	224	131	83	162	87	152	285	58	285	58	337	314	259	150	224	131	83	162	87	152	285	58
700	166	275	162	348	98	196	22	176	308	209	198	105	166	275	166	275	162	348	98	196	22	176	308	209	198	105	166	275

**Table 15 Fluorescence emission data for sensitive ssDNA detection of PNA1-GO complex (Figure 44a).**

nm	Concentration of DNAI (nM)															
	0	20	40	60	80	100	120	140	160	180	200	220	240	300	400	
500	386	933	1978	2541	3223	4163	4518	5227	5482	5587	5605	5883	5517	6455	6832	
510	1023	1980	4433	5997	7611	9755	10909	12295	13076	13413	13369	13927	13307	15508	16870	
520	1576	2711	6047	8081	10332	13192	14917	16753	18004	18225	18269	19132	18174	21141	22721	
530	1773	2705	5951	7973	10180	12946	14623	16507	17630	17830	17767	18688	17720	20648	22161	
540	1577	2277	4878	6611	8272	10497	11798	13313	14294	14545	14452	15197	14513	16923	17837	
550	1299	1834	3823	5195	6564	8258	9260	10468	11218	11212	11309	11930	11286	13081	13751	
560	983	1476	2897	3956	4966	6287	6979	7909	8468	8432	8588	9049	8555	9953	10491	
570	819	1193	2301	3171	3981	4976	5574	6312	6697	6683	6844	7246	6793	7969	8388	
580	609	898	1682	2257	2846	3600	3989	4465	4807	4832	4894	5067	4889	5708	5873	
590	456	684	1269	1746	2209	2711	2968	3383	3577	3717	3663	3859	3699	4297	4387	
600	368	555	933	1271	1599	2000	2117	2370	2600	2648	2659	2715	2633	2972	3181	
610	278	413	696	970	1142	1461	1551	1756	1866	1869	1905	2023	1939	2199	2234	
620	231	367	554	735	920	1069	1205	1335	1431	1353	1495	1519	1510	1722	1733	
630	191	270	454	529	674	831	883	1031	1061	1068	1084	1120	1114	1352	1309	
640	138	229	363	458	521	639	771	804	834	787	851	899	893	884	1006	
650	118	188	269	295	397	508	511	501	631	665	747	652	609	682	710	
660	144	153	182	296	334	350	399	364	537	576	513	562	489	723	647	
670	81	51	202	184	300	351	415	303	307	331	437	464	378	258	344	
680	90	65	71	234	179	434	265	260	498	290	423	389	439	590	385	
690	100	228	338	485	120	197	13	259	590	105	250	286	214	67	374	
700	164	0	424	15	87	342	546	395	468	60	566	313	353	0	158	

**Table 16 Fluorescence emission data for sensitive ssDNA detection of PNA2-GO complex (Figure 44b).**

nm	Concentration of DNAI (nM)															
	0	20	40	60	80	100	120	140	160	180	200	220	240	300	400	
500	234	865	1467	1838	2566	2766	3066	3229	3524	3676	3850	3700	4308	5192	5323	
510	494	1945	3563	4427	6194	6824	7657	7978	8587	9233	9611	9315	10839	13180	13474	
520	746	2935	5161	6413	8875	9708	10845	11306	12197	13190	13707	13402	15506	18745	19305	
530	844	3143	5439	6609	8982	9815	10790	11410	12258	13271	13699	13538	15591	18861	19204	
540	809	2763	4601	5499	7291	8042	8917	9266	10106	10787	11160	11073	12701	15250	15399	
550	701	2256	3702	4391	5729	6293	6926	7262	7838	8319	8588	8681	9806	11709	11911	
560	535	1714	2781	3304	4313	4735	5228	5481	5976	6366	6530	6512	7334	8849	9015	
570	435	1426	2249	2629	3479	3788	4123	4362	4845	5058	5196	5293	5910	6945	7099	
580	328	1072	1649	1933	2494	2744	3022	3193	3457	3663	3695	3792	4188	4929	5036	
590	285	886	1261	1500	1927	2094	2294	2347	2638	2763	2843	2816	3164	3681	3752	
600	210	656	928	1081	1389	1516	1650	1714	1897	1916	2003	2003	2225	2557	2653	
610	181	508	724	778	989	1081	1229	1281	1335	1416	1423	1551	1596	1907	1905	
620	147	395	553	680	820	836	927	976	1074	1132	1148	1075	1226	1370	1438	
630	128	311	409	500	573	585	711	739	740	850	833	848	904	1067	1036	
640	145	267	343	394	489	462	518	518	604	622	718	637	725	805	882	
650	78	177	266	275	375	364	397	447	451	509	493	499	532	587	594	
660	83	252	249	215	364	309	303	329	351	395	367	385	356	450	447	
670	96	178	208	135	311	247	206	221	303	368	182	330	264	230	345	
680	82	174	151	201	236	163	232	203	266	201	290	206	294	223	227	
690	58	192	164	142	85	263	186	151	156	216	192	185	337	287	209	
700	275	157	81	146	177	358	50	68	187	187	212	181	162	188	393	

**Table 17** The linearity range of relative fluorescence intensities at 530 nm ( $F_{530\text{nm}}$ ) and concentration of DNA1 of PNA/GO system towards targeted ssDNA detection (Figure 41c-d).

DNA1 (nM)	$F_{530\text{ nm}}$	
	PNA1·DNA1/GO	PNA2·DNA1/GO
0	1773	844
20	2705	3143
40	5951	5439
60	7973	6609
80	10180	8982
100	12946	9815
120	14623	10790
140	16507	-
160	17630	-

**Table 18** Average fluorescence intensities of PNA-GO complex in PCR reaction-solution; n = 3 (Figure 47).

Experiments	PNA1 only		PNA1-GO complex		$F_1 / F_0$
	$F_1$	SD	$F_0$	SD	
EX1	12156.06	1268.98	943.57	155.43	12.88
EX2	11091.13	1455.87	4065.47	588.01	2.73
EX3	10318.47	261.56	4333.47	270.49	2.38
EX4	10082.47	171.23	2992.80	214.01	3.37
EX5	9437.80	440.92	5506.13	275.71	1.71

**Table 19 Fluorescence intensity of PNA1 in PCR reaction-solution with different concentrations of GO which was re-determined and their percentage of fluorescence quenching (Figure 49).**

GO ( $\mu\text{g}/\text{mL}$ )	PNA1 in PCR solution (50 nM)	
	Fluorescence intensity	%Q
0	24404.47	0.00
10	8429.80	65.50
20	3400.13	86.10
30	2096.80	91.40
40	1529.47	93.70
50	1109.47	95.50

**Table 20 The percentage of fluorescence quenching (%Q) of 10 pmol PNA1 when adding different amounts of GO in range of 0-9.6  $\mu\text{g}$ ; n = 3 (Figure 57a).**

GO ( $\mu\text{g}$ )	<i>F</i> (average)	SD	%Q	SD
0	4513.32	145.27	0.00	0.00
1.2	1438.65	69.85	68.12	1.55
2.4	750.22	50.83	83.38	1.13
4.8	522.04	21.53	88.43	0.48
7.2	314.65	2.76	93.03	0.06
9.6	219.51	1.28	95.11	0.06

**Table 21 Measured fluorescence for the detection of targeted RPA products; n = 3 (Figure 57b).**

RPA/PNA-GO system	<i>F</i> (average) $\pm$ SD	
	Without DNase I	With DNase I
with target dsDNA	255.27 $\pm$ 3.56	232.94 $\pm$ 3.68
without target dsDNA	291.10 $\pm$ 3.52	1039.89 $\pm$ 50.98

**Table 22 Optimization of the hybridization time for the binding of the PNA probe to the dsDNA target; n = 3 (Figure 57d).**

Times (min)	<i>F</i> (average) ± SD	
	Without DNase I	With DNase I
0	129.74 ± 3.87	219.51 ± 1.28
5	308.45 ± 10.51	770.10 ± 22.64
10	466.69 ± 9.13	714.21 ± 29.20
15	444.33 ± 15.16	886.39 ± 12.04
20	505.62 ± 16.22	1236.98 ± 10.14
25	517.42 ± 28.05	1181.09 ± 25.18

**Table 23 The fluorescence intensity for *E. canis* detection by RPA-DPG assay; n = 3 (Figure 58).**

Canine blood parasites	<i>F</i> (average) ± SD
<i>E. canis</i>	936.33 ± 45.04
<i>A. platys</i>	187.65 ± 19.16
<i>B. vogeli</i>	210.36 ± 13.21
<i>H. canis</i>	190.17 ± 12.61
Milli Q (control)	187.82 ± 9.59

**Table 24 The absolute fluorescence read-out of the RPA-PDG for the detection of *E. canis* pUC57-plasmid DNA at different concentrations; n = 3 (Figure 59).**

Template (fg/μL)	<i>F</i> (average) ± SD
0 (control)	225.04 ± 4.26
1×10 <sup>0</sup>	236.77 ± 39.83
1×10 <sup>1</sup>	242.15 ± 17.14
1×10 <sup>2</sup>	292.19 ± 40.86
1×10 <sup>3</sup>	347.11 ± 42.42
1×10 <sup>4</sup>	371.54 ± 17.36
1×10 <sup>5</sup>	519.35 ± 21.50
1×10 <sup>6</sup>	936.33 ± 45.04

## 1. The calculation for the optimizing GO-quenching PNA probe

### 1.1 Preparation for stock solution

#### 1.25 M Tris-HCl buffer pH 8.0 and 2.5 M NaCl

*1.25 M Tris base in 10 mL of Milli Q water*

$$\frac{g}{Mw} = \frac{cv}{1000}$$

$$\frac{g}{121.14 \text{ g/mol}} = \frac{1.25 \text{ M} \times 10 \text{ mL}}{1000}$$

$$g = 1.51 \text{ g}$$

*2.5 M NaCl in 10 mL of Milli Q water*

$$\frac{g}{Mw} = \frac{cv}{1000}$$

$$\frac{g}{58.44 \text{ g/mol}} = \frac{2.5 \text{ M} \times 10 \text{ mL}}{1000}$$

$$g = 1.46 \text{ g}$$

1.51 g of Tris base and 1.46 g of NaCl were dissolved in 9.0 mL of Milli Q water. 37% HCl was slowly added into the solution to reduce pH to 8.0 and adjusted into 10 mL by Milli Q water.

#### 8 $\mu$ M PNA1

$$c_1v_1 = c_2v_2$$

$$948.28 \mu\text{M} \times v_1 = 8 \mu\text{M} \times 1000 \mu\text{L}$$

$$V_1 = 8.44 \mu\text{L} + 991.56 \mu\text{L of H}_2\text{O}$$

#### 8 $\mu$ M PNA2

$$c_1v_1 = c_2V_2$$

$$918.70 \mu\text{M} \times v_1 = 8 \mu\text{M} \times 1000 \mu\text{L}$$

$$v_1 = 8.71 \mu\text{L} + 991.29 \mu\text{L of H}_2\text{O}$$



**Stock GO solution (0, 20, 40, 60, 80, 100, 120, 140  $\mu\text{g}/\text{mL}$ )**

$$\begin{aligned}
 c_1 v_1 &= c_2 v_2 \\
 10,000 \mu\text{g}/\text{mL} \times v_1 &= c_2 (\mu\text{g}/\text{mL}) \times 1000 \mu\text{L} \\
 v_1 &= \frac{c_2}{10} (\mu\text{L}) + [1000 - v_1 (\mu\text{L})] \text{ of } H_2O
 \end{aligned}$$

*Example for 20  $\mu\text{g}/\text{mL}$* 

$$\begin{aligned}
 c_1 v_1 &= c_2 v_2 \\
 10,000 \mu\text{g}/\text{mL} \times v_1 &= 20 \mu\text{g}/\text{mL} \times 1000 \mu\text{L} \\
 v_1 &= 2 \mu\text{L} + 998 \mu\text{L} \text{ of } H_2O
 \end{aligned}$$

**1.2 Calculation for a final concentration**

Conditions; [PNA] = 200 nM in 25 mM Tris-HCl buffer pH 8.0 and 50 mM NaCl, [GO] = 0 - 14  $\mu\text{g}/\text{mL}$ , total volume = 200  $\mu\text{L}$ .

**25 mM Tris-HCl buffer pH 8.0 and 50 mM NaCl***25 mM Tris-HCl*

$$\begin{aligned}
 c_1 v_1 &= c_2 v_2 \\
 1.25 \text{ M} \times 4 \mu\text{L} &= c_2 \times 200 \mu\text{L} \\
 c_2 &= 25 \text{ mM}
 \end{aligned}$$

*50 mM NaCl*

$$\begin{aligned}
 c_1 v_1 &= c_2 v_2 \\
 2.5 \text{ M} \times 4 \mu\text{L} &= c_2 \times 200 \mu\text{L} \\
 c_2 &= 50 \text{ mM}
 \end{aligned}$$

**200 nM PNA**

$$\begin{aligned}
 c_1 v_1 &= c_2 v_2 \\
 8 \mu\text{M} \times 5 \mu\text{L} &= c_2 \times 200 \mu\text{L} \\
 c_2 &= 200 \text{ nM}
 \end{aligned}$$

**0 - 14  $\mu\text{g}/\text{mL}$  GO**

*Example for 2  $\mu\text{g}/\text{mL}$  GO*

$$\begin{aligned}
 c_1 v_1 &= c_2 v_2 \\
 20 \mu\text{g}/\text{mL} \times 20 \mu\text{L} &= c_2 (\mu\text{g}/\text{mL}) \times 200 \mu\text{L} \\
 c_2 &= 2 \mu\text{g}/\text{mL}
 \end{aligned}$$

**1.3 Percentage of fluorescence quenching (%Q)**

(%Q was calculated by using  $F_{530}$  in the absence and presence of GO. The  $Q_1$ ,  $Q_2$ ,  $Q_3$  are %Q in triplicate measurements)

$$\%Q = \frac{F_{SSPNA} - F_{SSPNA+GO}}{F_{SSPNA}} \times 100\%$$

*Example for 2  $\mu\text{g}/\text{mL}$  GO*

$$\%Q_1 = \frac{53767 - 14358}{53767} \times 100\%$$

$$\%Q_1 = 73.3 \%$$

$$\%Q_2 = \frac{46159 - 12726}{46159} \times 100\%$$

$$\%Q_2 = 72.4 \%$$

$$\%Q_3 = \frac{41530 - 9957}{41530} \times 100\%$$

$$\%Q_3 = 76.0 \%$$

$$\text{Average \%Q} = \frac{73.3 + 72.4 + 76.0}{3} = 73.9 \%$$

#### 1.4 Limit of detection (LOD)<sup>20</sup>

$$LOD = \frac{3.3 \times SD_{PNA-GO \text{ complex}}}{Slope}$$

For PNA1

$$LOD = \frac{3.3 \times 283.89}{105.9570} = 8.84 \text{ nM}$$

For PNA2

$$LOD = \frac{3.3 \times 186.56}{83.4423} = 7.38 \text{ nM}$$

## 2. The calculation for the studying ssDNA detection by PNA/GO system

Conditions; [PNA] = 200 nM in 25 mM Tris-HCl buffer pH 8.0 and 50 mM NaCl, [GO] = 10 µg/mL, [DNA1-5] = 240 nM or [DNA1] = 0 - 400 nM, volume = 200 µL.

### 2.1 Calculation for 1.2 equiv. of DNA1-5 used for specificity study

(Each ssDNA1-5 was diluted into 9.6 µM of stock concentration before used.)

$$\begin{aligned} c_1 v_1 &= c_2 v_2 \\ 9.6 \mu\text{M} \times 5 \mu\text{L} &= c_2 \times 200 \mu\text{L} \\ c_2 &= 240 \text{ nM} \end{aligned}$$

### 2.2 Preparation of stock DNA1 in a range of 0 - 16 µM in using for sensitivity study (The stock concentration of DNA1 = 20 µM)

$$\begin{aligned} c_1 v_1 &= c_2 v_2 \\ 20 \mu\text{M} \times v_1 &= c_2 \times 40 \mu\text{L} \\ v_1 &= 2 \times c_2 \end{aligned}$$

*Example for 0.8  $\mu\text{M}$*

$$\begin{aligned} c_1 v_1 &= c_2 v_2 \\ 20 \mu\text{M} \times v_1 &= 0.8 \mu\text{M} \times 40 \mu\text{L} \\ v_1 &= 1.6 \mu\text{L} + 38.4 \mu\text{L of } H_2O \end{aligned}$$

### 2.3 Calculation for 0 - 2.0 equiv. of DNA1 used for sensitivity study

**10  $\mu\text{g}/\text{mL}$  GO**

$$\begin{aligned} c_1 v_1 &= c_2 v_2 \\ 100 \mu\text{g}/\text{mL} \times 20 \mu\text{L} &= c_2 (\mu\text{g}/\text{mL}) \times 200 \mu\text{L} \\ c_2 &= 10 \mu\text{g}/\text{mL} \end{aligned}$$

**Example for 0.8  $\mu\text{M}$  (0.1 equiv. DNA)**

$$\begin{aligned} c_1 v_1 &= c_2 v_2 \\ 0.8 \mu\text{M} \times 5 \mu\text{L} &= c_2 \times 200 \mu\text{L} \\ c_2 &= 20 \text{ nM} \end{aligned}$$

### 3. Calculation for the studying dsDNA detection by RPA-DPG

**3.1 stock GO solution (0.2, 0.4, 0.8, 1.2, 1.6  $\mu\text{g}/\mu\text{L}$ )**

*Example for 0.2  $\mu\text{g}/\mu\text{L}$*

$$\begin{aligned} c_1 v_1 &= c_2 v_2 \\ 10 \mu\text{g}/\mu\text{L} \times v_1 &= 0.2 \mu\text{g}/\mu\text{L} \times 500 \mu\text{L} \\ v_1 &= 10 \mu\text{L} + 490 \mu\text{L of } H_2O \end{aligned}$$

(Used 6  $\mu\text{L}$  for quenching 10 pmol **PNA1**)

$$\text{amounts of GO in used} = 0.2 \mu\text{g} \times 6 \mu\text{L} = 1.2 \mu\text{g}$$

### 3.2 Concentration of pUC57-plasmid DNA (1 ng/ $\mu$ L)

*copies/ $\mu$ L*

$$\text{number of copies} = \frac{(ng \times 6.022 \times 10^{23})}{(\text{length} \times 1 \times 10^9 \times 650 \text{ g/mol})}$$

$$\text{number of copies} = \frac{(1 \text{ ng} \times 6.022 \times 10^{23})}{(1,380 \text{ bp} \times 1 \times 10^9 \times 650 \text{ g/mol})}$$

$$\text{number of copies} = 6.71 \times 10^8 \text{ copies}/\mu\text{L}$$

*mol/L*

$$\frac{cv}{1000} = \frac{g}{(\text{length} \times 650 \text{ g/mol})}$$

$$\frac{c \times (1 \times 10^{-3} \text{ mL})}{1000} = \frac{1 \text{ ng}}{(1,380 \text{ bp} \times 650 \text{ g/mol})}$$

$$c = \frac{(1 \times 10^{-9} \text{ g}) \times 10^3}{(1,380 \text{ bp} \times 650 \text{ g/mol}) \times 10^{-3}}$$

$$c = \frac{(1 \times 10^{-9} \text{ g}) \times 10^3}{(897 \times 10^3) \times 10^{-3}} \text{ (mol/L)}$$

$$c = 1.11 \times 10^{-9} \text{ (mol/L)}$$

$$c = 1.11 \text{ nM}$$

### 3.3 Limit of detection (LOD) <sup>20</sup>

$$\log_{10}(\text{LOD}) = \left( \frac{3.3 \times SD_{\text{PNA-GO complex}}}{\text{Slope}} \right)$$

$$\log_{10}(\text{LOD}) = \left( \frac{3.3 \times 4.26}{40.575} \right) = 0.346$$

$$\text{LOD} = 10^{0.346}$$

$$\text{LOD} = 2.22 \text{ fg}/\mu\text{L}$$

*mol/L*

$$c = \frac{(2.22 \times 10^{-15} \text{ g}) \times 10^3}{(897 \times 10^3) \times 10^{-3}} \text{ (mol/L)}$$

$$c = 2.47 \times 10^{-15} \text{ (mol/L)}$$

$$c = 2.47 \text{ fM}$$

### 3.3 LOD for visualization

$$\text{mol/L} \quad LOD = 10 \text{ pg}/\mu\text{L}$$

$$c = \frac{(10 \times 10^{-12} \text{ g}) \times 10^3}{(897 \times 10^3) \times 10^{-3}} \text{ (mol/L)}$$

$$c = 11.15 \times 10^{-12} \text{ (mol/L)}$$

$$c = 11.15 \text{ pM}$$

